

THE UNIVERSITY OF HULL

Two phase problems and two phase flow

being a Thesis submitted for the Degree of

Doctor of Philosophy

in the University of Hull

by

Wilkinson Kunda B.Sc. (UNZA), M.Sc. (Aston)

June 1986.

To

Aseli Carol Kunda

Acknowledgements

I would like to express my gratitude and appreciation to Professor Graham Poots for proposing this interesting field of research and for his encouragement, support and advice throughout the last three years.

I also wish to thank Dr. P. Beckett and the staff of the University Computer Centre for assistance during some of the numerical work.

I am also grateful to Mrs. Gillian Chilton for her speedy and efficient typing of the thesis and to the University of Zambia for financing this study.

Abstract

In section 1 of this thesis a two-dimensional mathematical model is used to investigate the circulation in a gas-bubble agitation system of a cylindrical vessel for the case of an orifice located at the centre of the base. The two-phase (liquid/gas) region is assumed to be confined to a cone-shaped region and is investigated using Wallis' Drift Flux Model. In the single-phase (liquid) region the turbulent Navier-Stokes equations, written in terms of the stream function, are used for the mathematical model. The analysis in the two-phase region yields the boundary conditions on the two-phase/single-phase boundary. The velocity field in the two-phase region is solved analytically giving results in closed form. A numerical algorithm is developed for calculating liquid flow in the single phase region, and numerical results are presented graphically in terms of the stream function.

In section 2 two moving interface problems are investigated. Small time analytic solutions are found for three-dimensional inward solidification of a half space initially at fusion temperature in the first problem. In the second problem, perturbation solutions for melting of a cylindrical annulus with constant heat flux on inner surface are given. In both problems the interface immobilization technique is used. Interface locations at various times are calculated for the inward solidification problem and

the results shown in three-dimensional graphs. First and second perturbation terms for the interface location are given for the second problem and graphs of each are presented for a particular case.

Contents

	<u>Page</u>
Section 1. <u>Two phase flow</u>	
<u>Chapter 1</u>	
Introduction	2
<u>Chapter 2</u>	
Flow model in bubble stream	11
<u>Chapter 3</u>	
Mathematical model	18
<u>Chapter 4</u>	
Calculation of liquid flow	28
<u>Chapter 5</u>	
Numerical Solutions	37
Section 2. <u>Two phase problems</u>	
<u>Chapter 1</u>	
Introduction	41

Chapter 2

Analytical solutions to a class of
three-dimensional solidification problems 48

Chapter 3

Perturbation solutions for melting of a
cylindrical annulus with constant heat
flux on inner surface 67

Tables 91
Figures 93
Appendix 1 117
Appendix 2 121
Appendix 3 130
References 137

Nomenclature

Section 1

A	cross-section area
C.	distribution parameter
g	gravitational constant
H	height of liquid column
j	volumetric flux density
p	pressure
Q	volumetric flow rate
r	radial position
R	dimensionless radial position
R.	radius of cylindrical container
Re	Reynolds number
u	velocity
u.	gas velocity outlet orifice
u _∞	rising velocity of bubbles
v.	velocity
W	mass flow rate
z	axial position
z.	height above base of inlet orifice
Z	dimensionless axial position
α	void fraction
β	dimensionless parameter
δ	dimensionless parameter
η	dimensionless independent variable
λ	angular measure
μ	viscosity
ξ	dimensionless independent variable

ρ	density
ψ	stream function
Ψ	dimensionless stream function

subscripts

1	liquid property
2	gas property
eff	effective
l	liquid property
r	radial direction property

Section 2

a	radius of inner boundary of annulus
b	radius of outer boundary of annulus
Bi	Biot number
C	positional function of the interface
c_p	specific heat
g	wall temperature function
h	heat transfer coefficient
k	thermal diffusivity
K	thermal conductivity
L	latent heat of fusion
Q	heat flux
r	radial position
r_i	position of interface
t	time
T	temperature
x	independent variable
\underline{x}	the vector (x, y) or (ϕ, ψ)
X	dimensionless independent variable

y	independent variable
Y	dimensionless independent variable
z	independent variable
Z	dimensionless independent variable
α	dimensionless parameter
ϵ	perturbation parameter $(C_p(T_F - T_I) / L_s)$
η	dimensionless independent variable
θ	dimensionless temperature
ξ	dimensionless independent variable
ρ	density
σ	dimensionless position of interface
τ	dimensionless time
Ω	dimensionless parameter

subscripts

o	initial property
F	fusion property
I	initial property
L	liquid property
S	solid property

local to Chapter 2

β	Stefan number
ϕ	dimensionless independent variable
ψ	dimensionless independent variable

local to Chapter 3

β	dimensionless parameter
ϕ	dimensionless temperature of liquid
ψ	dimensionless temperature of solid

SECTION 1

Two phase flow

CHAPTER 1

INTRODUCTION

Gas injection into molten metal has been used in commercial steel making operations since the 1850's when Bessemer injected gas into the base of a steel making ladle. The ultimate objective of bubbling gas into molten metal is to effect a chemical change in the liquid phase. Development of gas injection processes in steel making continues but the means for effectively assessing proposed process designs and their potential operational benefits are not as complete or reliable as desired.

When gas is issued from an orifice at a low superficial velocity into a liquid, a swarm of bubbles rises uniformly within a gas-bubble column. When gas velocity is increased, the bubble flow ceases to be uniform and becomes unstable, intense recirculation is observed in the gas-liquid two-phase region, and the column operates in the recirculation flow regime. Until very recent times the quantitative characterization of flow patterns and mixing in argon-stirred ladles was very difficult and the most that could be done was to estimate mixing times and flow features from water models. Typical apparatus for the experimental study of water models consist of a transparent cylindrical tank filled with water and stirred by a metered continuous jet of air admitted through an orifice centrally placed in the bottom of the tank. Polystyrene particles are added to

the water and illuminated by a light source. The flow pattern is observed by the motion of the polystyrene particles through the transparent tank. While the information obtained from the flow visualization test is very helpful it is only qualitative. Over a period of years quantitative description of the flow field was obtained using hot film anemometry. Hot film anemometry relies on the fact that if a metal film heated by a current is immersed in a moving fluid, the rate of heat loss from the film is related to the velocity of the fluid adjacent to the probe. Since the electrical conductivity of the film is temperature dependent, if the current required to maintain the probe at a constant temperature is determined, this current can be related to the local fluid velocity. The probe is mounted on a frame and attached to a suitable travelling mechanism which allows the positioning of the probe at any desired point within the system. Current experimental measurements on velocity fields in a cylindrical tank, containing water, are carried out using laser-doppler anemometry, which is an improvement over the hot film anemometry, making use of recent developments in laser technology.

Laser-doppler or hot film anemometry methods cannot be used to measure directly the velocity fields in molten metal baths because the temperatures in the baths are too high for the apparatus to withstand. Alternative approaches have been developed which are based on the turbulent

Navier-Stokes equations together with models for the turbulent viscosity. Turbulence models developed give predictions on velocity profiles which can be compared with experimental measurements. Szekely, Wang and Kiser (1976) predicted the velocity field in a water model of an argon-stirred ladle. They compared their results to quantitatively measured velocity using hot-film anemometry. Their theoretical prediction was based on the numerical solution of the turbulent Navier-Stokes equations using the two-equation k-W model for the turbulence viscosity. Comparison of the predicted and measured results showed that the agreement was only qualitative.

DebRoy, Majumdar and Spalding (1978) used a mathematical model for the water model of an argon stirred ladle of Szekely et al (1976) to predict the velocity field. In their model, DebRoy et al assumed that the two-phase (gas/liquid) was confined to a cylinder, whose axis was the axis of the container, and radius being an estimate of the radial width of gas-liquid mixture at the surface. The no-slip condition on velocity was used at the walls and at the free surface the conditions imposed were that vertical velocity is zero and that the surface shear stress is zero. A constant effective viscosity was used. In the numerical solution was included a procedure for predicting the average volumetric concentration of gas (void fraction) from the gas flow rate. DebRoy et al examined two idealized cases: the case when gas and liquid move with the same speed; and the case when the gas moves at a higher speed than the liquid so

allowing for slip. A comparison was made between the predictions of velocity field with the no-slip model along with the experimental measurements of Szekely et al (1976). Agreement between the measurements and the predicted values was reasonable.

Grevet, Szekely and El-Kaddah (1982) performed more detailed experimental studies where the air-water system was used to simulate the behaviour of the argon-stirred ladle and laser-doppler anemometry was employed to determine the velocity fields. In addition to the laser velocimetry a photographic record was made of the system in order to define the geometry of the bubble column and the two-phase region. Grevet et al (1982) also made a mathematical model of the gas bubble circulating system of their experiment which represented an axisymmetrical turbulent recirculation flow problem. In the mathematical model Grevet et al make the assumption that the two-phase region is confined to a jet cone, the dimensions of which are determined from the experiment. The boundary conditions used are the same as those of DebRoy et al (1976) with the addition of an initial gas velocity at the orifice. The whole domain was represented in terms of a single set of equations. The void fraction was calculated using the drift flux model. The governing equations were solved numerically retaining the primitive variables, and using the $k - \epsilon$ model for the turbulent viscosity. The numerical computations were performed using a general computer program of Pun and

Spalding (1977). The comparisons made between predicted and measured velocities showed reasonable agreement and speculation was made as to whether the discrepancies were due to the experimental data or to the mathematical model.

A mathematical model using the continuous mixture approach was devised by Aldham, Cross and Markatos (see Hudson and O'Carroll (1982)) for the purpose of comparing the predicted velocities with the experimental results of Grevet et al (1982). In their paper Aldham et al conclude that their model predictions compare favourably with the measurements of Grevet et al. Investigations of bubble driven circulation in an axis^mymmetric vessel were carried out numerically and experimentally, using Laser-doppler anemometry, by Durst, Taylor and Whitelaw (1984). In this investigation liquid flow was caused by a steady column of air bubbles rising through castor oil in a cylindrical vessel. Measurements of the liquid velocity were obtained across the diameter of the vessel and confirmed that the only region of asymmetry was confined to the vicinity of the bubble column near the free surface. In the mathematical model, Durst et al assumed liquid flow to have constant properties, be incompressible, steady and axisymmetric. The no-slip condition on velocity was used at the walls and the free surface was assumed to be stationary. The time-average of the measured values of velocity were imposed on a cylinder whose axis was that of the container and radius specified. The governing equations were solved numerically retaining the primitive variables using a method derived

from that of Spalding (1972). The results of the calculations were in close agreement with the experiment.

When modelling an argon-stirred ladle through the statement of the turbulent Navier-Stokes equations and comparison of the model made with experimental measurements, the main difficulties are those regarding the boundary conditions and experimental inaccuracies. Szekely, Dilawari and Metz (1979) devised an experiment for which the system was so constructed that the boundary conditions may be stated unambiguously. The system consisted of a cylindrical tank containing water and recirculating motion was induced in the tank by means of a tube which was made to pass through the axis of the tank in the upward direction. The tube was driven by a pulley which was driven by a variable speed motor. This system is referred to as the Belt Driven Circulating Flow System. In this system the conditions on solid boundaries are known and the condition on the moving boundary is also known. In their experiment, Szekely et al measured the velocities in the tank using Laser-doppler anemometry. For the mathematical model the turbulent Navier-Stokes equations were written in terms of the stream function and the k-W model of turbulence used. A numerical method was used to solve the governing equations and the solutions compared to the experimental results. It was found that the theoretical predictions of the velocity profiles represented the experimentally obtained profiles quite well.

One purpose of this work is to produce theoretical results which may help in development of gas injection processes in steel making. The primary objective is to provide a numerical algorithm which can be used to effectively predict the circulation in a steel making ladle.

It is an aim of this section of the thesis to produce a two-dimensional model capable of predicting the circulation in a gas-bubble agitation system of a cylindrical vessel for the case of an orifice located at the centre of the base.

Current practice has shown that the turbulent Navier-Stokes equations govern flow in turbulent recirculation systems such as the gas bubble recirculation of a ladle. One of the main problems encountered in previous theoretical investigations of the gas bubble driven circulation systems was to obtain proper representation of the boundary between the gas bubble-rich region and the bulk of the liquid both in terms of shape and in terms of stating the proper boundary conditions for the velocity and velocity gradients.

To construct a mathematical model the following assumptions are made:

(i) the bubble-stream is confined to a cone-shaped region;

(ii) the two-phase region is confined to the bubble-stream.

The assumptions result in the flow domain being divided into

two regions, namely the two-phase cone region and the remainder which is a single-phase region. The problem in the single-phase region becomes that of turbulent recirculating flow with the velocity on the two-phase/single-phase boundary being derived from the velocity fields in the two-phase region.

A consequence of the assumptions is that the model for the recirculating liquid flow is now reduced to a 'belt-driven' model, where the belt is a conical surface moving with variable speed along a cone generator. The reduced problem for recirculating liquid is related to the 'belt-driven' square cavity recirculating liquid flow problem for which numerical results have been contributed by many researchers using a variety of finite difference and finite element methods. Olson (1979) compared methods and results to the square cavity recirculating liquid flow problem. The problem consisted of a square (two-dimensional) cavity containing liquid with a lid at the top sliding at a constant velocity causing flow of the liquid. The results considered were for when the sliding top was moving at a Reynold's number of 1 and at Reynolds number of 400. Contour plots of stream function, vorticity and pressure as well as velocity profiles across the cavity's centre lines are considered in the comparison of results by Olson. For the case Reynolds number (Re) equal to 1, Olson reports that all the contributed numerical results showed very good agreement. However, the agreement

between the various contributors are reported not to be as good for $Re = 400$. Reasonable agreement is reported for $Re = 400$ from contributors who used very fine grids. Flows in steel making ladles are of Reynolds number in the range $10^3 - 10^4$ and results of any recirculating flows of Reynolds number in this range are very few. Tuann and Olson (1978) report about obtained results for the square cavity for Reynold number flows of up to 3000 in their review of computing methods for recirculating flows and are inconclusive about which method of solution is best.

In Chapter 2 flow in the two-phase region is analysed using the drift flux model. The boundary conditions on the two-phase/single-phase boundary are obtained.

In Chapter 3 a two-dimensional mathematical model which represents an axysymmetric turbulent recirculating system driven by gas is constructed. The governing equations and boundary conditions for the single-phase flow are stated in terms of the stream function.

In Chapter 4 an algorithm is developed for calculating liquid flow in the single-phase region.

In Chapter 5 a selection of numerical solutions is presented. As data for bath agitation in the steel industry were not available, operating data for a water tank is used. A discussion of the results is also included.

CHAPTER 2

FLOW MODEL IN BUBBLE STREAM

The aim of this chapter is to analyse the flow in the two-phase region by using the drift flux model. In this model suitable average properties in the bubble stream are determined and the mixture is treated as a pseudo-fluid that obeys the usual equations of single component flow. The components of two-phase flow are distinguished by subscripts 1, for liquid, and 2, for gas.

Consider here one-dimensional two-phase flow. The total mass rate is represented by W and the volumetric flow rate is represented by Q . Using the subscript notation

$$W = W_1 + W_2 \quad (1.2.1)$$

and

$$Q = Q_1 + Q_2 \quad (1.2.2)$$

The average volumetric concentration, also called the void fraction, is the fraction of the volume which is occupied at any instant by gas and is represented by the symbol α . The volumetric flow rate per unit area (volumetric flux) is represented by j and is related to the void fraction and velocity v as follows:

$$j_1 = (1 - \alpha) v_1 \quad ; \quad (1.2.3)$$

$$j_2 = \alpha v_2 \quad ; \quad \text{and} \quad (1.2.4)$$

$$j = j_1 + j_2 \quad . \quad (1.2.5)$$

Let A denote cross-section area, then

$$Q_1 = \int j_1 dA \quad , \quad \text{and} \quad (1.2.6)$$

$$Q_2 = \int j_2 dA \quad (1.2.7)$$

The drift flux represents the volumetric flux of a component relative to a surface moving at the average velocity. The drift flux^{density} of liquid is represented by j_{12} and is related to the void fraction as follows:

$$j_{12} = (1 - \alpha)(v_1 - j) \quad . \quad (1.2.8)$$

The drift flux^{density} of gas is represented by j_{21} and satisfies the following relation:

$$j_{21} = \alpha(v_2 - j) \quad . \quad (1.2.9)$$

In order to take into account variations in concentrations and velocity across the cross-section, averages over the

cross-section are taken. Let z be any quantity, define \bar{z} as follows:

$$\bar{z} = \int z dA / A \quad . \quad (1.2.10)$$

To derive expressions for the drift flux \bar{j}_{21} ^{density} and the void fraction $\bar{\alpha}$, introduce the definitions:

$$\langle v_1 \rangle = \bar{j}_1 / (1 - \bar{\alpha}) \quad ; \quad (1.2.11)$$

$$\langle v_2 \rangle = \bar{j}_2 / \bar{\alpha} \quad ; \quad \text{and} \quad (1.2.12)$$

$$c_0 = \bar{\alpha} \bar{j} / \bar{\alpha} \bar{j} \quad (1.2.13)$$

c_0 is called the distribution parameter. Using (1.2.12), (1.2.13) and (1.2.9) yields the expression

$$\bar{j}_{21} = \bar{\alpha} \langle v_2 \rangle - c_0 \bar{\alpha} \bar{j} \quad , \quad (1.2.14)$$

and applying (1.2.5) and definitions (1.2.11) and (1.2.12) to (1.2.14) gives \bar{j}_{21} as

$$\bar{j}_{21} = \bar{\alpha} \langle v_2 \rangle - \bar{\alpha} c_0 (\langle v_1 \rangle - \bar{\alpha} (\langle v_2 \rangle - \langle v_1 \rangle)) \quad . \quad (1.2.15)$$

Using (1.2.4), (1.2.9) and (1.2.13) in (1.2.12) gives

$$\langle v_2 \rangle = c_0 \bar{j} + \bar{j}_{21} / \bar{\alpha} \quad (1.2.16)$$

Using (1.2.7) in (1.2.12) gives the expression

$$\langle v_2 \rangle = Q_2 / A \bar{\alpha} \quad (1.2.17)$$

Equating the right hand sides of (1.2.16) and (1.2.17) yields

$$\bar{\alpha} = (Q_2 - A j_{21}) / A c_o \bar{j} \quad (1.2.18)$$

Finally, on substituting into (1.2.18) the expression (1.2.15) for the drift flux, $\bar{\alpha}$ is given by:

$$\bar{\alpha} = \frac{Q_2 - \bar{\alpha} (\langle v_2 \rangle - c_o (\langle v_1 \rangle + \bar{\alpha} (\langle v_2 \rangle - \langle v_1 \rangle)))}{A c_o \bar{j}} \quad (1.2.19)$$

In the particular system under consideration, the two-phase flow occurs within a (right circular) cone region. Let the centre of the orifice be taken as the origin of a three-dimensional co-ordinate system with the line through the origin and perpendicular to the plane of the base taken as the z-axis. Let $A(z)$ be the cross-section area at height z and assume that at any vertical height z , the vertical velocity u_z of the pseudo-fluid is uniform, i.e., does not vary with r (or θ). A momentum balance over a volume in the axial direction gives

$$\frac{d}{dz} \left(\rho u_z (A u_z) \right) = \bar{\alpha} \frac{d}{dz} \left(\rho g \frac{z A}{3} \right) \quad (1.2.20)$$

The void fraction $\bar{\alpha}$ is given in terms of relative velocities. As with all other analyses of this kind assume that the distribution parameter is unity,

$$\text{i.e. } C_0 = 1 \quad ; \quad (1.2.21)$$

and that

$$\langle v_2 \rangle - \langle v_1 \rangle = v_2 - v_1 \quad , \quad (1.2.22)$$

where $v_2 - v_1$ is the rising velocity of the gas phase denoted by u_∞ . Then using the declared coordinate system the void fraction is given by

$$\bar{\alpha} = \frac{Q_2 - \bar{\alpha}(1-\bar{\alpha})u_\infty}{2\pi \int_0^r r(v_1 - \bar{\alpha}u_\infty) dr} \quad (1.2.23)$$

In this model it is further assumed that there is no slip between the gas and liquid phases, hence

$$u_\infty = 0 \quad , \quad \text{and} \quad (1.2.24)$$

$$v_1 = u_z \quad (1.2.25)$$

Substituting (1.2.24) and (1.2.25) in (1.2.23) gives

$$\bar{\alpha} = Q_2 / \pi r^2 u_z \quad (1.2.26)$$

Let the base angle of the cone be 2λ . Then r and z are related by

$$r = z \tan \lambda \quad , \text{ hence} \quad (1.2.27)$$

$$A(z) = \pi z^2 \tan^2 \lambda \quad , \text{ giving} \quad (1.2.28)$$

$$\bar{\alpha} = Q_2 / A u_z \quad (1.2.29)$$

Q_2 is the volumetric gas flow rate taken at $z = z_0$.

Imposing the condition that

$$u_z = u_0 \quad \text{at} \quad z = z_0 \quad (1.2.30)$$

gives the following expression for Q_2 :

$$Q_2 = \pi u_0 z_0^2 \tan^2 \lambda \quad (1.2.31)$$

Using the equations (1.2.28), (1.2.29) and (1.2.31) in (1.2.20) and adopting the boundary conditions (1.2.30) results in the following equations governing the vertical velocity u_z in the two phase region:

$$\frac{d}{dz} (z^2 u_z^2) = \frac{\pi g z_0^2 u_0}{u_z} \quad (1.2.32)$$

$$u_z(z_0) = u_0 \quad (1.2.33)$$

The solution to the system (1.2.32) and (1.2.33) is

$$\frac{u_z}{u_0} = \frac{1}{z} \left(\frac{3\pi g}{4u_0^2} z_0^2 (z^2 - z_0^2) + z_0^3 \right)^{\frac{1}{3}} \quad (1.2.34)$$

The model also assumes that there is no motion in the radial direction, therefore at any height z in the cone region, the components of the pseudo-fluid velocity are:

$$u_z = u_z(z) \quad , \quad u_r = 0 \quad (1.2.35)$$

For small λ these led to the velocity condition along and normal to a generator of the cone given by

$$u_t = u_z \cos \lambda \approx u_z(z) \quad (1.2.36)$$

$$u_n = 0 \quad (1.2.37)$$

CHAPTER 3

MATHEMATICAL MODEL

Consider a system consisting of a cylindrical vessel with an orifice at the centre of the base containing a fluid and inert gas being injected into the container through the orifice. This constitutes what is generally called a gas bubble driven circulating system. A mathematical model of this system which represents an axisymmetrical turbulent recirculating flow problem is to be developed. The model supposes that the system has attained steady state and the following assumptions are made:

- (i) the bubble-stream is confined to a cone shaped region;
- (ii) the two phase region (liquid/inert gas) is confined to the bubble stream; and
- (iii) the velocity and momentum flux are continuous across the boundary of the two-phase region, see figure 1.

The centre of the orifice is taken as the origin of a three-dimensional co-ordinate system and the line through the centre of the orifice and perpendicular to the plane of the base is taken as the z-axis. Due to symmetry with respect to the z-axis, there is no variation with θ .

Let (u_r, u_z) be the velocity components in the (r, z) directions. The equations to be solved for the liquid flow are derived from the continuity and Navier-Stokes equations and are the following:

continuity:

$$\frac{1}{r} \frac{\partial}{\partial r} (r u_r) + \frac{\partial u_z}{\partial z} = 0 \quad ; \quad (1.3.1)$$

momentum:

z-direction

$$u_r \frac{\partial u_z}{\partial r} + u_z \frac{\partial u_z}{\partial z} = -\frac{1}{\rho} \frac{\partial p}{\partial z} + \frac{1}{\rho} \left(2 \frac{\partial}{\partial z} \left(\mu_{\text{eff}} \frac{\partial u_z}{\partial z} \right) + \frac{1}{r} \frac{\partial}{\partial r} \left(r \mu_{\text{eff}} \left(\frac{\partial u_z}{\partial r} + \frac{\partial u_r}{\partial z} \right) \right) \right) \quad (1.3.2)$$

r-direction

$$u_r \frac{\partial u_r}{\partial r} + u_z \frac{\partial u_r}{\partial z} = -\frac{1}{\rho} \frac{\partial p}{\partial r} + \frac{1}{\rho} \left(\frac{2}{r} \frac{\partial}{\partial r} \left(r \mu_{\text{eff}} \frac{\partial u_r}{\partial r} \right) + \frac{\partial}{\partial z} \left(\mu_{\text{eff}} \left(\frac{\partial u_r}{\partial z} + \frac{\partial u_z}{\partial r} \right) \right) - 2 \mu_{\text{eff}} \frac{u_r}{r^2} \right) \quad (1.3.3)$$

boundary conditions

$$u_r = 0, \quad u_z = 0 \quad \text{on } z = 0, \quad 0 < r \leq R_0 \quad ; \quad (1.3.4)$$

$$u_r = 0 \quad , \quad u_z = 0 \quad , \quad \text{on } r = R_0 \quad , \quad 0 \leq z \leq H \quad ; \quad (1.3.5)$$

$$u_z = 0 \quad , \quad \frac{\partial u_r}{\partial z} = 0 \quad , \quad \text{on } z = H \quad , \quad 0 \leq r \leq R_0 \quad (1.3.6)$$

$$u_z = u_0 \quad \text{at} \quad r = 0 \quad , \quad z = z_0 \quad (1.3.7)$$

The effective viscosity μ_{eff} used is calculated by a viscosity hypothesis proposed by Pun and Spalding that provides a reasonable prediction of the velocity fields in systems such as the one under consideration. The following expression has been used:

$$\mu_{\text{eff}} = k (2R_0)^{\frac{2}{3}} (H)^{-\frac{1}{3}} \rho_l^{\frac{2}{3}} (Q_{\text{gas}} u_0^2)^{\frac{1}{3}} \quad , \quad (1.3.8)$$

where Q_{gas} is the volumetric gas flow rate, u_0 is the constant velocity of the gas at the orifice, k is a constant given by

$$k = 0.012 \quad , \quad \text{and} \quad (1.3.9)$$

ρ_l is the density of the liquid.

The two-phase flow occurs within the cone region

$$0 \leq r \leq z \tan \lambda \quad , \quad z_0 \leq z \leq H \quad , \quad (1.3.10)$$

where 2λ is the angle of the cone whose vertex is at $r = z = 0$

It is assumed that the two-phase flow at any height $z \gg z_0$.

has uniform vertical velocity

$$u_z = U(z) \quad , \quad \text{and} \quad (1.3.11)$$

radial velocity

$$u_r = 0 \quad (1.3.12)$$

The expression for $U(z)$ is as derived in Chapter 2 and given by equation (1.2.34). Consequently, the model for recirculating liquid flow is now reduced to a "belt-driven" model. Here the belt is a conical surface moving with variable speed along a cone generator.

Using the constant effective viscosity and the conditions on the two-phase/liquid interface, (see figure 2,) the equations governing liquid flow are as follows:

continuity:

$$\frac{1}{r} \frac{\partial}{\partial r} (r u_r) + \frac{\partial u_z}{\partial z} = 0 \quad ; \quad (1.3.13)$$

z-direction:

$$u_r \frac{\partial u_z}{\partial r} + u_z \frac{\partial u_z}{\partial z} = - \frac{1}{\rho} \frac{\partial p}{\partial z} + \frac{\mu_{eff}}{\rho} \left(2 \frac{\partial^2 u_z}{\partial z^2} + \frac{1}{r} \frac{\partial}{\partial r} \left(r \left(\frac{\partial u_z}{\partial r} + \frac{\partial u_r}{\partial z} \right) \right) \right) \quad ; \quad (1.3.14)$$

r-direction:

$$u_r \frac{\partial u_r}{\partial r} + u_z \frac{\partial u_r}{\partial z} = -\frac{1}{\rho} \frac{\partial p}{\partial r} + \frac{\mu_{\text{eff}}}{\rho} \left(\frac{z}{r} \frac{\partial}{\partial z} \left(r \frac{\partial u_r}{\partial r} \right) + \frac{\partial}{\partial z} \left(\frac{\partial u_r}{\partial z} + \frac{\partial u_z}{\partial r} \right) - 2 \frac{u_r}{r^2} \right) ; \quad (1.3.15)$$

boundary conditions:

$$u_r = 0, \quad u_z = 0, \quad \text{on } z=0, \quad 0 < r < R_0 ; \quad (1.3.16)$$

$$u_r = 0, \quad u_z = 0, \quad \text{on } r=R_0, \quad 0 \leq z \leq H ; \quad (1.3.17)$$

$$u_z = 0, \quad \frac{\partial u_r}{\partial z} = 0, \quad \text{on } z=H, \quad 0 < r < H \tan \lambda ; \quad (1.3.18)$$

$$u_r = 0, \quad u_z = U(z) \quad \text{on } r = z \tan \lambda, \quad z_0 \leq z \leq H. \quad (1.3.19)$$

When the equations for the second derivative $\partial^2 p / \partial r \partial z$ are determined from the z- and r- components of the momentum equation and equated, p is eliminated from the governing equations resulting in the following equation holding in the flow field:

$$\frac{\partial}{\partial z} \left(u_r \frac{\partial u_r}{\partial r} + u_z \frac{\partial u_r}{\partial z} \right) - \frac{\partial}{\partial r} \left(u_r \frac{\partial u_z}{\partial r} + u_z \frac{\partial u_z}{\partial z} \right) = \frac{\mu_{\text{eff}}}{\rho} \left(\frac{z}{r} \frac{\partial}{\partial z} \left(r \frac{\partial^2 u_z}{\partial r \partial z} \right) - \frac{\partial}{\partial r} \left(\frac{1}{r} \frac{\partial}{\partial r} \left(r \left(\frac{\partial u_z}{\partial r} + \frac{\partial u_r}{\partial z} \right) \right) \right) \right) +$$

$$\frac{\partial^2}{\partial z^2} \left(\frac{\partial u_r}{\partial z} - \frac{\partial u_z}{\partial r} \right) - \frac{2}{r^2} \frac{\partial u_r}{\partial z} \quad (1.3.20)$$

The stream function defined by

$$u_r = -\frac{1}{r} \frac{\partial \psi}{\partial r}, \quad u_z = \frac{1}{r} \frac{\partial \psi}{\partial z} \quad (1.3.21)$$

is introduced, reducing the number of dependent variables to one, and the following dimensionless variables are introduced:

$$R = \frac{r}{R_0} \quad (1.3.22)$$

$$Z = \frac{z}{H} \quad (1.3.23)$$

$$\Psi = \frac{\psi}{u_0 R_0^2} \quad \text{and} \quad (1.3.24)$$

$$\gamma = \frac{R_0}{H} \quad (1.3.25)$$

Using the stream function and the dimensionless variables the governing equations become:

$$\gamma \frac{Re}{R} \left(\frac{\partial \Psi}{\partial Z} \left(\frac{\partial^3 \Psi}{\partial R^3} + \gamma^2 \frac{\partial^3 \Psi}{\partial R \partial Z} - \frac{3}{R} \frac{\partial^2 \Psi}{\partial R^2} - \frac{2\gamma^2}{R} \frac{\partial^2 \Psi}{\partial Z^2} \right) + \right. \\ \left. \frac{\partial \Psi}{\partial R} \left(\frac{3}{R^2} \frac{\partial \Psi}{\partial Z} + \frac{1}{R} \frac{\partial^2 \Psi}{\partial R \partial Z} - \frac{\partial^3 \Psi}{\partial R^2 \partial Z} - \gamma^2 \frac{\partial^3 \Psi}{\partial Z^3} \right) \right) =$$

$$\begin{aligned} & \frac{3}{R^3} \frac{\partial \bar{\Psi}}{\partial R} - \frac{3}{R} \frac{\partial^2 \bar{\Psi}}{\partial R^2} + \frac{2}{R} \frac{\partial^3 \bar{\Psi}}{\partial R^3} + \frac{2\gamma^2}{R} \frac{\partial^3 \bar{\Psi}}{\partial R \partial Z^2} - \frac{\partial^4 \bar{\Psi}}{\partial R^4} \\ & - 2\gamma^2 \frac{\partial^4 \bar{\Psi}}{\partial R^2 \partial Z^2} - \gamma^4 \frac{\partial^4 \bar{\Psi}}{\partial Z^4} ; \end{aligned} \quad (1.3.26)$$

boundary conditions:

$$\bar{\Psi} = 0, \quad \frac{\partial \bar{\Psi}}{\partial Z} = 0, \quad \text{on } Z = 0, 0 \leq R \leq 1; \quad (1.3.27)$$

$$\bar{\Psi} = 0, \quad \frac{\partial \bar{\Psi}}{\partial R} = 0, \quad \text{on } R = 1, 0 \leq Z \leq 1; \quad (1.3.28)$$

$$\bar{\Psi} = 0, \quad \frac{\partial^2 \bar{\Psi}}{\partial Z^2} = 0, \quad \text{on } Z = 1, 1 < R < \beta \quad (1.3.29)$$

$$\bar{\Psi} = 0, \quad \frac{\partial \bar{\Psi}}{\partial R} = \beta \left(\frac{3\pi}{4} k^2 \frac{Hg}{u_0^2} (Z^2 - k^2) + k^3 \right)^{\frac{1}{3}},$$

$$\text{on } R = \beta, \quad 0 < Z < 1; \quad (1.3.30)$$

$$\text{where } Re = \frac{\rho R_0 u_0}{\mu_{\text{eff}}} \quad (\text{Reynolds number}), \quad (1.3.31)$$

$$k = \frac{z_0}{H}, \quad \text{and} \quad (1.3.32)$$

$$\beta = \frac{\tan \lambda}{\gamma}. \quad (1.3.33)$$

The domain of integration is turned into a square domain $[0, 1] \times [0, 1]$ by introducing the following new

variables:

$$\eta = Z \quad ; \quad (1.3.34)$$

$$\xi = \frac{R-1}{\beta Z-1} \quad . \quad (1.3.35)$$

For brevity, the following differential operators are introduced:

$$L = L_1 \frac{\partial}{\partial \xi} + L_2 \frac{\partial^2}{\partial \xi^2} + L_3 \frac{\partial^2}{\partial \xi \partial \eta} + L_4 \frac{\partial^2}{\partial \eta^2} + L_5 \frac{\partial^3}{\partial \xi^3} +$$

$$L_6 \frac{\partial^3}{\partial \xi^2 \partial \eta} + L_7 \frac{\partial^3}{\partial \xi \partial \eta^2} \quad ; \quad (1.3.36)$$

$$M = M_1 \frac{\partial}{\partial \xi} + M_2 \frac{\partial}{\partial \eta} + M_3 \frac{\partial^2}{\partial \xi^2} + M_4 \frac{\partial^2}{\partial \xi \partial \eta} + M_5 \frac{\partial^3}{\partial \xi^3} +$$

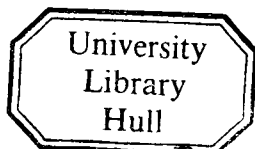
$$M_6 \frac{\partial^3}{\partial \xi^2 \partial \eta} + M_7 \frac{\partial^3}{\partial \xi \partial \eta^2} + M_8 \frac{\partial^3}{\partial \eta^3} \quad ; \quad (1.3.37)$$

$$N = N_1 \frac{\partial}{\partial \xi} + N_2 \frac{\partial^2}{\partial \xi^2} + N_3 \frac{\partial^2}{\partial \xi \partial \eta} + N_4 \frac{\partial^3}{\partial \xi^3} + N_5 \frac{\partial^3}{\partial \xi^2 \partial \eta} +$$

$$N_6 \frac{\partial^3}{\partial \xi \partial \eta^2} + N_7 \frac{\partial^4}{\partial \xi^4} + N_8 \frac{\partial^4}{\partial \xi^3 \partial \eta} + N_9 \frac{\partial^4}{\partial \xi^2 \partial \eta^2} + N_{10} \frac{\partial^4}{\partial \xi \partial \eta^3} +$$

(1.3.38)

$$N_{11} \frac{\partial^4}{\partial \eta^4} \quad ;$$



where $L_1, \dots, L_7, M_1, \dots, M_8$, and N_1, \dots, N_u are functions of ξ and η as given in appendix I. Introduce the following differential operators as well:

$$D_1 = \frac{-\beta\xi}{-1 + \beta\eta} \frac{\partial}{\partial \xi} + \frac{\partial}{\partial \eta}, \text{ and} \quad (1.3.39)$$

$$D_2 = \frac{1}{-1 + \beta\eta} \frac{\partial}{\partial \xi}. \quad (1.3.40)$$

Substituting the variables ξ and η into the governing equations results in the following set of governing equations:

$$N\Psi = \text{Re}(D_1\Psi M\Psi + D_2\Psi L\Psi) \quad ; \quad (1.3.41)$$

boundary conditions

$$\Psi = 0, \quad \frac{\partial \Psi}{\partial \eta} = 0, \quad \text{on } \eta = 0, \quad 0 \leq \xi \leq 1; \quad (1.3.42)$$

$$\Psi = 0, \quad \frac{\partial \Psi}{\partial \xi} = 0, \quad \text{on } \xi = 0, \quad 0 \leq \eta \leq 1; \quad (1.3.43)$$

$$\Psi = 0, \quad \frac{\partial^2 \Psi}{\partial \eta^2} = 0, \quad \text{on } \eta = 1, \quad 0 \leq \xi \leq 1; \quad (1.3.44)$$

$$\bar{\Psi} = 0, \quad \frac{\partial \bar{\Psi}}{\partial \xi} = \beta(\beta\eta - 1) \left(\frac{3\pi}{4} k^2 \frac{Hg}{u_0^2} (\eta^2 - k^2) + k^3 \right)^{\frac{1}{3}},$$

$$\text{on } \xi = 1, \quad 0 \leq \eta < 1. \quad (1.3.45)$$

In the special case of the tangential velocity along a generator of the cone being taken constant at u_0 then (1.3.45) is replaced by

$$\bar{\Psi} = 0, \quad \frac{\partial \bar{\Psi}}{\partial \xi} = \beta \eta (-1 + \beta \eta) \quad . \quad (1.3.46)$$

CHAPTER 4

CALCULATION OF LIQUID FLOW

The elliptic partial differential equation governing liquid flow is non-linear and of the fourth order. The equation cannot be treated by any of the very extensive methods for integrating partial differential equations and recourse is made to treat the problem by a numerical method. The numerical algorithm developed for solving the system of equations (1.3.41) - (1.3.45) of chapter 3 uses the technique of quasi-linearization. On quasi-linearizing the nonlinear governing equation, a convergent and stable procedure is achieved.

The governing equations are quasi-linearized on writing

$$\Psi = \bar{\Psi} + \Psi^* \quad , \quad (1.4.1)$$

where

$$\frac{|\Psi^*|}{|\bar{\Psi}|} \ll 1 \quad , \quad (1.4.2)$$

The governing equation in quasi-linearized form is

$$\begin{aligned} -N\Psi + \operatorname{Re}(D_1\bar{\Psi}L\Psi + L\bar{\Psi}D_1\Psi + D_2\bar{\Psi}M\Psi + \\ M\bar{\Psi}D_2\Psi) = \operatorname{Re}(D_1\bar{\Psi}M\bar{\Psi} + D_2\bar{\Psi}L\bar{\Psi}) \quad , \quad (1.4.3) \end{aligned}$$

the differential operators L, M, N, D_1 and D_2 are as defined in chapter 3 and the bar is now used to denote the previous iterate.

The boundary conditions for (1.4.3) are:

$$\Psi = 0, \quad \frac{\partial \Psi}{\partial \eta} = 0, \quad \text{on } \eta = 0, \quad 0 \leq \xi \leq 1; \quad (1.4.4)$$

$$\Psi = 0, \quad \frac{\partial \Psi}{\partial \xi} = 0, \quad \text{on } \xi = 0, \quad 0 \leq \eta \leq 1; \quad (1.4.5)$$

$$\Psi = 0, \quad \frac{\partial^2 \Psi}{\partial \eta^2} \quad \text{on } \eta = 1, \quad 0 \leq \xi \leq 1; \quad (1.4.6)$$

$$\Psi = 0, \quad \frac{\partial \Psi}{\partial \xi} = \beta(\beta\eta^{-1}) \left(\frac{3\pi}{4} R^2 \frac{Hq}{u_0^2} (\eta^2 - k^2) + R^3 \right)^{1/3},$$

$$\text{on } \xi = 1, \quad 0 \leq \eta < 1. \quad (1.4.7)$$

In the special case of the tangential velocity along a generator of the cone being taken as u_0 then (1.4.7) is replaced by

$$\Psi = 0, \quad \frac{\partial \Psi}{\partial \xi} = \beta\eta(-1 + \beta\eta) \quad \text{on } \xi = 1, \quad 0 \leq \eta < 1. \quad (1.4.8)$$

The transformation from the (R, Z) to the (ξ, η) coordinate system transformed the flow domain into a square region. The convenience of this transformation is appreciated during discretization of the flow domain as it guarantees that for any value of λ the boundary intersects

the rectangular mesh at mesh points. Discretization in the ξ and η directions by means of standard central differences in the square domain $0 \leq \xi \leq 1$, $0 \leq \eta \leq 1$ leads to mn nodes (m in the ξ -direction and n in the η -direction). Of the mn nodes $2(m+n)-4$ are boundary nodes at which Ψ is known. For convenience define the mesh lengths h and k such that

$$h = 1/(m-1), \quad \text{and} \quad (1.4.9)$$

$$k = 1/(n-1). \quad (1.4.10)$$

The k defined by equation (1.4.10) defines z_0 through equation (1.3.32) which is then given by

$$z_0 = H/(n-1) \quad (1.4.11)$$

also define the values of Ψ at the nodes by

$$\Psi_{i,j} = \Psi(ih, jk), \quad (1.4.12)$$

for $i = 0, 1, 2, \dots, m-1$, and $(1.4.13)$

$$j = 0, 1, 2, \dots, n-1.$$

Using central difference finite approximations on the

actions of linear operators gives the following:

$$\begin{aligned}
N\Psi_{i,j} &= C_1\Psi_{i-1,j-2} + C_2\Psi_{i,j-2} + C_3\Psi_{i+1,j-2} + C_4\Psi_{i-2,j-1} \\
&+ C_5\Psi_{i-1,j-1} + C_6\Psi_{i,j-1} + C_7\Psi_{i+1,j-1} + C_8\Psi_{i+2,j-1} + C_9\Psi_{i-2,j} \\
&+ C_{10}\Psi_{i-1,j} + C_{11}\Psi_{i,j} + C_{12}\Psi_{i+1,j} + C_{13}\Psi_{i+2,j} + \\
&C_{14}\Psi_{i-2,j+1} + C_{15}\Psi_{i-1,j+1} + C_{16}\Psi_{i,j+1} + C_{17}\Psi_{i+1,j+1} + \\
&C_{18}\Psi_{i+2,j+1} + C_{19}\Psi_{i-1,j+2} + C_{20}\Psi_{i,j+2} + C_{21}\Psi_{i+1,j+2} .
\end{aligned}
\tag{1.4.14}$$

$$\begin{aligned}
M\Psi_{i,j} &= D_2\Psi_{i,j-2} + D_5\Psi_{i,j-1} + D_6\Psi_{i,j-1} + D_2\Psi_{i+1,j} \\
&+ D_9\Psi_{i-2,j} + D_{10}\Psi_{i-1,j} + D_{11}\Psi_{i,j} + D_{12}\Psi_{i+1,j} + D_{13}\Psi_{i+2,j} \\
&+ D_{15}\Psi_{i-1,j+1} + D_{16}\Psi_{i,j+1} + D_{17}\Psi_{i+1,j+1} + D_{20}\Psi_{i,j+2} .
\end{aligned}
\tag{1.4.15}$$

$$\begin{aligned}
L\Psi_{i,j} &= E_5\Psi_{i-1,j-1} + E_6\Psi_{i,j-1} + E_7\Psi_{i+1,j-1} + E_9\Psi_{i-2,j} \\
&+ E_{10}\Psi_{i-1,j} + E_{11}\Psi_{i,j} + E_{12}\Psi_{i+1,j} + E_{13}\Psi_{i+2,j} + \\
&E_{15}\Psi_{i-1,j+1} + E_{16}\Psi_{i,j+1} .
\end{aligned}
\tag{1.4.16}$$

where $C_1, \dots, C_{12}, D_1, \dots, D_{20}$ and E_1, \dots, E_{20} are given in appendix 2.

The other differential operators are approximated by:

$$D_1 \Psi_{i,j} = - \frac{\Psi_{i,j-1}}{2k} + \frac{\beta \xi_i \Psi_{i-1,j}}{2h(1+\beta\eta_j)} - \frac{\beta \xi_i \Psi_{i+1,j}}{2h(1+\beta\eta_j)} + \frac{\Psi_{i,j+1}}{2k} \quad ; \quad (1.4.17a)$$

$$D_2 \Psi_{i,j} = \frac{-\Psi_{i-1,j}}{2h(1+\beta\eta_j)} + \frac{\Psi_{i+1,j}}{2h(1+\beta\eta_j)} \quad ; \quad (1.4.17b)$$

where

$$\xi_i = ih \quad , \quad \text{and} \quad (1.4.18a, b)$$

$$\eta_j = jk \quad .$$

At each node point (ij,jk) inside the flow field the following finite difference approximation is used:

$$\begin{aligned} & S_1 \Psi_{i-1,j-2} + S_2 \Psi_{i,j-2} + S_3 \Psi_{i+1,j-2} + S_4 \Psi_{i-2,j-1} + S_5 \Psi_{i-1,j-1} \\ & + S_6 \Psi_{i,j-1} + S_7 \Psi_{i+1,j-1} + S_8 \Psi_{i+2,j-1} + S_9 \Psi_{i-2,j} + S_{10} \Psi_{i-1,j} \\ & + S_{11} \Psi_{i,j} + S_{12} \Psi_{i+1,j} + S_{13} \Psi_{i+2,j} + S_{14} \Psi_{i-2,j+1} + \\ & S_{15} \Psi_{i-1,j+1} + S_{16} \Psi_{i,j+1} + S_{17} \Psi_{i+1,j+1} + S_{18} \Psi_{i+2,j+1} \\ & + S_{19} \Psi_{i-1,j+2} + S_{20} \Psi_{i,j+2} + S_{21} \Psi_{i+1,j+2} = V_{i,j} \end{aligned} \quad (1.4.19)$$

where S_1, \dots, S_{21} and $V_{i,j}$ are given in appendix 2. On the boundary points, the following approximations are applied:

$$\Psi_{i,n-1} = 0 \quad , \quad \Psi_{i,n} = \Psi_{i,n-2} \quad , \quad 0 \leq i \leq m-1 \quad ; \quad (1.4.20)$$

$$\Psi_{0,j} = 0 \quad , \quad \Psi_{-1,j} = \Psi_{1,j} \quad , \quad 0 \leq j \leq n \quad ; \quad (1.4.21)$$

$$\Psi_{i,n-1} = 0 \quad , \quad -\Psi_{i,n} = \Psi_{i,n-2} \quad , \quad 0 \leq i \leq m \quad ; \quad (1.4.22)$$

$$\Psi_{m-1,j} = 0 \quad , \quad \Psi_{m,j} = \Psi_{m-2,j} +$$

$$\beta(-1 + \beta\eta_j) \left(\frac{3\pi}{4} k^2 \frac{Hq}{\omega_0^2} (\eta_j^2 - k^2) + k^3 \right)^{\frac{1}{3}} \quad ,$$

$$1 \leq j \leq n \quad . \quad (1.4.23)$$

In the case of constant velocity along a cone generator (1.4.23) is replaced by

$$\Psi_{m-1,j} = 0 \quad , \quad \Psi_{m,j} = \Psi_{m-2,j} + \beta\eta_j(-1 + \beta\eta_j) \quad . \quad (1.4.24)$$

Writing the equations obtained by using equation (1.4.19) and boundary conditions (1.4.20) - (1.4.23) in matrix form after removing prescribed boundary values to the right hand side of each equation when each line of the grid, from bottom to top, is successively traversed in order from left to right results in the matrix equation for $\Psi_{i,j}$ of the form

$$WX = Y \quad , \quad (1.4.25)$$

where X is a column vector the transpose of which is given by

$$X^T = \left(\Psi_{1,1}, \Psi_{2,1}, \dots, \Psi_{m-2,j}, \Psi_{1,2}, \Psi_{2,2}, \dots, \Psi_{m-2,2}, \right. \\ \left. \Psi_{2,3}, \dots, \Psi_{m-2,3}, \dots, \Psi_{m-2,1}, \dots, \Psi_{m-2,n-2} \right) \quad (1.4.26)$$

and W is a banded matrix with $2m-3$ bands on either side of the main diagonal the structure of which is displayed in figure 3.

The method used to solve the equation (1.4.25) is based on Choleski's method of triangular^A decomposition. The matrix is factorized into a product of a lower-triangular matrix with ones on the main diagonal and an upper-triangular matrix. This mode of factorization has the advantage that the two factor matrix can be displayed in one matrix with the interpretation that the strictly lower triangle of the matrix represents the lower-triangular matrix, without the main diagonal, and the upper triangle represents the upper-triangular matrix. The algorithm for factorization proceeds sequentially by row starting with the first row in both the lower and upper-triangular matrices. Hence the process of factorization of the matrix W is carried out using a representation displaying only one matrix.

Let the matrix W be factored as follows:

$$W = W_L W_u \quad (1.4.27)$$

where W_L is a lower-triangular triangular matrix with ones on the main diagonal and W_u is an upper-triangular matrix. Using forward substitution the equation

$$W_L Z = Y \quad , \quad (1.4.28)$$

is solved and then the equation

$$W_u X = Z \quad (1.4.29)$$

is solved by back substitution to give the required solution X .

The matrix W is $(m-2) \times (n-2)$ which requires large storage on the computer for any reasonable values of m and n . The method of solution used for solving (1.4.25) requires only a single two-dimensional array to be declared in a computer program making a saving in computer storage over standard methods that use matrix inversion techniques. A further reduction in computer storage is achieved by realizing that the locations in the matrix, above and below the band, which contain zeros will contain zeros even after triangular decomposition. The further reduction is effected by declaring storage for the elements in the band only.

An iterative scheme is used to evaluate the unknowns $\bar{\Psi}_{i,j}$ ($i = 1, \dots, m-2$, $j = 1, 2, \dots, n-2$). The solution being acceptable when the difference between the new solution and the previous iterate (the barred quantities) is less than some prescribed tolerance. In the first instance the special case of the tangential velocity along the cone generator being taken as u_0 is considered. The linear Stokes problem obtained by putting $Re = 0$ in (1.4.3) is solved initially. Next, a small Reynolds number is set and a solution found for it using the solution to the linear Stokes problem as the previous iterate. The converged solution at this Reynolds number is used as the initial estimate for the iteration of the next larger Reynolds number. In this fashion there is created a number of initial estimates for any Reynolds number required. In the second instance the converged solution for a given Reynolds number in the special case is used as the initial estimate for the case when the velocity on a cone generator is not constant (for the same Reynolds number).

CHAPTER 5

NUMERICAL SOLUTIONS

In this chapter a selection of numerical solutions of the stream function will be presented. Of particular interest to the steel making industry is the change in circulation pattern as the Reynolds number increases. The number of figures necessary to convey the full extent of the numerical information available would be excessive and so only a selection of figures is displayed. Both the cases when the liquid velocity along a cone generator is taken as constant and when there is variable velocity along a cone generator are included. Data for bath agitation in steel making are not available, instead operating data for a cylindrical tank containing water which is being agitated by an air-bubble stream are taken from Grevet, Szekeley and El-Kaddah (1981).

The governing equations were solved by the method described in chapter 4 using a program developed for the purpose on an ICL 2900. The finite difference grid possessed 21 intervals in each direction. For $Re \leq 5000$ the belt driven model, with constant velocity along the generator, is employed. For $Re \geq 5000$ the solutions using both boundary conditions (1.4.23) and (1.4.24) are given. The program is first employed to obtain a solution for the linear Stokes problem when $Re = 0$. The stream function so obtained is then used as $\bar{\Psi}$ in the calculation for $Re = 10$.

At the end of each solution of (1.4.25) $\bar{\Psi}$ is updated. Convergence of Ψ to five significant figures was achieved in 3 iterations. In this fashion the Reynolds number was increased to $Re = 500$ taking $\Delta Re = 10$, 3 iterations per case being required. From $Re = 500 - 1000$ with $\Delta Re = 50$ each case converged in 5 or 6 iterations; from $Re = 1000 - 4000$ with $\Delta Re = 200$ each case converged in 4 iterations; finally from $Re = 4000 - 10,000$ with $\Delta Re = 500$ convergence was achieved in 2 iterations. Solutions for the case of variable velocity along a cone generator were obtained using the converged solution Ψ for the case of constant velocity as the initial Ψ . Convergence for both $Re = 5000$ and $Re = 10,000$ for variable velocity was achieved in 2 iterations.

Figures 4 - 9 give the streamlines for $Re = 0, 1, 10, 100, 500$ and $1,000$ respectively; in these cases the liquid velocity along the cone generators is taken as constant. For $Re = 5,000$ figures 10(a) and 10(b) display the streamlines for (a) constant velocity along cone generator, and (b) variable velocity along cone generator as predicted by the drift flux model; in figure 10(c) the graph of u_z / u_0 against z as used in the computation of 10(b) is given. The results for $Re = 10,000$ are displayed in figures 11(a), for constant velocity along a cone generator, 11(b) for variable velocity along a cone generator as predicted by the drift-flux model, and 11(c), the graph of u_z / u_0 as used in the computation of 11(c). The system parameters used for the water model are given in table 1.

The development of the flow with Reynolds number is shown in figures 4 - 9. The centre of the primary vortex is moving towards the top left hand part of the vessel as the Reynolds number increases through 0, 1, 10, 100, 500 and 1,000. For $Re = 5,000$ the streamlines in models (a) and (b) are almost identical except in the upper left hand part of the flow field where the circulation in (a) is more vigorous than that in (b) as is expected. The results for $Re = 10,000$ show that the final (boundary-layer) structure of the recirculating flow at large Reynolds number is now established. The stagnant region at the lower left hand portion of the vessel is now quite extensive and stirring is confined to the liquid/two-phase interface and near the upper free surface of the vessel. The main features of the flow for $Re = 10,000$ are well predicted using the simple model (a).

SECTION 2

Two phase problems

CHAPTER 1

INTRODUCTION

A large number of technically important problems involve solutions of the equations describing diffusion of heat, mass or some other scalar quantity subject to boundaries that are neither fixed in space nor known a priori. Problems of this type arise in crystal growth from melts and solutions, purification of materials, freezing of water and melting of ice, solidification of molten metals and many other problems arising in such diverse fields as refrigeration of food, metallurgy, thermalplastics, electrochemistry, latent heat of fusion energy storage and geophysics.

A feature of these problems is the existence of a moving interface between the phases at which thermal energy in the form of latent heat is liberated. The mathematical condition at this interface is non-linear and, in consequence, generalized analytical solutions are not readily available. Neumann's solution (see Carslaw and Jaeger (1959)) to the problem of freezing in a semi-infinite region which was presented in the 1860's remains one of the few exact solutions available. In more recent years considerable progress has been made in analytical work in the case of one-dimensional solidification problems. Small time solutions in the case of inward solidification of a sphere initially at fusion temperature were first studied by

Poots (1962). Pedroso and Domoto (1973) were the first to give perturbation expansion solutions for large Stefan number ($\beta = L/c_p \Delta T$) and noting that it is a singular perturbation problem, new perturbation expansion solutions in the case of one-dimensional solidification problems have been given by Riley, Smith and Poots (1974), Stewartson and Waechter (1976) and Soward (1980). The surveys of Bankoff (see Drew, Hoopes and Vermuelen (1964)), Muehlbauer and Sunderland (1965), Ockendon and Hodgkins (1975), Furzeland (1980) and Jiji and Weinbaum (1978) cite many works in the case of one-dimensional solidification problems.

In the case of two-dimensional solidification problems solutions have been obtained using approximate methods. Heat balance integral methods were used by Poots (1962) to discuss the inward solidification of a square prism of fluid initially at fusion temperature. Rathjen and Jiji (1971) studied the solidification of a quarter space initially at fusion temperature by extending Lightfoot's method (see Carslaw and Jaeger (1959)) to two-dimensions. Sikarskie and Boley (1965) have studied the solidification of a semi-finite insulated strip using a method that involves solving integro-differential equations analytically. Schulze, Beckett, Howarth and Poots (1982) have given small time analytical solutions to two-dimensional inward solidification of a half space initially at fusion temperature using methods based on the immobilization technique first used by Landau (1950) in a

one-dimensional investigation. The technique is to introduce a single coordinate transformation in which the moving interface is immobilized by scaling the independent distance co-ordinate by the instantaneous interface location. This transformation shifts the non-linearity from the interface boundary conditions to the governing differential equations.

Other methods have been used to study the two-dimensional moving interface problems. Springer and Olson (1962), Tien and Wilkes (1970) and Lazaridis (1970) have used fixed grid methods. Movement of the interface through a fixed finite differential grid is traced in fixed grid methods and finite difference explicit schemes are used for all solidified nodes. Crowley (1978) used a heat enthalpy method in studying multi-dimensional moving interface problems. In the heat enthalpy methods the interface is not considered in the finite difference scheme instead when the cell temperature straddles the fusion temperature the cell temperature is set equal to fusion temperature when the thermal energy input to it is equal to latent heat liberated.

Boley and Yogoda (1971) have obtained solutions for small time for three-dimensional solidification of a half space by a general surface heat input, such that change of phase starts at a point of the surface, and then spreads simultaneously both toward the interior of the body and along the surface. The small time solutions are obtained by means of a technique (referred to by Boley and Yogoda as the

embedding technique) in which the actual body is embedded in a fictitious one with known shape, a fictitious heat input is then applied over the fictitious boundary and the temperature deduced as a function of the fictitious heat input and boundaries resulting in a set of integro-differential equations which are solved analytically. In general, three-dimensional moving interface problems are studied using numerical methods as no exact analytical solutions of such problems exist for all time. Small time solutions such as that of Boley and Yogoda are useful in producing reliable computer algorithms for the numerical solution. One of the purposes of this section of the thesis is to present analytical solutions to a certain class of three-dimensional solidification problems. The solutions augment the small time two-dimensional solutions of Schulze et al (1982) and those of Boley and Yogoda (1971). Note that the embedding technique of Boley et al is difficult to apply and gives rather limited results for practical reasons.

Most of the work on moving interface problems is presented using rectangular^a Cartesian co-ordinates. Hence solutions given by those studies preclude their application to several practical geometries like, pipes and cylindrical containers, that involve cylindrical co-ordinates having an extra radial term in the original heat conduction equation. At present there are no general exact solutions to the moving interface problem in cylindrical coordinates. In

1943 London and Seban obtained approximate analytic solutions to the problems of inward solidification of cylinders and spheres (see Talwar and Dipare (1978)) initially at fusion temperature and later the exposed surface maintained at a temperature equal to freezing temperature. Jiji and Weinbaum (1978) found small time analytical solutions to the moving interface problem (also called the Stefan problem) of inward solidification in an annulus which is initially not at fusion temperature with outside boundary maintained at constant temperature below fusion while the inside boundary is either insulated or maintained at a constant temperature above the fusion level. Jiji and Weinbaum (1978) used the immobilization technique and the resulting equations solved by the method of singular perturbation. Analytical solutions of London and Seban (1948) and of Jiji and Weinbaum (1978) are desirable in attempting numerical solutions to Stefan problems in cylindrical polar co-ordinate. This section of the thesis also presents perturbation solutions for melting of a solid in an annulus which is initially at a sub-freezing temperature with outside boundary maintained at the sub-freezing temperature while the inner boundary emits heat at a constant rate. The solutions augment these of London and Seban (1948) and Jiji and Weinbaum (1978).

In chapter 2 the following three-dimensional two phase problems are investigated:

- (i) At time $t = 0$, the half space $z > 0$ is filled

with liquid at fusion temperature and for $t > 0$ the wall is maintained at a lower temperature given by

$T_0 - (T_F - T_0)g(x/a, y/a)$, where x and y are measured along the wall and a is a representative length. Here $g(x/a, y/a) > -1$ for $|x| < \infty$ and $T_0 < T_F$.

(ii) At time $t = 0$ the half space $z > 0$ is filled with liquid at fusion temperature T_F and for $t > 0$ there is Newton cooling at the wall $z = 0$ into the environment. The wall heat transfer coefficient is taken as varying with co-ordinates x and y measured along the wall. Following the method developed by Schulze et al (1982) small time solutions are obtained. For specific examples results on the location of the solidification surface are presented graphically for various times.

In chapter 3 perturbation solutions of the Stefan problem are given for the case of an infinite cylinder existing initially at a sub-freezing temperature. For all times greater than zero the outside boundary is maintained at the constant sub-freezing temperature while at the inner boundary there is constant heat flux. This problem is considered in two parts, namely, the warm-up period before fusion temperature is attained by any part of the solid and the period after this. An analytic solution is obtained for the warm-up period and perturbation solutions found for the Stefan problem. For a specific example results for values of the first two perturbation functions of the location of

the interface are given graphically.

The work in chapter 2 is now available in Kunda and Poots (1984), see appendix 3.

CHAPTER 2

ANALYTICAL SOLUTIONS TO A CLASS OF THREE-DIMENSIONAL SOLIDIFICATION PROBLEMS.

The purpose of this chapter is to present analytical solutions to a class of three-dimensional solidification problems. The analytical solutions presented are generalizations of the classical one-dimensional problem of Neumann (see Carslaw and Jaeger (1959)), for the half space domain. They augment the small time two-dimensional solutions of Schulze, Beckett, Howarth and Poots (1982) and the earlier work of Boley and Yogoda (1971).

The condition controlling the motion of the liquid/solid interface at the change of phase is non-linear. This shall be derived prior to the formulation of the three-dimensional problems.

In a Cartesian frame of reference (x, y, z) , at time $t = 0$, the half space $z > 0$ is filled with liquid at fusion temperature x and y are measured along the wall $z = 0$. Let the equation of the interface be

$$C(x, y, z, t) = 0 \quad (2.2.1)$$

when \underline{v} is the normal velocity of the interface the latent heat liberated as the interface moves escapes by conduction across the solidified region and the heat balance at the interface results in the equation

$$K \nabla T \cdot \frac{\nabla C}{|\nabla C|} = \rho L \underline{v} \cdot \frac{\nabla C}{|\nabla C|} \quad , \quad (2.2.2)$$

where L is the latent heat of fusion, ρ is the density of both the solid and liquid phases, K is the thermal conductivity and T is the temperature of the solid. To find \underline{v} let $P(\underline{x}_0)$ be a point on the interface $C(\underline{x}, t_0) = 0$ and Q a point on the interface $C(\underline{x}, t_0 + \Delta t) = 0$ at which the normal through P intersects it. Then

$$\underline{v} = \lim_{\Delta t \rightarrow 0} \frac{\overrightarrow{PQ}}{\Delta t} \quad . \quad (2.2.3)$$

Let the vector equation of the normal at P be

$$\underline{r} = \underline{r}_0 + \lambda \nabla C \quad , \quad (2.2.4)$$

where ∇C is evaluated at P . Then at the point Q , λ satisfies $C(\underline{r}_0 + \lambda \nabla C, t_0 + \Delta t) = 0$. A linear approximation to this equation, taking λ and Δt small and that $C(\underline{x}, t_0) = 0$ is the following:

$$\nabla C \cdot (\lambda \nabla C) + \frac{\partial C}{\partial t} \Delta t = 0 \quad . \quad (2.2.5)$$

therefore

$$\lambda = - \frac{\partial C}{\partial t} \frac{\Delta t}{|\nabla C|^2} \quad , \quad (2.2.6)$$

and

$$\vec{p} \vec{q} = \underline{r} - \underline{r}_0 \approx -\frac{\partial C}{\partial t} \frac{\Delta t}{|\nabla C|^2} \nabla C \quad (2.2.7)$$

Hence

$$\underline{v} \approx -\frac{\partial C}{\partial t} \frac{\nabla C}{|\nabla C|^2} \quad (2.2.8)$$

Substituting for \underline{v} the expression in (2.2.8) in (2.2.2) gives the equation

$$K \nabla T \cdot \nabla C = -\rho L \frac{\partial C}{\partial t} \quad (2.2.9)$$

Using the same reference frame as above, assume that at $t = 0$, the half space $z > 0$ is filled with liquid at fusion temperature T_F and for $t > 0$ the situations involve either a variation of wall temperature with x and y or non-uniform Newton cooling into the environment $z < 0$. Then the governing equations for the solidified phase are the following:

$$K \nabla^2 T = \rho c_p \frac{\partial T}{\partial t} \quad ; \quad (2.2.10)$$

$$T = T_F \quad , \quad K \nabla T \cdot \nabla C = -\rho L \frac{\partial C}{\partial t} \quad ,$$

$$\text{on } C(x, y, z, t) = z - \tilde{\chi}(x, y, t) = 0 \quad ; \quad (2.2.11)$$

either

$$T = T_0 - (T_F - T_0) g(x/a, y/a) \quad , \quad (2.2.12)$$

or

$$K \frac{\partial T}{\partial z} = h(x/a, y/a)(T - T_0) \quad \text{on } z = 0 \quad ; \quad (2.2.13)$$

together with the initial conditions

$$T = T_F \quad \text{for } t = 0, \quad z > 0 \quad ; \quad (2.2.14)$$

and
$$\tilde{\chi}(x/a, y/a, 0) = 0 \quad . \quad (2.2.15)$$

In the condition (2.2.12) it is assumed that $-1 < g\left(\frac{x}{a}, \frac{y}{a}\right) < \infty$ for $x^2 + y^2 < \infty$. The wall heat transfer coefficient is also bounded with $h\left(\frac{x}{a}, \frac{y}{a}\right) \geq 0$ for $x^2 + y^2 < \infty$ and the temperature T_0 ($< T_F$) is used to denote a reference condition of the environment. a is a representative length. In the above L is the latent heat of fusion. ρ the density of both the liquid and the solid, K the thermal conductivity, C_p the specific heat and T the temperature of the solid.

With use of the dimensionless variables

$$X = \frac{x}{a}, \quad Y = \frac{y}{a}, \quad Z = \frac{z}{a}$$

$$\tau = \frac{kt}{a^2}, \quad \theta = \frac{T - T_0}{T_F - T_0}, \quad \chi = \frac{\tilde{\chi}}{a} \quad . \quad (2.2.16)$$

where $k = \frac{K}{\rho c_p}$ is the thermal diffusivity, the governing

equations (2.2.10) - (2.2.15) transform to the following:

$$\frac{\partial^2 \theta}{\partial x^2} + \frac{\partial^2 \theta}{\partial y^2} + \frac{\partial^2 \theta}{\partial z^2} = \frac{\partial \theta}{\partial \tau} \quad ; (2.2.17)$$

$$\theta(x, y, z, \tau) = 1, \nabla \theta \cdot \nabla C = -\beta \frac{\partial C}{\partial \tau} \text{ on } Z = \chi(x, y, \tau) \quad ; (2.2.18)$$

Either

$$\theta = -g(x, y) \quad \text{on } Z = 0 \quad ; (2.2.19)$$

or

$$\frac{\partial \theta}{\partial Z} = Bi(x, y) \theta \quad \text{on } Z = 0 \quad ; (2.2.20)$$

together with the initial conditions

$$\theta(x, y, z, 0) = 1 \quad ; (2.2.21)$$

$$\chi(x, y, 0) = 0 \quad . (2.2.22)$$

Here the Stefan number is defined as $\beta = \frac{L}{c_p(T_F - T_0)}$

and the wall Biot number $Bi = \frac{ah(x, y)}{K}$

Small time solutions for variable wall temperature

The case considered now is with the wall temperature specified by (2.2.19). Employing the interface immobilization technique, introduce the new variables

$$\phi = x \quad , \quad \psi = y \quad , \quad \eta = \frac{z}{\chi(x, y, \tau)}$$

In the solid phase the dimensionless temperature satisfies

$$\begin{aligned} \nabla_1^2 \theta + \frac{1}{\chi} \frac{\partial^2 \theta}{\partial \eta^2} + \frac{2\eta}{\chi^2} |\nabla_1 \chi|^2 \frac{\partial \theta}{\partial \eta} - \frac{\eta}{\chi} \nabla_1^2 \chi \frac{\partial \theta}{\partial \eta} + \frac{2\eta}{\chi} \nabla_1 \chi \cdot \nabla_1 \left(\frac{\partial \theta}{\partial \eta} \right) \\ + \eta^2 |\nabla_1 \chi|^2 \frac{\partial^2 \theta}{\partial \eta^2} = -\frac{\eta}{\chi} \frac{\partial \chi}{\partial \tau} \frac{\partial \theta}{\partial \eta} + \frac{\partial \theta}{\partial \tau} \end{aligned} \quad (2.2.23)$$

subject to the conditions

$$\theta = 1 \quad , \quad (1 + |\nabla_1 \chi|^2) \frac{\partial \theta}{\partial \eta} = \beta \chi \frac{\partial \chi}{\partial \tau} \quad \text{on} \quad \eta = 1 \quad , \quad (2.2.24)$$

$$\theta = -q(\underline{x}) \quad \text{on} \quad \eta = 0 \quad , \quad (2.2.25)$$

$$\theta(\underline{x}, \eta, 0) = 1 \quad , \quad \chi(\underline{x}, 0) = 0 \quad , \quad (2.2.26)$$

In the above $\nabla_1 = \text{grad} = \left(\frac{\partial}{\partial \phi}, \frac{\partial}{\partial \psi} \right)$,

$$\nabla_1^2 = \frac{\partial^2}{\partial \phi^2} + \frac{\partial^2}{\partial \psi^2} \quad \text{and} \quad \underline{x} = (\phi, \psi)$$

For small time assume regular perturbation expansions:

$$\theta(x, \eta, \tau) = \theta_0(x, \eta) + \theta_1(x, \eta)\tau + O(\tau^2), \quad (2.2.27)$$

$$\text{and } \chi(x, \tau) = 2\tau^{\frac{1}{2}}\chi_0(x) + 2\tau^{\frac{3}{2}}\chi_1(x) + O(\tau^{\frac{5}{2}}), \quad (2.2.28)$$

substitution of (2.2.27) and (2.2.28) into (2.2.23) - (2.2.26) gives

$$\begin{aligned} & 2\chi_0^2\eta \frac{\partial \theta_0}{\partial \eta} + \frac{\partial^2 \theta_0}{\partial \eta^2} + \tau \left(4\chi_0^2 \nabla_1^2 \theta_0 + 8\chi_0\eta \nabla_1 \chi_0 \cdot \nabla_1 \left(\frac{\partial \theta_0}{\partial \eta} \right) + \right. \\ & \left. 4\eta^2 |\nabla_1 \chi_0|^2 \frac{\partial^2 \theta_0}{\partial \eta^2} + 4\eta (2|\nabla_1 \chi_0|^2 - \chi_0 \nabla_1^2 \chi_0 + 2\chi_0 \chi_1) \frac{\partial \theta_0}{\partial \eta} + \right. \\ & \left. \frac{\partial^2 \theta_1}{\partial \eta^2} + 2\chi_0^2\eta \frac{\partial \theta_1}{\partial \eta} \right) = 4\chi_0^2 \theta_1 \tau + O(\tau^2), \quad (2.2.29) \end{aligned}$$

$$\theta_0(x, 1) + \tau \theta_1(x, 1) + O(\tau^2) = 1, \quad (2.2.29a)$$

$$\begin{aligned} & \frac{\partial \theta_0}{\partial \eta} + \tau \left(\frac{\partial \theta_1}{\partial \eta} + 4|\nabla_1 \chi_0|^2 \frac{\partial \theta_0}{\partial \eta} \right) \\ & = 2\beta\chi_0^2 + \tau 8\beta\chi_0\chi_1 + O(\tau^2). \quad (2.2.30) \end{aligned}$$

$$\theta_0(x, 0) + \tau \theta_1(x, 0) + O(\tau^2) = -g(x) \quad , \quad (2.2.31)$$

$$\theta_0(x, \eta) + \tau \theta_1(x, \eta) + O(\tau^2) = 1 \quad , \quad (2.2.32)$$

The zeroth and first order perturbation terms will now be solved.

Zeroth order

Equating the coefficients of the zeroth power of τ in (2.2.25) gives

$$2\chi_0^2 \eta \frac{\partial \theta_0}{\partial \eta} + \frac{\partial^2 \theta_0}{\partial \eta^2} = 0 \quad , \quad (2.2.33)$$

which after integration yields

$$\theta_0(x) = A(x) \frac{2 \operatorname{erf}[\chi_0 \eta]}{\chi_0 \sqrt{\pi}} + B(x) \quad , \quad (2.2.34)$$

where $A(x)$ and $B(x)$ are arbitrary functions. Using boundary conditions (2.2.31) and (2.2.32) determines $A(x)$ and $B(x)$ uniquely to give

$$\theta_0(x) = \frac{(1+g) \operatorname{erf}[\chi_0 \eta]}{\operatorname{erf}[\chi_0]} - g(x) \quad (2.2.35)$$

Equating the coefficients of the zeroth power of τ in

(2.2.29) gives

$$\frac{\partial \theta_0}{\partial \eta} = 2 \chi_0^2 \beta \quad . \quad (2.2.36)$$

Differentiating (2.2.35) and substituting in (2.2.36) gives the following transcendental equation for $\chi_0(\lambda)$

$$\chi_0 \exp(\chi_0^2) \operatorname{erf}[\chi_0] = \frac{1+g}{\beta \sqrt{\pi}} \quad (2.2.37)$$

First order

Equating the coefficient of τ in (2.2.29) we have

$$\begin{aligned} \frac{\partial^2 \theta_0}{\partial \eta^2} + 2 \chi_0^2 \eta \frac{\partial \theta_0}{\partial \eta} - 4 \chi_0^2 \theta_0 &= -4 \chi_0^2 \nabla_1^2 \theta_0 \\ -8 \chi_0 \eta \nabla_1 \chi_0 \cdot \nabla_1 \left(\frac{\partial \theta_0}{\partial \eta} \right) - 4 \eta^2 |\nabla_1 \chi_0|^2 \frac{\partial^2 \theta_0}{\partial \eta^2} \\ - 4 \eta (2 |\nabla_1 \chi_0|^2 - \chi_0 \nabla_1^2 \chi_0 + 2 \chi_0 \chi_1) \frac{\partial \theta_0}{\partial \eta} & \quad . \quad (2.2.38) \\ \nabla_1 &= \left(\frac{\partial}{\partial \phi}, \frac{\partial}{\partial \psi} \right) \quad . \end{aligned}$$

Using (2.2.35) for the value of θ_0 we obtain

$$\frac{\partial \theta_0}{\partial \phi} = \frac{\operatorname{erf}[\chi_0 \eta]}{\operatorname{erf}[\chi_0]} \left(\frac{\partial g}{\partial \phi} - \frac{2(1+g)}{\sqrt{\pi} \exp(\chi_0^2) \operatorname{erf}[\chi_0]} \frac{\partial \chi_0}{\partial \phi} + \right.$$

$$\frac{2(1+g)\eta \exp(-\chi_0^2 \eta^2)}{\sqrt{\pi} \operatorname{erf}[\chi_0]} \frac{\partial \chi_0}{\partial \phi} - \frac{\partial g}{\partial \phi} \quad (2.2.39)$$

$$\frac{\partial \theta_0}{\partial \psi} = \frac{\operatorname{erf}[\chi_0 \eta]}{\operatorname{erf}[\chi_0]} \frac{\partial g}{\partial \psi} - \frac{\partial g}{\partial \psi} \quad (2.2.40)$$

$$\frac{\partial \theta_0}{\partial \eta} = 2\beta \chi_0 \exp(-\chi_0^2 (\eta^2 - 1)) \quad (2.2.40a)$$

$$\begin{aligned} \frac{\partial^2 \theta_0}{\partial \phi^2} = & -\frac{\partial^2 g}{\partial \phi^2} + \frac{\operatorname{erf}[\chi_0 \eta]}{\operatorname{erf}[\chi_0]} \left(\frac{\partial^2 g}{\partial \phi^2} - 2\beta \left(\frac{\partial \chi_0}{\partial \phi} \right)^2 - 2\beta \chi_0 \frac{\partial^2 \chi_0}{\partial \phi^2} \right. \\ & \left. - \frac{2\beta \chi_0}{1+g} \frac{\partial \chi_0}{\partial \phi} \frac{\partial g}{\partial \phi} + \frac{4\beta^2 \chi_0^2}{1+g} \left(\frac{\partial \chi_0}{\partial \phi} \right)^2 \right) + \\ & \eta \exp(-\chi_0^2 (\eta^2 - 1)) \left(\frac{4\beta \chi_0}{1+g} \frac{\partial \chi_0}{\partial \phi} \frac{\partial g}{\partial \phi} - \frac{8\beta^2 \chi_0^2}{1+g} \left(\frac{\partial \chi_0}{\partial \phi} \right)^2 + 2\beta \chi_0 \frac{\partial^2 \chi_0}{\partial \phi^2} \right) \\ & - 4\beta \chi_0^2 \eta^3 \exp(-\chi_0^2 (\eta^2 - 1)) \left(\frac{\partial \chi_0}{\partial \phi} \right)^2. \quad (2.2.41) \end{aligned}$$

$$\begin{aligned} \frac{\partial^2 \theta_0}{\partial \psi^2} = & -\frac{\partial^2 g}{\partial \psi^2} + \frac{\operatorname{erf}[\chi_0 \eta]}{\operatorname{erf}[\chi_0]} \left(\frac{\partial^2 g}{\partial \psi^2} - 2\beta \left(\frac{\partial \chi_0}{\partial \psi} \right)^2 - 2\beta \chi_0 \frac{\partial^2 \chi_0}{\partial \psi^2} \right. \\ & \left. - \frac{2\beta \chi_0}{1+g} \frac{\partial \chi_0}{\partial \psi} \frac{\partial g}{\partial \psi} + \frac{4\beta^2 \chi_0^2}{1+g} \left(\frac{\partial \chi_0}{\partial \psi} \right)^2 \right) + \end{aligned}$$

$$\eta \exp(-\chi_0^2(\eta^2-1)) \left(\frac{4\beta\chi_0}{1+g} \frac{\partial\chi_0}{\partial\psi} \frac{\partial g}{\partial\psi} - \frac{8\beta^2\chi_0^2}{1+g} \left(\frac{\partial\chi_0}{\partial\psi} \right)^2 + \right. \\ \left. 2\beta\chi_0 \frac{\partial^2\chi_0}{\partial\psi^2} \right) - 4\beta\chi_0^3\eta^3 \exp(-\chi_0^2(\eta^2-1)) \left(\frac{\partial\chi_0}{\partial\psi} \right)^2 \\ \frac{\partial^2\theta_0}{\partial\eta^2} = -4\beta\chi_0^2\eta \exp(-\chi_0^2(\eta^2-1)) \quad (2.3.42)$$

$$\frac{\partial^2\theta_0}{\partial\phi\partial\eta} = \exp(-\chi_0^2(\eta^2-1)) \left(\frac{2\beta\chi_0^2}{1+g} \left(\frac{\partial g}{\partial\phi} - 2\beta\chi_0 \frac{\partial\chi_0}{\partial\phi} \right) + 2\beta\chi_0 \frac{\partial\chi_0}{\partial\phi} - 4\beta\chi_0^3\eta^2 \frac{\partial\chi_0}{\partial\phi} \right) \quad (2.3.42a) \\ (2.2.43)$$

$$\frac{\partial^2\theta_0}{\partial\psi\partial\eta} = \exp(-\chi_0^2(\eta^2-1)) \left(\frac{2\beta\chi_0^2}{1+g} \left(\frac{\partial g}{\partial\psi} - 2\beta\chi_0 \frac{\partial\chi_0}{\partial\psi} \right) + 2\beta\chi_0 \frac{\partial\chi_0}{\partial\psi} - 4\beta\chi_0^3\eta^2 \frac{\partial\chi_0}{\partial\psi} \right) \quad (2.2.44)$$

Substituting the expressions (2.2.39) - (2.2.44) in (2.2.38)

we obtain the equation of first order terms as

$$\frac{\partial^2\theta_1}{\partial\eta^2} + 2\chi_0^2\eta \frac{\partial\theta_1}{\partial\eta} - 4\chi_0^2\theta_1 = 4\chi_0^2 \left(\nabla_1^2 g + \right.$$

$$\left. P(x)\text{erf}[\chi_0\eta] - 2Q(x)\eta \exp(-\chi_0^2\eta^2) \right) .$$

(2.2.45)

where

$$P(x) = \frac{1}{\text{erf}[\chi_0]} \left(\frac{2\beta\chi_0}{1+g} \nabla_1 \chi_0 \frac{\partial g}{\partial \phi} - \nabla_1^2 g + \right.$$

$$\left. 2\beta \left(1 - \frac{2\beta\chi_0^2}{1+g} \right) |\nabla_1 \chi_0|^2 + 2\beta\chi_0 \nabla_1^2 \chi_0 \right) , \text{ and } (2.2.46)$$

$$Q(x) = \frac{2\chi_1(1+g)}{\text{erf}[\chi_0]\sqrt{\pi}} . \quad (2.2.47)$$

The homogeneous first order equation is

$$\frac{\partial^2 \theta_1}{\partial \eta^2} + 2\chi_0^2 \eta \frac{\partial \theta_1}{\partial \eta} - 4\chi_0^2 \theta_1 = 0 . \quad (2.2.48)$$

This has solutions

$$\theta_1 = 1 - 2\chi_0^2 \eta^2 , \text{ and } (2.2.49)$$

$$\theta_1 = i^2 \text{erfc}[\eta\chi_0] . \quad (2.2.50)$$

The particular integral is

$$\theta_1 = Q\eta \exp(-\chi_0^2 \eta^2) - \text{Perf}[\chi_0 \eta] - \nabla_1^2 g . \quad (2.2.51)$$

Thus the general solution is

$$\theta_1 = A(1 + 2\chi_0^2 \eta^2) + B i^2 \text{erfc}[\chi_0 \eta] - \nabla_1^2 g - \text{Perf}[\chi_0 \eta] + Q\eta \exp(-\chi_0^2 \eta^2) . \quad (2.2.52)$$

Applying the boundary conditions (2.2.31) and (2.2.32) gives the first order function as

$$\begin{aligned}
 \theta_1 = & 2\chi_0^2 \eta^2 \nabla_1^2 g + \frac{1+2\chi_0^2 \eta^2 - 4i^2 \operatorname{erfc}[\chi_0 \eta]}{(1+g)(1+2\gamma\chi_0^2) \operatorname{erf}[\chi_0]} (4\chi_0^2(\gamma-1)|\nabla_1 g|^2 \\
 & - (1+g)(1+2\gamma\chi_0^2)^2 (2\chi_0 \chi_1 (\gamma-1)(1+g)(1+2\gamma\chi_0^2) + \\
 & (1+4\chi_0^2 + 4\gamma\chi_0^4) \nabla_1^2 g) + \frac{2\chi_1(1+g)\eta \exp(-\chi_0^2 \eta^2)}{\sqrt{\pi} \operatorname{erf}[\chi_0]} \\
 & - \frac{\operatorname{erf}[\chi_0 \eta] (4\chi_0^2(\gamma-1)|\nabla_1 g|^2 - (1+g)(1+2\gamma\chi_0^2)(1+2\chi_0^2) \nabla_1^2 g)}{(1+g)(1+2\gamma\chi_0^2)^3 \operatorname{erf}[\chi_0]} .
 \end{aligned}
 \tag{2.2.53}$$

Equating the coefficients of τ in (2.2.30) gives

$$4|\nabla_1 \chi_0|^2 \frac{\partial \theta_0}{\partial \eta} + \frac{\partial \theta_1}{\partial \eta} - 8\beta \chi_0 \chi_1 = 0 \tag{2.2.54}$$

Using the found expressions for θ_0 and θ_1 , the interface perturbation function $\chi_1(x)$ is determined from

$$\begin{aligned}
 \chi_1 \beta (3 + 2\chi_0^2 + 10\gamma\chi_0^2 + 4\gamma\chi_0^4) = & \\
 & \frac{\chi_0 (1 - 2\chi_0^2 - \gamma - 4\gamma\chi_0^4 + 2\gamma^2\chi_0^2 + 4\gamma^2\chi_0^4) \nabla_1^2 g}{1 + 2\gamma\chi_0^2} + \\
 & \frac{4\chi_0^3 (\gamma-1) (2 + \gamma + 6\gamma\chi_0^2 - 2\gamma^2\chi_0^2 + 4\gamma^2\chi_0^4) |\nabla_1 g|^2}{(1+g)(1+2\gamma\chi_0^2)^3} .
 \end{aligned}
 \tag{2.2.55}$$

For any Stefan number β , the expansions (2.2.27) and (2.2.28) are valid for small time and all X and also for large $|X|$ and all time.

Small time solutions for variable Newton cooling

The case considered next is with the condition specified by (2.2.19). This case is examined using the method of Megerlin (1968). Firstly introduce the variable

$$\tilde{\tau} = \frac{\tau}{\beta} \quad (2.2.56)$$

The governing equations transform to the following:

$$\frac{\partial^2 \theta}{\partial X^2} + \frac{\partial^2 \theta}{\partial Y^2} + \frac{\partial^2 \theta}{\partial Z^2} = \frac{1}{\beta} \frac{\partial \theta}{\partial \tilde{\tau}} \quad ; (2.2.57)$$

$$\theta(X, Y, Z, \tilde{\tau}) = 1, \quad \nabla \theta \cdot \nabla C = \partial C / \partial \tilde{\tau},$$

on $C = Z - \chi(X, Y, \tilde{\tau}) = 0 \quad (2.2.58)$

$$\frac{\partial \theta}{\partial Z} = Bi(X, Y) \theta \quad \text{on} \quad Z = 0 \quad (2.2.59)$$

$$(2.2.60)$$

$$\theta(X, Y, Z, 0) = 1, \quad \chi(X, Y, 0) = 0.$$

Following the method of Megerlin (1968) the temperature field is written as

$$\theta(x, y, z, \tilde{z}) = 1 + \sum_{n=1}^{\infty} G_n(x, y, \tilde{z}) (z - \chi(x, y, \tilde{z})) \quad (2.2.61)$$

and the following subsidiary expansions are used:

$$\chi(x, y, \tilde{z}) = \sum_{r=1}^{\infty} \tilde{z}^r \chi_r(x, y) \quad (2.2.62)$$

$$G_n(x, y, \tilde{z}) = \sum_{r=0}^{\infty} \tilde{z}^r b_{n,r}(x, y) \quad (2.2.63)$$

Substitute (2.2.61) into (2.2.57) - (2.2.59) and equate coefficients of the same power of $(z - \chi)$ to obtain

$$2G_2(1 + |\nabla_1 \chi|^2) - 2\nabla_1 G_1 \cdot \nabla_1 \chi - G_1 \nabla_1^2 \chi - \frac{G_1}{\beta} \frac{\partial \chi}{\partial \tilde{z}} = 0 \quad (2.2.64)$$

$$6G_3(1 + |\nabla_1 \chi|^2) - 4\nabla_1 G_2 \cdot \nabla_1 \chi + \nabla_1^2 G_1 - 2G_2 \nabla_1^2 \chi + \frac{1}{\beta} \left(2G_2 \frac{\partial \chi}{\partial \tilde{z}} - \frac{\partial G_1}{\partial \tilde{z}} \right) = 0 \quad (2.2.65)$$

$$G_1(1 + |\nabla_1 \chi|^2) = \frac{\partial \chi}{\partial \tilde{z}} \quad (2.2.66)$$

$$G_1 - 2G_2 \chi + 3G_3 \chi^2 = Bi(1 - G_1 \chi + G_2 \chi^2) \quad (2.2.67)$$

In the above $\underline{x} = (x, y)$, $\nabla_1 = \left(\frac{\partial}{\partial x}, \frac{\partial}{\partial y} \right)$ and $\nabla_1^2 = \frac{\partial^2}{\partial x^2} + \frac{\partial^2}{\partial y^2}$

Substitute (2.2.62) and (2.2.63) into (2.2.64) - (2.2.67) and equate coefficients of the same powers of \tilde{z} to obtain

$$b_{1,0} \chi_1 + 2\beta b_{2,0} = 0 \quad ; \quad (2.2.68)$$

$$b_{1,1} \chi_1 + 2\beta b_{2,1} + 2b_{1,0} \chi_2 - \beta b_{1,0} \nabla_1^2 \chi_1$$

$$- 2\beta \nabla_1 b_{1,0} \cdot \nabla_1 \chi_1 = 0 ; \quad (2.2.69)$$

$$b_{1,2} \chi_1 + 2\beta b_{2,2} + 2b_{1,1} \chi_2 + 3b_{1,0} \chi_3$$

$$- \beta b_{1,0} \nabla_1^2 \chi_2 - \beta b_{1,1} \nabla_1^2 \chi_1 - 2\beta \nabla_1 b_{1,0} \cdot \nabla_1 \chi_2$$

$$- 2\beta \nabla_1 b_{1,1} \cdot \nabla_1 \chi_1 = 0 ; \quad (2.2.70)$$

$$6\beta b_{3,0} - b_{1,1} + \beta \nabla_1^2 b_{1,0} + 2b_{2,0} \chi_1 = 0 \quad (2.2.71)$$

$$6\beta b_{3,1} + 4b_{2,0} \chi_2 + 2b_{2,1} \chi_1 - 2b_{1,2} + \beta \nabla_1^2 b_{1,1}$$

$$- 2\beta \nabla_1^2 \chi_1 - 4\nabla_1 b_{2,0} \cdot \nabla_1 \chi_1 = 0 ; \quad (2.2.72)$$

$$6\beta b_{3,2} + 6b_{2,1} \chi_3 + 4b_{2,1} \chi_2 + 2b_{2,2} \chi_1 - 3b_{1,3}$$

$$+ \beta \nabla_1^2 b_{1,2} - 2\beta b_{2,0} \nabla_1^2 \chi_2 - 2\beta b_{2,1} \nabla_1^2 \chi_1 + 6\beta b_{3,0} |\nabla_1 \chi_1|^2$$

$$- 4\beta \nabla_1 b_{2,0} \cdot \nabla_1 \chi_2 - 4\nabla_1 b_{2,1} \cdot \nabla_1 \chi_1 = 0 ; \quad (2.2.73)$$

$$b_{1,0} - \chi_1 = 0 ; \quad (2.2.74)$$

$$b_{1,1} - 2\chi_2 = 0 ; \quad (2.2.75)$$

$$b_{1,2} + b_{1,0} |\nabla_1 \chi_1|^2 - 3\chi_3 = 0 ; \quad (2.2.76)$$

$$b_{1,0} - Bi = 0 ; \quad (2.2.77)$$

$$b_{1,1} - 2b_{2,0} \chi_1 + Bi b_{1,0} \chi_1 = 0 ; \quad (2.2.78)$$

$$b_{1,2} - 2b_{2,0} \chi_2 - 2b_{2,1} \chi_1 + 3b_{3,0} \chi_1^2 + \\ Bi (b_{1,0} \chi_2 + b_{1,1} \chi_1 - b_{2,0} \chi_1^2) = 0 . \quad (2.2.79)$$

The equations (2.2.68) - (2.2.79) are solved to give

$$\chi_1 = Bi , \quad (2.2.80)$$

$$\chi_2 = -\frac{(Bi)^3}{2} \left(1 + \frac{1}{\beta} \right) , \quad (2.2.81)$$

$$\chi_3 = Bi |\nabla_1 Bi|^2 + \frac{(Bi)^2}{2} \nabla_1^2 Bi + \frac{(Bi)^5}{2} \left(1 + \frac{8}{3\beta} + \frac{5}{3\beta^2} \right) \\ (2.2.82)$$

yielding the solution

$$\chi(\Delta, \tau) = Bi \frac{\tau}{\beta} - \frac{(Bi)^3}{2} \left(1 + \frac{1}{\beta} \right) \left(\frac{\tau}{\beta} \right)^2 + \\ Bi \left(|\nabla_1 Bi|^2 + \frac{Bi}{2} \nabla_1^2 Bi + \frac{(Bi)^4}{2} \left(1 + \frac{8}{3\beta} + \frac{5}{3\beta^2} \right) \left(\frac{\tau}{\beta} \right)^3 \right) . \quad (2.2.83)$$

The expansion (2.2.61) is valid for large β only and thus so is (2.2.83).

Numerical solutions

Interface locations have been calculated from the two-term expansion (2.2.28) when the wall temperature is given in the form

$$g(\phi, \psi) = 0.3 \left((1 + \tanh \phi)(1 + \tanh \psi) - 1 \right) \quad (2.2.84)$$

for $\beta = 0.3$. The two-dimensional equivalent of (2.2.28) is shown in Schulze et al (1982) to yield results in ^{excellent} agreement with numerical finite difference solutions up to dimensionless time $\tau = 0.5$. It follows that expansion (2.2.28) may also be valid in this region of time. Note that for the solidification of steel ingots $\tau = 0.5$ is roughly the complete time of ingot solidification (see Schulze et al (1982)). Consequently the results given here are highly relevant to three-dimensional effects in ingot solidification.

At dimensionless time $\tau = 0.2, 0.4$ and 0.6 the values of χ have been calculated using step lengths of $\Delta\phi = 0.4$ and $\Delta\psi = 0.4$ and the resulting forms of the interface are displayed in figures 12, 13 and 14 respectively.

In figure 15 the interface location at $\tau = 0.6$ for $\beta = 0.3$ and the bounded wall temperature given by

$$Bi(x, y) = 0.9 \sin x \sin y, \quad |x| \leq 2\pi, |y| \leq 2\pi. \quad (2.2.85)$$

is displayed.

Conclusion

The analytical and numerical results presented in this chapter can be utilized in producing and checking computer algorithms that may be developed for the numerical solution of three-dimensional moving interface problems. Moreover, the vector form of the analytical results can be utilized in other applications where the geometry is expressed in curvilinear co-ordinates.

CHAPTER 3

PERTURBATION SOLUTIONS FOR MELTING OF A CYLINDRICAL ANNULUS WITH CONSTANT HEAT FLUX ON INNER SURFACE.

This chapter presents perturbation solutions for melting of a cylindrical annulus of a solid which is initially at a sub-freezing temperature^a, with outside boundary maintained at the sub-freezing temperature and constant heat flux on inner surface. This problem has arisen in the following way. When snow sticks to an overhead transmission line, an ice spike grows out into the wind, see Poots and Rodgers (1976), Poots and Baker (1984) and Rodgers and Poots (1986). As the ice spike grows it rotates due to its weight and this rotation is opposed by the torsional couple of the cable. Figure 16 shows how the ice spike may grow in an overnight snow environment, going from fig 16 (a), to (b) to (c) and finally in fig 16 (d). It is during the growth period that the ice spike is aerodynamically unstable. Low frequency high amplitude oscillations are set up, called galloping, and can put the grid at risk. How can the transmission line be rid of this ice? Can the ice be prevented from forming? One possibility is to try and melt the ice by joule heating. This chapter deals with such a model for de-icing.

The problem for melting of a cylindrical annulus with constant heat flux on the inner surface reduces to a two-dimensional problem because the temperature on the

surface of any cylinder co-axial with the outer boundary (and thus also the inner boundary) of the cylindrical annulus is uniform. The solutions presented here add to the analytical solution of the Stefan problem in cylindrical co-ordinates of London and Seban (1943) (see Talwar and Dilpare (1978)) and those of Jiji and Weinbaum (1978).

There are two parts to the problem considered; the first being the determination of the temperature profile in the annulus at the time when the solid on the inner boundary attains fusion temperature. This will be referred to as the warm-up problem. The second part will be the Stefan problem itself.

The geometry of the system considered in the warm up problem is shown in figure 17. The solid in the annulus is initially at temperature T_i which is below the freezing temperature T_f . At time $t = 0$ heat suddenly starts to emit from the inner boundary at $r = a$ while the boundary at $r = b$ is maintained at the sub-freezing temperature T_i .

Using the cylindrical polar co-ordinates, the equations governing the temperature distribution are the following:

$$\frac{1}{r} \frac{\partial}{\partial r} \left(r \frac{\partial T}{\partial r} \right) = \frac{1}{k} \frac{\partial T}{\partial t}, \quad a < r < b \quad ; \quad (2.3.1)$$

$$k \frac{\partial T}{\partial r} = q, \quad r = a \quad (2.3.2)$$

$$T = T_I \quad , \quad r = b \quad ; \quad (2.3.3)$$

$$T = T_I \quad , \quad t = 0 \quad ; \quad (2.3.4)$$

where K is thermal conductivity, k is diffusivity of heat given by $k = K / \rho c_p$, where ρ is density and c_p is the specific heat.

To non-dimensionalize the governing equations, the following dimensionless quantities are defined:

$$\theta = - \frac{T_F - T}{T_F - T_I} \quad ; \quad (2.3.5)$$

$$\xi = \frac{b - r}{b - a} \quad ; \quad (2.3.6)$$

$$\tau = \frac{kt}{b^2} \quad ; \quad (2.3.7)$$

$$\Omega = \frac{(b-a)Q}{K(T_F - T_I)} \quad ; \quad (2.3.8)$$

$$\text{and } \beta = \frac{a}{b} \quad . \quad (2.3.9)$$

Using the dimensionless quantities above the governing equations for the warm-up problem become:

$$\frac{1}{1 - (1-\beta)\xi} \frac{\partial}{\partial \xi} \left((1 - (1-\beta)\xi) \frac{\partial \theta}{\partial \xi} \right) = (1-\beta)^2 \frac{\partial \theta}{\partial \tau} \quad , \quad 0 < \xi < 1 \quad ; \quad (2.3.10)$$

$$\frac{\partial \theta}{\partial \xi}(1, \tau) = -\Omega \quad ; \quad (2.3.11)$$

$$\theta(0, \tau) = -1 \quad ; \quad (2.3.12)$$

and the initial condition is

$$\theta(\xi, 0) = -1 \quad . \quad (2.3.13)$$

The geometry of the system considered for the moving interface problem is shown in figure 18.

The solid in the annular space has initial temperature distribution that which is attained in the heat-up problem when the inner boundary attains fusion temperature. At time $t = 0$ heat starts to emit from the inner boundary at $r = a$ while the outer boundary at $r = b$ is maintained at the sub-freezing temperature T_1 .

It is assumed that the fluid properties in each phase are constant and that the volumetric expansions or contractions due to phase change are non-existent. Free convection currents in the liquid phase are also ignored. Using the cylindrical polar co-ordinates, the equations governing the temperature distribution in both the liquid and solid phases, based on the given assumptions, are the following:

$$\frac{1}{r} \frac{\partial}{\partial r} \left(r \frac{\partial T_L}{\partial r} \right) = \frac{1}{k_L} \frac{\partial T_L}{\partial t} \quad , \quad a < r < r_i \quad ; \quad (2.3.14)$$

$$\frac{1}{r} \frac{\partial}{\partial r} \left(r \frac{\partial T_S}{\partial r} \right) = \frac{1}{k_S} \frac{\partial T_S}{\partial t} \quad , \quad r_i < r < b \quad ; \quad (2.3.15)$$

$$K_L \frac{\partial T_L}{\partial r} = Q, \quad r = a \quad ; \quad (2.3.16)$$

$$T_s = T_I, \quad r = b \quad ; \quad (2.3.17)$$

$$T_s = T(r_i, t_M), \quad t = 0 \quad ; \quad (2.3.18)$$

$$r_i = a, \quad t = 0 \quad ; \quad (2.3.19)$$

where $r_i(t)$ is the position of the solid-liquid interface and subscripts **s** and **L** denote solid and liquid phases respectively. The energy balance at the interface gives

$$K_s \frac{\partial T_s}{\partial r} - K_L \frac{\partial T_L}{\partial r} = L_s \rho_s \frac{dr_i}{dt}, \quad r = r_i(t), \quad (2.3.20)$$

where L is the latent heat of fusion.

To non-dimensionalize the governing equations and immobilize the interface, the following dimensionless quantities are defined:

$$\psi = - \frac{T_F - T_s}{T_F - T_I} \quad ; \quad (2.3.21)$$

$$\xi = \frac{b - r}{b - r_i} \quad ; \quad (2.3.22)$$

$$\phi = - \frac{K_L}{K_s} \frac{T_F - T_L}{T_F - T_I} \quad ; \quad (2.3.23)$$

$$\eta = \frac{r_i - r}{r_i - a} \quad ; \quad (2.3.24)$$

$$\epsilon = \frac{c_{ps} (T_F - T_I)}{L_s} \quad ; \quad (2.3.25)$$

$$\tau = \epsilon \frac{k_s t}{b^2} \quad ; \quad (2.3.26)$$

$$\sigma = \frac{r_i - a}{a} \quad ; \quad (2.3.27)$$

$$\Omega = \frac{a Q}{k_s (T_F - T_I)} \quad ; \quad (2.3.28)$$

$$k = \frac{k_s}{k_h} \quad ; \quad (2.3.29)$$

$$\beta = a/b \quad \text{and} \quad \alpha = 1/\beta \quad (2.3.30a, b)$$

Using the dimensionless quantities above the governing equations for the Stefan problem become:

$$\frac{1}{1+\sigma(1-\eta)} \frac{\partial}{\partial \eta} \left((1+\sigma(1-\eta)) \frac{\partial \phi}{\partial \eta} \right) = \epsilon k \beta^2 \sigma \left(\sigma \frac{\partial \phi}{\partial \tau} + (1-\eta) \frac{d\sigma}{d\tau} \frac{\partial \phi}{\partial \eta} \right), \quad 0 < \eta < 1 \quad ; \quad (2.3.31)$$

$$\frac{1}{\alpha + (1-\alpha+\sigma)\xi} \frac{\partial}{\partial \xi} \left((\alpha + (1-\alpha+\sigma)\xi) \frac{\partial \psi}{\partial \xi} \right) = \epsilon \beta^2 (1-\alpha+\sigma) \times$$

$$\left((1-\alpha+\sigma) \frac{\partial \psi}{\partial \tau} - \xi \frac{d\sigma}{d\tau} \frac{\partial \psi}{\partial \xi} \right), \quad 0 < \xi < 1 \quad ; \quad (2.3.32)$$

$$(2.3.33)$$

$$\phi(0, \tau) = 0 \quad ;$$

$$\frac{\partial \phi(1, \tau)}{\partial \eta} = -\sigma \Omega \quad ; \quad (2.3.34)$$

$$\psi(0, \tau) = -1 \quad ; \quad (2.3.35)$$

$$\psi(1, \tau) = 0 \quad ; \quad (2.3.36)$$

$$\psi(\xi, 0) = \theta(\xi, \tau_M) \quad ; \quad (2.3.37)$$

$$\sigma(0) = 0 \quad ; \quad (2.3.38)$$

$$\sigma \frac{\partial \psi(1, \tau)}{\partial \xi} + (1 - \alpha + \sigma) \frac{\partial \phi(0, \tau)}{\partial \eta} = \beta^2 \sigma (1 - \alpha + \sigma) \frac{d\sigma}{d\tau} \quad (2.3.39)$$

Solution of the warm-up problem

Using the method of variation of parameter, the system of equations (2.3.10) - (2.3.13) governing the warm-up problem are assumed to have a solution of the form

$$\theta(\xi, \tau) = u(\xi) + v(\xi, \tau) \quad . \quad (2.3.40)$$

u satisfies the equations

$$\frac{d}{d\xi} \left((1 - (1 - \beta)\xi) \frac{du}{d\xi} \right) = 0 \quad , \quad 0 < \xi < 1 \quad ; \quad (2.3.41)$$

$$\frac{du(1)}{d\xi} = -\Omega \quad ; \quad (2.3.42)$$

$$u(0) = -1 \quad . \quad (2.3.43)$$

V satisfies the set of equations

$$\frac{1}{1-(1-\beta)\xi} \frac{\partial}{\partial \xi} \left((1-(1-\beta)\xi) \frac{\partial V}{\partial \xi} \right) - (1-\beta)^2 \frac{\partial V}{\partial \tau} = 0 \quad ; \quad (2.3.44)$$

$$\frac{\partial V}{\partial \xi}(1, \tau) = 0 \quad ; \quad (2.3.45)$$

$$V(0, \tau) = 0 \quad ; \quad (2.3.46)$$

$$V(\xi, 0) = -1 - u(\xi) \quad . \quad (2.3.47)$$

The set of equations (2.3.41)-(2.3.43) is easily solved to give

$$u(\xi) = \frac{-2\beta}{1-\beta} \ln(1-(1-\beta)\xi) - 1 \quad . \quad (2.3.48)$$

To solve for $V(\xi, \tau)$ introduce the following transformations:

$$X = 1 - (1-\beta)\xi \quad ; \quad \text{and} \quad (2.3.49)$$

$$\underline{\tau} = \tau \quad (2.3.50)$$

The equations for $V(X, \underline{\tau})$ are

$$\frac{1}{X} \frac{\partial}{\partial X} \left(X \frac{\partial V}{\partial X} \right) - \frac{\partial V}{\partial \underline{\tau}} = 0 \quad , \quad \beta < X < 1 \quad ; \quad (2.3.51)$$

$$\frac{\partial v}{\partial x}(\beta, \tau) = 0 \quad ; \quad (2.3.52)$$

$$v(1, \tau) = 0 \quad ; \quad (2.3.53)$$

$$v(x, 0) = -\frac{\beta \Omega \ln x}{1 - \beta} \quad . \quad (2.3.54)$$

Assume v has the following form

$$v(x, \tau) = y(x) e^{-\alpha^2 \tau} \quad , \quad (2.3.55)$$

then the equation for y is

$$\frac{1}{x} \frac{d}{dx} \left(x \frac{dy}{dx} \right) + \alpha^2 y = 0 \quad . \quad (2.3.56)$$

This is Bessel's equation of order zero. The range of x does not include the origin, hence Bessel functions of the second kind are not excluded. Consider the function

$$u_0(\alpha x) = J_0(\alpha x) Y_0(\alpha) - Y_0(\alpha x) J_0(\alpha) \quad , \quad (2.3.57)$$

where J_0 and Y_0 are Bessel functions of order zero of the first and second kind respectively. This function vanishes when $x = 1$ and $\frac{du_0}{dx} = 0$ at $x = \beta$ provided that α is

a root of the equation

$$Y_1(\alpha \beta) J_0(\alpha) - J_1(\alpha \beta) Y_0(\alpha) = 0 \quad , \quad (2.3.58)$$

where J_1 and Y_1 are Bessel functions of the first order of

the first and second kind respectively. Assume the initial temperature can be expanded in the series

$$\frac{-\beta \ln x}{1-\beta} = \sum_{n=1}^{\infty} A_n U_0(\alpha_n x) \quad , \quad (2.3.59)$$

where $\alpha_1, \alpha_2, \dots$ are zeros of $\frac{dU_0(\beta)}{dx}$ in ascending

order. To find the constants A_n , establish the orthogonality of the functions $y_n(x) = U_0(\alpha_n x)$.

Let m and n be integers, then y_n and y_m satisfy (2.3.56) with α replaced by α_n and α_m respectively. The resulting equations are combined to yield the equation

$$(\alpha_m^2 - \alpha_n^2) x y_n y_m = y_n \frac{d}{dx} \left(x \frac{dy_m}{dx} \right) - y_m \frac{d}{dx} \left(x \frac{dy_n}{dx} \right). \quad (2.3.60)$$

Therefore if $m \neq n$ (so that $\alpha_m \neq \alpha_n$),

$$\int_1^{\beta} x y_n y_m dx = \frac{1}{\alpha_m^2 - \alpha_n^2} \int_1^{\beta} \frac{d}{dx} \left(x \left(y_n \frac{dy_m}{dx} - y_m \frac{dy_n}{dx} \right) \right) dx = 0 \quad (2.3.61)$$

For the case $m = n$

$$\frac{1}{x} \frac{d}{dx} \left(x \frac{dy_n}{dx} \right) + \alpha_n^2 y_n = 0 \quad (2.3.62)$$

gives rise to the equation

$$\frac{d}{dx} \left(\left(x \frac{dy_n}{dx} \right)^2 \right) + 2\alpha_n^2 x y_n \frac{dy_n}{dx} = 0 \quad (2.3.63)$$

Integrating (2.3.63) once gives

$$\alpha_n^2 \int_1^\beta x^2 \frac{dy_n^2}{dx} dx = \left(\frac{dy_n(1)}{dx} \right)^2 \quad (2.3.64)$$

On integrating the left-hand side by parts

$$2\alpha_n^2 \int_1^\beta x y_n^2 dx = \alpha_n^2 \beta^2 y_n^2(\beta) - \left(\frac{dy_n(1)}{dx} \right)^2 \quad (2.3.65)$$

Finally obtain

$$\int_1^\beta x y_n^2 dx = \frac{1}{2} \left(\beta^2 U_0(\alpha_n \beta) - (J_1(\alpha_n) Y_0(\alpha_n) - Y_1(\alpha_n) J_0(\alpha_n)) \right) \quad (2.3.66)$$

To find the constants A_n also required is the integral

$$\int_1^\beta x \ln x U_0(\alpha_n x) dx .$$

Using the heat conduction equation, obtain

$$\ln x \frac{d}{dx} \left(x \frac{dU_0}{dx} \right) + \alpha_n^2 x \ln x U_0 = 0 \quad (2.3.67)$$

Integrating (2.3.67) once gives

$$\int_1^\beta x \ln x U_0(\alpha_n x) dx = \frac{U_0(\alpha_n \beta)}{\alpha_n^2} \quad (2.3.68)$$

Hence, using the orthogonality of the functions $U_0(\alpha_n x)$ the constants A_n of (2.3.59) are given by

$$A_n = \frac{-2\beta - 2 U_0(\alpha_n \beta)}{\alpha_n^2 (1-\beta) (\beta^2 U_0^2(\alpha_n \beta) - (J_1(\alpha_n) Y_0(\alpha_n) - Y_1(\alpha_n) J_0(\alpha_n))^2)} \quad (2.3.69)$$

Thus the solution $U(x, \tau)$ is given by

$$U(x, \tau) = \sum_{n=1}^{\infty} A_n U_0(\alpha_n x) \exp(-\alpha_n^2 \tau) \quad (2.3.70)$$

The solution to the system of equations (2.3.10) - (2.3.13) is thus given by

$$\theta(\xi, \tau) = -1 + \frac{-2\beta \ln(1-(1-\beta)\xi)}{1-\beta} + \sum_{n=1}^{\infty} A_n U_0(\alpha_n (1-(1-\beta)\xi)) \times \exp(-\alpha_n^2 \tau) \quad (2.3.71)$$

Solution of the Stefan problem

The method of singular perturbations is used to solve the equations (2.3.31) - (2.3.39). The perturbation

parameter ϵ used is the same as that used by Jiji and Weinbaum (1978) which is given by (2.3.25). In this method two separate solutions, the outer solution and the inner solution, emerge in the form of infinite series in powers of ϵ which when matched term by term in a region of overlapping validity provide a solution valid for all time.

Outer solution.

To obtain the outer solution, the following perturbation expansions are assumed:

$$\phi(\eta, \tau) = \sum_{n=0}^{\infty} \epsilon^n \phi_n(\eta, \tau) \quad ; \quad (2.3.72)$$

$$\psi(\xi, \tau) = \sum_{n=0}^{\infty} \epsilon^n \psi_n(\xi, \tau) \quad ; \quad (2.3.73)$$

$$\sigma(\tau) = \sum_{n=0}^{\infty} \epsilon^n \sigma_n(\tau) \quad . \quad (2.3.74)$$

On substituting (2.3.72) - (2.3.74) into (2.3.31) - (2.3.39) and equating coefficients of the same power of ϵ , zeroth and first order terms are determined.

Equating the coefficients of the zeroth power of ϵ gives equations for ϕ_0 , ψ_0 and σ_0 . The equations governing ϕ_0 are the following

$$\frac{\partial}{\partial \eta} \left((1 + \sigma_0(1 - \eta)) \frac{\partial \phi_0}{\partial \eta} \right) = 0 \quad ; \quad (2.3.75)$$

$$\phi_0(0, \tau) = 0 \quad ; \quad (2.3.76)$$

$$\frac{\partial \phi_0}{\partial \eta}(1, \tau) = -\Omega \sigma_0 \quad . \quad (2.3.77)$$

are the following:

$$\begin{aligned} & \frac{1}{1+\sigma_0(1-\eta)} \frac{\partial}{\partial \eta} \left((1+\sigma_0(1-\eta)) \frac{\partial \phi_1}{\partial \eta} - \frac{\Omega \sigma_0 \sigma_1 (1-\eta)}{1+\sigma_0(1-\eta)} \right) \\ &= k \beta^2 \sigma_0 \left(\frac{-\Omega \sigma_0}{1+\sigma_0} \right) \frac{d\sigma_0}{d\tau} \quad ; \end{aligned} \quad (2.3.84)$$

$$\phi_1(0, \tau) = 0 \quad ; \quad (2.3.85)$$

$$\frac{\partial \phi_1(1, \tau)}{\partial \eta} = -\Omega \sigma_1 \quad . \quad (2.3.86)$$

The equation (2.3.84) - (2.3.86) give $\phi_1(\eta, \tau)$ as

$$\begin{aligned} \phi_1(\eta, \tau) &= \frac{k \Omega \beta^2}{2(1+\sigma_0)} \frac{d\sigma_0}{d\tau} \left(\ln(1+\sigma_0(1-\eta)) - \ln(1+\sigma_0) + \right. \\ & \left. \frac{(1+\sigma_0)^2 - (1+\sigma_0(1-\eta))^2}{2} \right) + \frac{\Omega \sigma_1}{\sigma_0} \left(\frac{1}{1+\sigma_0} - \frac{1}{1+\sigma_0(1-\eta)} \right) . \end{aligned} \quad (2.3.87)$$

The equations governing ψ_1 are the following:

$$\begin{aligned} & \frac{1}{\alpha + (1-\alpha + \sigma_0)\xi} \frac{\partial}{\partial \xi} \left((\alpha + (1-\alpha + \sigma_0)\xi) \frac{\partial \psi_1}{\partial \xi} + \frac{\sigma_1(1-\alpha + \sigma_0)\xi}{(\alpha + (1-\alpha + \sigma_0)\xi)(\ln(1+\sigma_0) - \ln \alpha)} \right) \\ &= \frac{d\sigma_0}{d\tau} \frac{\beta^2 (1-\alpha + \sigma_0)^2 (\ln \alpha - \ln(\alpha + (1-\alpha + \sigma_0)\xi))}{(1+\sigma_0)(\ln(1+\sigma_0) - \ln \alpha)} \quad ; \end{aligned} \quad (2.3.88)$$

$$\psi_1(0, \tau) = 0 \quad ; \quad (2.3.89)$$

The equations (2.3.75) - (2.3.77) have solution

$$\phi_0(\eta, \tau) = \Omega (\ln(1 + \sigma_0(1 - \eta)) - \ln(1 + \sigma_0)) . \quad (2.3.78)$$

The equations governing ψ_0 are the following

$$\frac{\partial}{\partial \xi} \left((\alpha + (1 - \alpha + \sigma_0) \frac{\xi}{\xi}) \frac{\partial \psi_0}{\partial \xi} \right) = 0 \quad ; \quad (2.3.79)$$

$$\psi_0(0, \tau) = -1 \quad ; \quad (2.3.80)$$

$$\psi_0(1, \tau) = 0 \quad ; \quad (2.3.81)$$

The equations (2.3.79) - (2.3.81) yield

$$\psi_0(\xi, \tau) = \frac{\ln(\alpha + (1 - \alpha + \sigma_0) \frac{\xi}{\xi}) - \ln(1 + \sigma_0)}{\ln(1 + \sigma_0) - \ln \alpha} \quad (2.3.82)$$

Using the solutions (2.3.78) and (2.3.82) in the zeroth order interface equation gives the following equation for σ_0 :

$$\beta^2 \frac{d\sigma_0}{d\tau} = \frac{1}{1 + \sigma_0} \left(\frac{1}{\ln(1 + \sigma_0) - \ln \alpha} - \Omega \right) . \quad (2.3.83)$$

Equations for ϕ_1 , ψ_1 and σ_1 are obtained by equating coefficients of ϵ . The equations governing ϕ_1

$$\psi_1(1, \tau) = 0 \quad ; \quad (2.3.90)$$

The equations (2.3.88) - (2.3.90) are solved to give

$$\begin{aligned} \psi_1(\xi, \tau) = & \frac{1}{1-\alpha+\sigma_0} \left(\left(1 - \frac{(1-\alpha+\sigma_0)(\ln(\alpha+(1-\alpha+\sigma_0)\xi) - \ln\alpha)}{(1+\sigma_0)(\ln(1+\sigma_0) - \ln\alpha)} \right. \right. \\ & \left. \left. - \frac{\alpha}{\alpha+(1-\alpha+\sigma_0)\xi} \right) \frac{\sigma_1}{\ln(1+\sigma_0) - \ln\alpha} - \frac{\beta^2(1-\alpha+\sigma_0)}{4(1+\sigma_0)(\ln(1+\sigma_0) - \ln\alpha)^2} \times \right. \\ & \left. \frac{d\sigma_0}{d\tau} \left(\alpha^2 + (\alpha+(1-\alpha+\sigma_0)\xi)^2 (\ln(\alpha+(1-\alpha+\sigma_0)\xi) - \ln\alpha - 1) + \right. \right. \\ & \left. \left. \frac{((1+\sigma_0)^2(1 - \ln(1+\sigma_0) + \ln\alpha) - \alpha^2)(\ln(\alpha+(1-\alpha+\sigma_0)\xi) - \ln\alpha)}{\ln(1+\sigma_0) - \ln\alpha} \right) \right) \end{aligned} \quad (2.3.91)$$

Substituting (2.3.78), (2.3.81), (2.3.87) and (2.3.91) in the first order interface equation gives the following equation for $\sigma_1(\tau)$:

$$\begin{aligned} \beta^2 \frac{d}{d\tau} (\sigma_1 \sigma_0 (1-\alpha+\sigma_0)) = & \sigma_1 \left(\frac{\sigma_0}{(1+\sigma_0) \ln(\frac{1+\sigma_0}{\alpha})} \left(\alpha - \frac{\sigma_0}{(1+\sigma_0) \ln(\frac{1+\sigma_0}{\alpha})} \right) \right. \\ & + \frac{1-\alpha+\sigma_0}{(1+\sigma_0) \ln(\frac{1+\sigma_0}{\alpha})} - \frac{2}{1+\sigma_0} \left(\sigma_0 + \frac{1-\alpha+\sigma_0}{1+\sigma_0} \right) + \frac{R \alpha \beta^2 \sigma_0^2 (2+\sigma_0)(1-\alpha+\sigma_0)}{2(1+\sigma_0)^2} \\ & \left. - \frac{d\sigma_0}{d\tau} \frac{\beta^2 \sigma_0 (1-\alpha+\sigma_0)}{4(1+\sigma_0) \left(\ln(\frac{1+\sigma_0}{\alpha}) \right)^2} \left(\frac{(1+\sigma_0)^2 - \alpha^2}{(1+\sigma_0) \ln(\frac{1+\sigma_0}{\alpha})} + 2(1+\sigma_0) \left(\ln(\frac{1+\sigma_0}{\alpha}) - 1 \right) \right) \right) \end{aligned} \quad (2.3.92)$$

To obtain the inner solution a magnified time variable is introduced into (2.3.31) - (2.3.39)

$$\hat{\tau} = \frac{\tau}{\epsilon} \quad . \quad (2.3.93)$$

The dependent inner variables are denoted by:

$$\hat{\phi}(\eta, \hat{\tau}) = \phi(\eta, \tau) \quad ; \quad (2.3.94)$$

$$\hat{\psi}(\xi, \hat{\tau}) = \psi(\xi, \tau) \quad ; \text{ and} \quad (2.3.95)$$

$$\hat{\sigma}(\hat{\tau}) = \sigma(\tau) \quad (2.3.96)$$

and the following perturbation expansions are assumed:

$$\hat{\phi}(\eta, \hat{\tau}) = \sum_{n=0}^{\infty} \epsilon^n \hat{\phi}_n(\eta, \hat{\tau}) \quad ; \quad (2.3.97)$$

$$\hat{\psi}(\xi, \hat{\tau}) = \sum_{n=0}^{\infty} \epsilon^n \hat{\psi}_n(\xi, \hat{\tau}) \quad ; \quad (2.3.98)$$

$$\hat{\sigma}(\hat{\tau}) = \sum_{n=0}^{\infty} \epsilon^n \hat{\sigma}_n(\hat{\tau}) \quad ; \quad (2.3.99)$$

On substituting (2.3.97) - (2.3.99) into the resulting governing equations of the inner variables and equating coefficients of the same powers of ϵ , zeroth and first order terms are determined.

The equations governing $\hat{\sigma}_0(\hat{\tau})$ are:

$$\frac{d\hat{\sigma}_0}{d\tau} = 0 \quad ; \quad \hat{\sigma}_0(0) = 0 \quad (2.3.100a, b)$$

These yield

$$\hat{\sigma}_0(\hat{\tau}) = 0 . \quad (2.3.101)$$

The equations governing $\hat{\phi}_0(\eta, \hat{\tau})$ are the following:

$$\frac{\partial^2 \hat{\phi}_0}{\partial \eta^2} = 0 , \quad 0 < \eta < 1 ; \quad (2.3.102)$$

$$\hat{\phi}_0(0, \hat{\tau}) = 0 ; \quad (2.3.103)$$

$$\frac{\partial \hat{\phi}_0}{\partial \eta}(1, \hat{\tau}) = 0 \quad (2.3.104)$$

The solution for the equations (2.3.102) - (2.3.104) is

$$\hat{\phi}_0(\eta, \hat{\tau}) = 0 . \quad (2.3.105)$$

The following equations govern $\hat{\psi}_0(\xi, \hat{\tau})$:

$$\frac{1}{(1-\beta)^2(1-(1-\beta)\xi)} \frac{\partial}{\partial \xi} \left((1-(1-\beta)\xi) \frac{\partial \hat{\psi}_0}{\partial \xi} \right) - \frac{\partial \hat{\psi}_0}{\partial \hat{\tau}} = 0 ; \quad (2.3.106)$$

$$\hat{\psi}_0(0, \hat{\tau}) = -1 ; \quad (2.3.107)$$

$$\hat{\psi}_0(1, \hat{\tau}) = 0 ; \quad \text{and} \quad (2.3.108)$$

$$\hat{\psi}_0(\xi, 0) = \theta(\xi, \tau_m) . \quad (2.3.109)$$

The system of equations (2.3.108) - (2.3.109) have solution

$$\hat{\psi}_0(\xi, \hat{\tau}) = -1 + \frac{\ln(1 - (1-\beta)\xi)}{\ln \beta} + \sum_{m=1}^{\infty} D_m V_0(\mu_m(1 - (1-\beta)\xi)) \exp(-\mu_m^2 \tau). \quad (2.3.110)$$

where, as in the case of warm-up solution

$$V_0(\mu x) = J_0(\mu x) Y_0(\mu) - Y_0(\mu x) J_0(\mu). \quad (2.3.111)$$

J_0 and Y_0 are Bessel functions of order zero of the first and second kind respectively. $\mu_1, \mu_2, \mu_3, \dots$ are roots of (2.3.111) in ascending order when $x = \beta$,

$$V_1(\mu x) = \mu Y_1(\mu x) J_0(\mu) - \mu J_1(\mu x) Y_0(\mu) \quad (2.3.112)$$

J_1 and Y_1 are Bessel functions of first order of first and second kind respectively,

$$E_m = \frac{1}{\mu_m} \left(\frac{V_1(\mu_m \beta)}{\beta^2 V_1^2(\mu_m \beta) - V_1^2(\mu_m)} \right), \quad (2.3.113)$$

$$D_m = E_m \left(\left(\frac{-2\beta}{1-\beta} - \frac{1}{\ln \beta} \right) \frac{\beta \ln \beta}{\mu_m} - \sum_{n=1}^{\infty} A_n U_0(\alpha_n \beta) e^{-\alpha_n^2 \tau_m} \right) \quad (2.3.114)$$

Equations for $\hat{\phi}_1(\eta, \hat{\tau})$ and $\hat{\sigma}_1(\hat{\tau})$ are obtained by equating coefficients of ϵ and ϵ^2 . The equations governing $\hat{\phi}_1(\eta, \hat{\tau})$ are:

$$\frac{\partial^2 \hat{\phi}_1}{\partial \eta^2} = 0, \quad 0 < \eta < 1; \quad (2.3.115)$$

$$\hat{\phi}_1(0, \hat{\tau}) = 0 \quad ; \quad (2.3.116)$$

$$\frac{\partial \hat{\phi}_1}{\partial \eta}(1, \hat{\tau}) = -\Omega \hat{\sigma}_1 \quad . \quad (2.3.117)$$

The equations (2.3.115) - (2.3.117) give $\hat{\phi}_1(\eta, \hat{\tau})$ as

$$\hat{\phi}_1(\eta, \hat{\tau}) = -\Omega \hat{\sigma}_1 \eta \quad . \quad (2.3.118)$$

$\hat{\sigma}_1(\hat{\tau})$ is governed by the equations:

$$\hat{\sigma}_1 \frac{d\hat{\sigma}_1}{d\tau} = \frac{\sigma_1}{\beta(1-\beta)} \frac{\partial \hat{\psi}_0}{\partial \xi}(1, \hat{\tau}) - \frac{1}{\beta^2} \frac{\partial \hat{\phi}_1}{\partial \eta}(0, \hat{\tau}) \quad ; \quad (2.3.119)$$

$$\hat{\sigma}_1(0) = 0 \quad . \quad (2.3.120)$$

The solution for the equations (2.3.118) and (2.3.120) is

$$\hat{\sigma}_1(\hat{\tau}) = C_0 + C_1 \hat{\tau} - \sum_{m=1}^{\infty} F_m e^{-\mu_m^2 \hat{\tau}} \quad , \quad (2.3.121)$$

where

$$F_m = \frac{D_m V_1(\mu_m \beta)}{\beta \mu_m^2} \quad , \quad (2.3.122)$$

$$C_1 = \frac{1}{\beta^2} \left(\frac{1}{\ln \beta} - \Omega \right) \quad , \quad \text{and} \quad (2.3.123)$$

$$C_0 = \sum_{m=1}^{\infty} F_m \quad . \quad (2.3.124)$$

To facilitate matching assume the power series expansions

$$\sigma_0(\tau) = \sum_{n=0}^{\infty} a_n \tau^n, \quad \sigma_1(\tau) = \sum_{n=0}^{\infty} b_n \tau^n. \quad (2.3.125a,b)$$

On substituting (2.3.120) and (2.3.121) and replacing the inner independent variable by the outer independent variable in (2.3.100), $\hat{\sigma}(\tau)$ is given by

$$\hat{\sigma}(\tau) = c_1 \tau + \epsilon c_0 - \epsilon \sum_{m=1}^{\infty} F_m e^{-\mu_m^2 \tau / \epsilon} + O(\epsilon^2). \quad (2.3.126)$$

Matching the inner and outer expansions gives

$$\sigma_0(0) = a_0 = 0, \quad \text{and} \quad (2.3.127)$$

$$\sigma_1(0) = b_0 = c_0. \quad (2.3.128)$$

Numerical solutions.

The zeroth and first terms in the expansion (2.3.46) for $\sigma(\tau)$ have been calculated using the data in table 2. The time τ_M required in (2.3.37) is calculated from (2.3.40) when $\theta = 0$ and $\xi = 1$ by using the Newton-Ralphson method. The values of $\sigma_0(\tau)$ and $\sigma_1(\tau)$ have been calculated from ((2.3.83) and (2.3.127)) and (2.3.92) and (2.3.128)) respectively using a Runge-Kutta method.

Asymptotic expansion for σ_0 and σ_1 are now calculated for comparison with the obtained graphs. In

(2.3.83) the equation for $\sigma_0(\tau)$ let

$$y = \frac{1 + \sigma_0}{\alpha} \quad (2.3.129)$$

when $\frac{dy}{d\tau} = 0$, $y = \exp(1/\Omega)$. (2.3.130)

Let $\bar{y} = \exp(1/\Omega)$ (2.3.131)

and assume that for large τ

$$y = \bar{y} + y^* \quad , \text{ then} \quad (2.3.132)$$

$$\frac{dy^*}{d\tau} = \frac{1 - \Omega \ln(\bar{y} + y^*)}{(\bar{y} + y^*) \ln(\bar{y} + y^*)} \quad (2.3.133)$$

Using the first two terms of the Taylor series

$$\ln(\bar{y} + y^*) = \ln \bar{y} + \frac{y^*}{\bar{y}} - \frac{1}{2} \left(\frac{y^*}{\bar{y}} \right)^2 + \dots \quad (2.3.134)$$

in (2.3.133) yields the expression

$$\frac{dy^*}{d\tau} = - \left(\frac{\Omega}{\bar{y}} \right)^2 \frac{y^*}{(1 + y^*/\bar{y})(1 + \Omega y^*/\bar{y})} \quad (2.3.135)$$

As $y \rightarrow \bar{y}$, $y^* \rightarrow 0$, hence

$$\frac{dy^*}{d\tau} = - y^* \left(\frac{\Omega}{\bar{y}} \right)^2 \quad (2.3.136)$$

giving

$$y^* = A \exp\left(-(\Omega/\bar{y})^2 \tau\right) \quad (2.3.137)$$

Therefore for large τ

$$\sigma_0(\tau) = \alpha \exp(\nu - \Omega) - 1 + B \exp\left(-(\Omega/\bar{y})^2 \tau\right) \quad (2.3.138)$$

where B is a constant.

The expression for $\sigma_1(\tau)$ is given by (2.3.97).

Using the data in table 2, for large τ

$$\sigma_0 = \alpha \exp(1/\Omega) - 1 = 0.53 \quad (2.3.139)$$

and

$$\frac{d\sigma_0}{d\tau} = 0 \quad (2.3.140)$$

Substituting (2.3.140) in (2.3.92) gives

$$\beta^2 \sigma_0 (1 - \alpha + \sigma_0) \frac{d\sigma_1}{d\tau} = \frac{\sigma_1}{1 + \sigma_0} \left(\frac{1}{\ln\left(\frac{1 + \sigma_0}{\alpha}\right)} \left(1 - \alpha + \sigma_0 + \sigma_0 \alpha - \frac{\sigma_0^2}{(1 + \sigma_0) \ln\left(\frac{1 + \sigma_0}{\alpha}\right)} \right) - \Omega \left(\sigma_0 + \frac{1 - \alpha + \sigma_0}{1 + \sigma_0} \right) \right) + \frac{k \Omega \beta^2 \sigma_0^2 (2 + \sigma_0) (1 - \alpha + \sigma_0)}{2 (1 + \sigma_0)^2}$$

Using (2.3.139) in (2.3.114) gives, approximately

$$\frac{d\sigma_1}{d\tau} = -\frac{140}{\beta^2} \sigma_1 \quad (2.3.142)$$

hence
$$\sigma_1(\tau) \approx C \exp(-s^2 \tau) \quad (2.3.143)$$

for large τ , where C is a constant.

Figure 19 and Figure 20 give the variation of $\sigma_0(\tau)$ and $\sigma_1(\tau)$ respectively and are as expected by the asymptotic expressions above.

Conclusion

The problem set forth in this chapter of the annulus initially at a sub-freezing temperature to the final stages where the annulus consists of both the liquid and solid phases marks a new development for the moving boundary problem. The development is that at the start of the boundary value problem the temperature in the solid is not uniform but more characteristic of a real life problem devoid of the laboratory condition of uniform initial temperature.

The results obtained give the first two terms in the expansion of the function giving the position of the interface. At considerable cost in terms of labour, more terms can be obtained but here are the two that are significant.

Table 1

Radius of vessel,	R_0 (M)	0.3
Height of water bath,	H (M)	0.6
Base angle of two-phase cone,	2λ	0.35
Radius of orifice,	r_0 (M)	0.0064
Velocity of gas at nozzle,	u_0 (Msec ⁻¹)	1.62
Density of water,	ρ_l (Kg M ⁻³)	1000
Acceleration due to gravity,	g (Msec ⁻²)	9.8

Table 2

		<u>Water</u>	<u>Ice</u>
Latent heat of fusion,	L (J Kg^{-1})		3.2×10
Density,	ρ (Kg M^{-3})	998	916
Thermal conductivity,	K ($\text{W M}^{-1}\text{K}^{-1}$)	0.57	2.3
Specific Heat,	c_p ($\text{J Kg}^{-1}\text{K}^{-1}$)	4250	2106
Fusion Temperature	T_F (K)		273
Initial Temperature,	T_I (K)		253
Heat flux,	Q (kW M^{-2})	20	
Inner radius of annulus	a (M)	.027	
Outer radius of annulus	b (M)	.045	

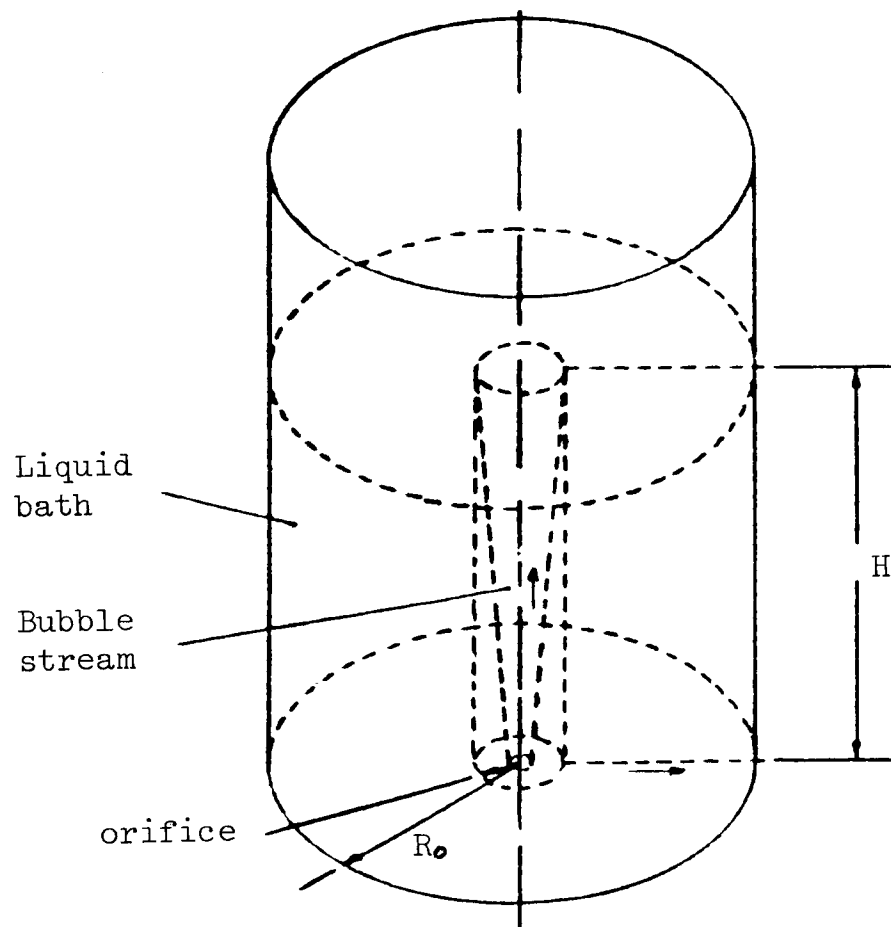


Figure 1. Schematic diagram of gas bubble-driven circulating system.

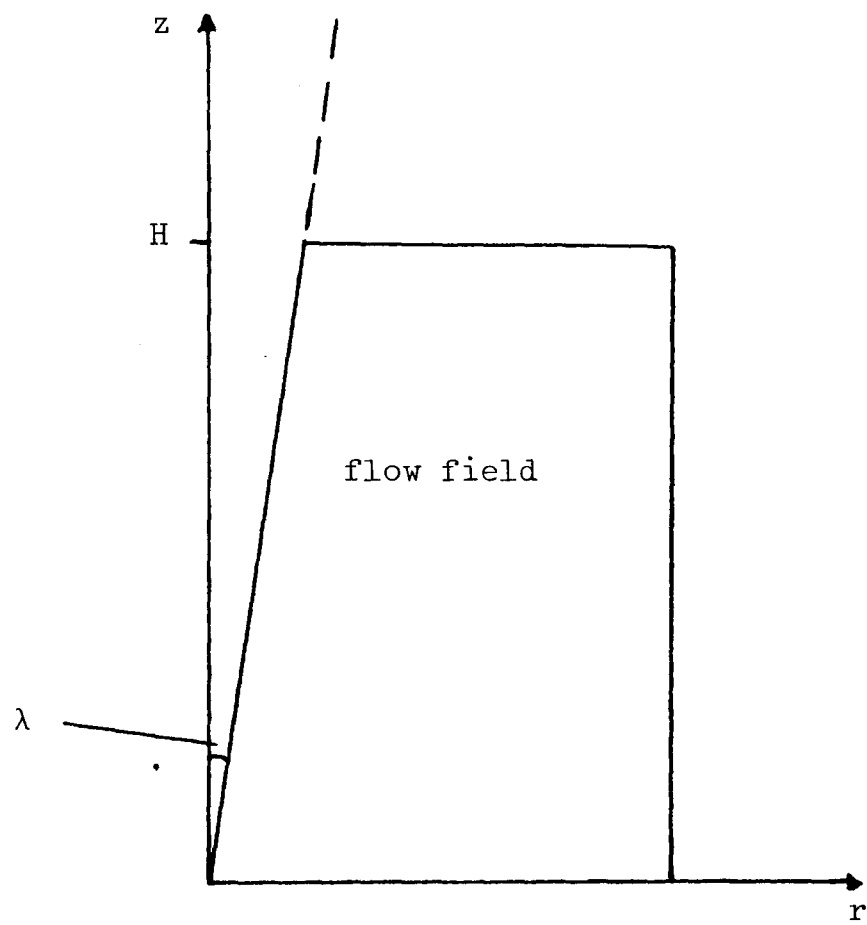


Figure 2. Geometry of flow field for recirculating flow

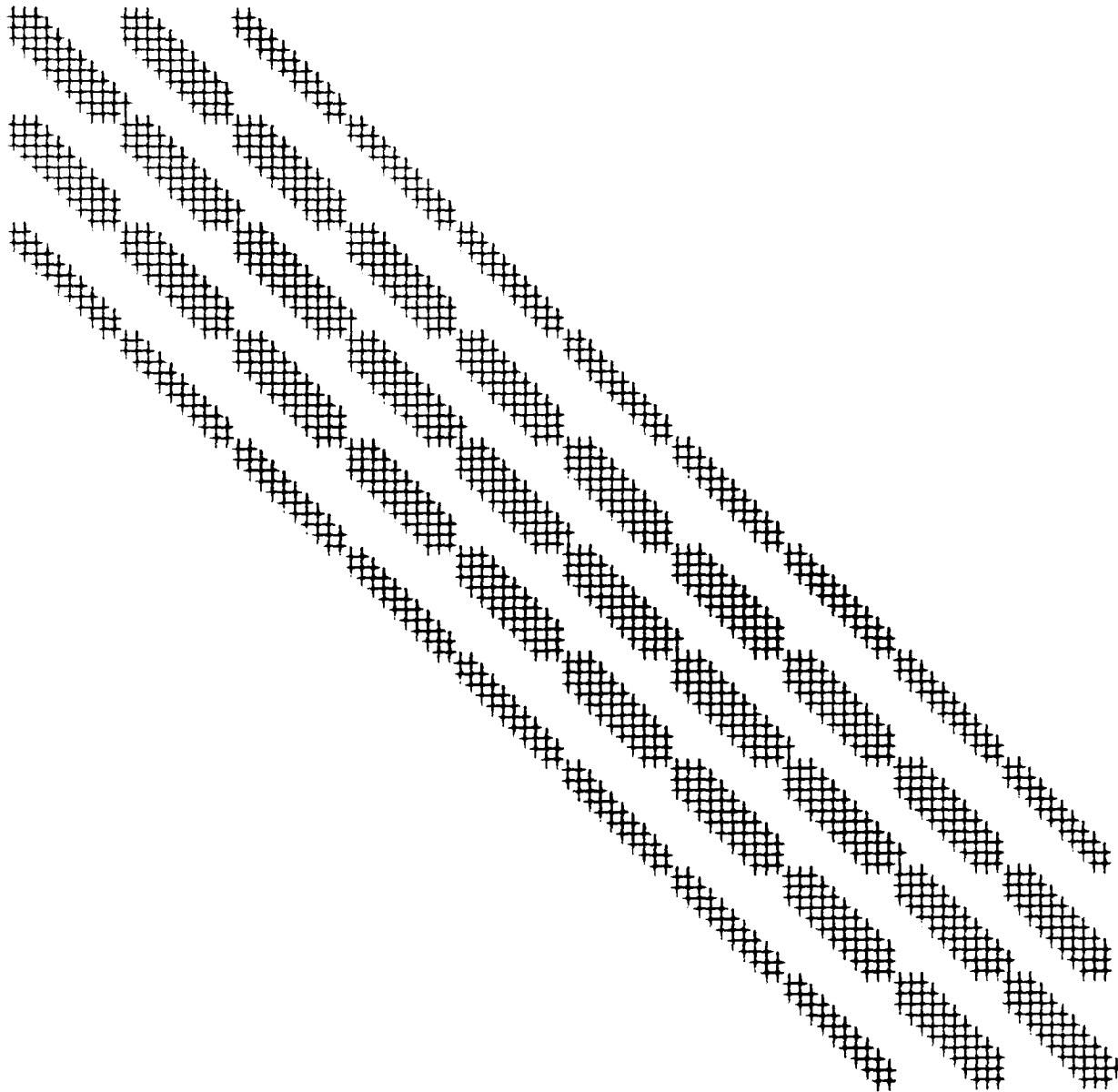


Figure 3. Structure of Banded matrix W appearing in equation 1.4.25.

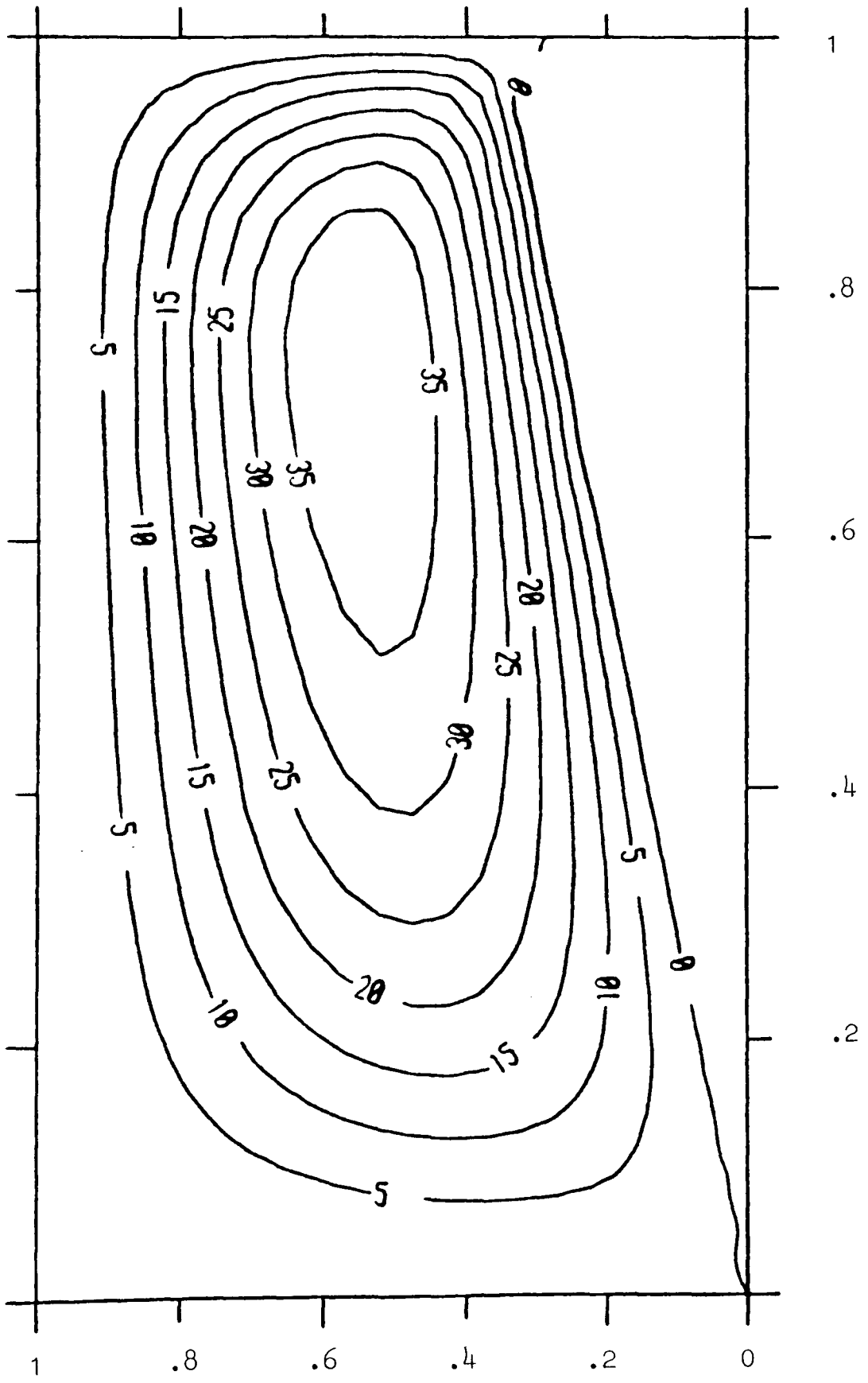


Figure 4.

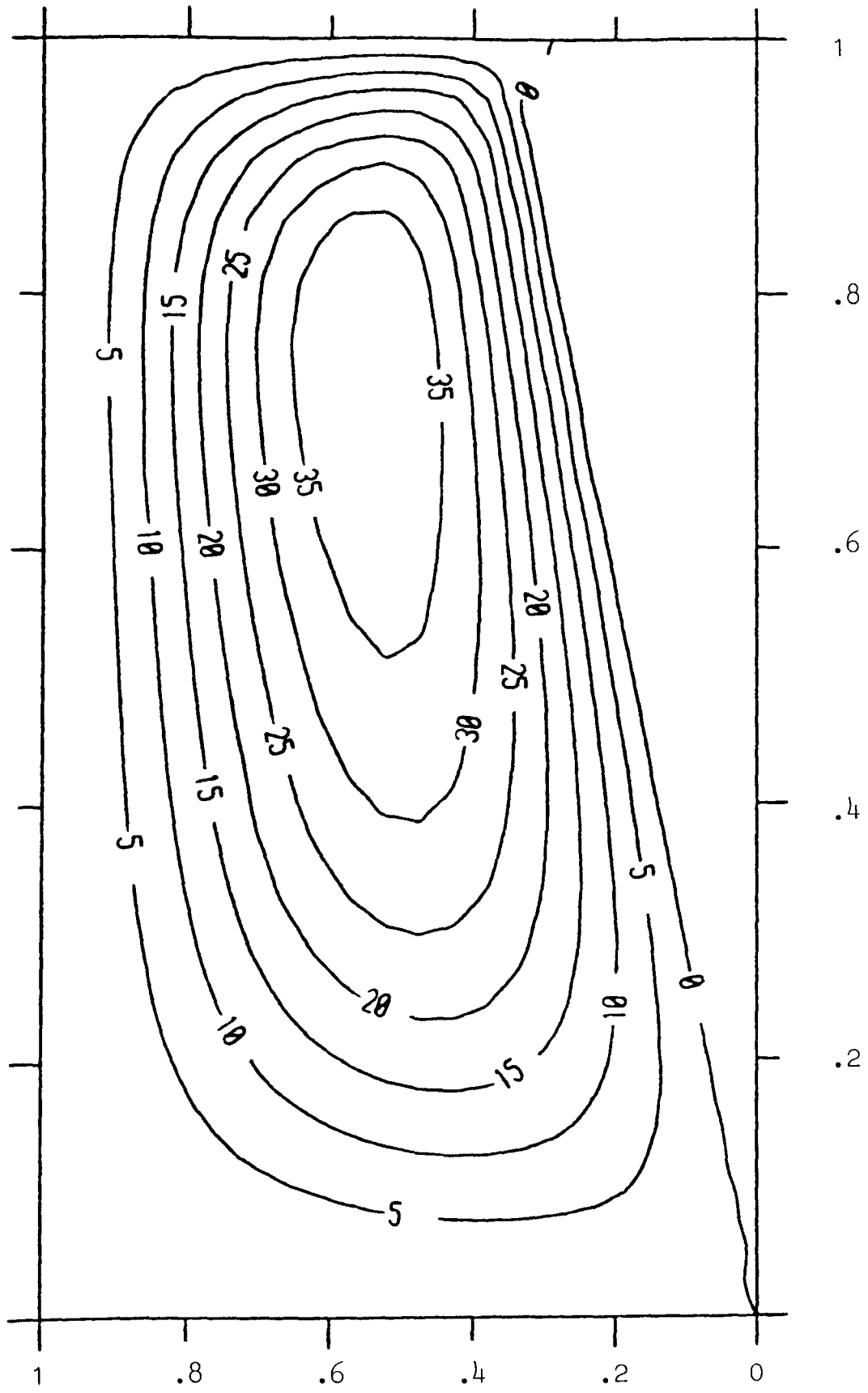


Figure 5.

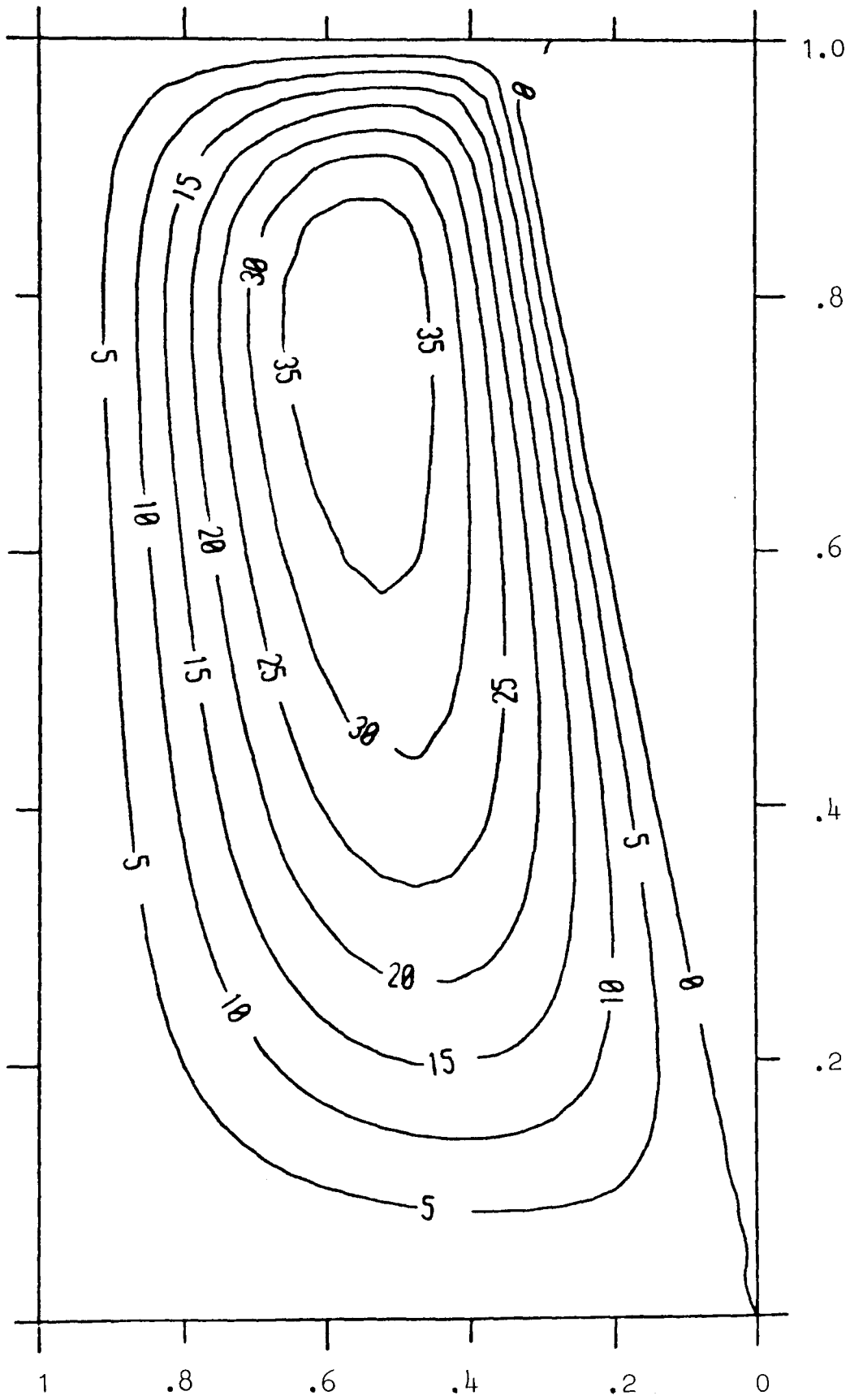


Figure 6.

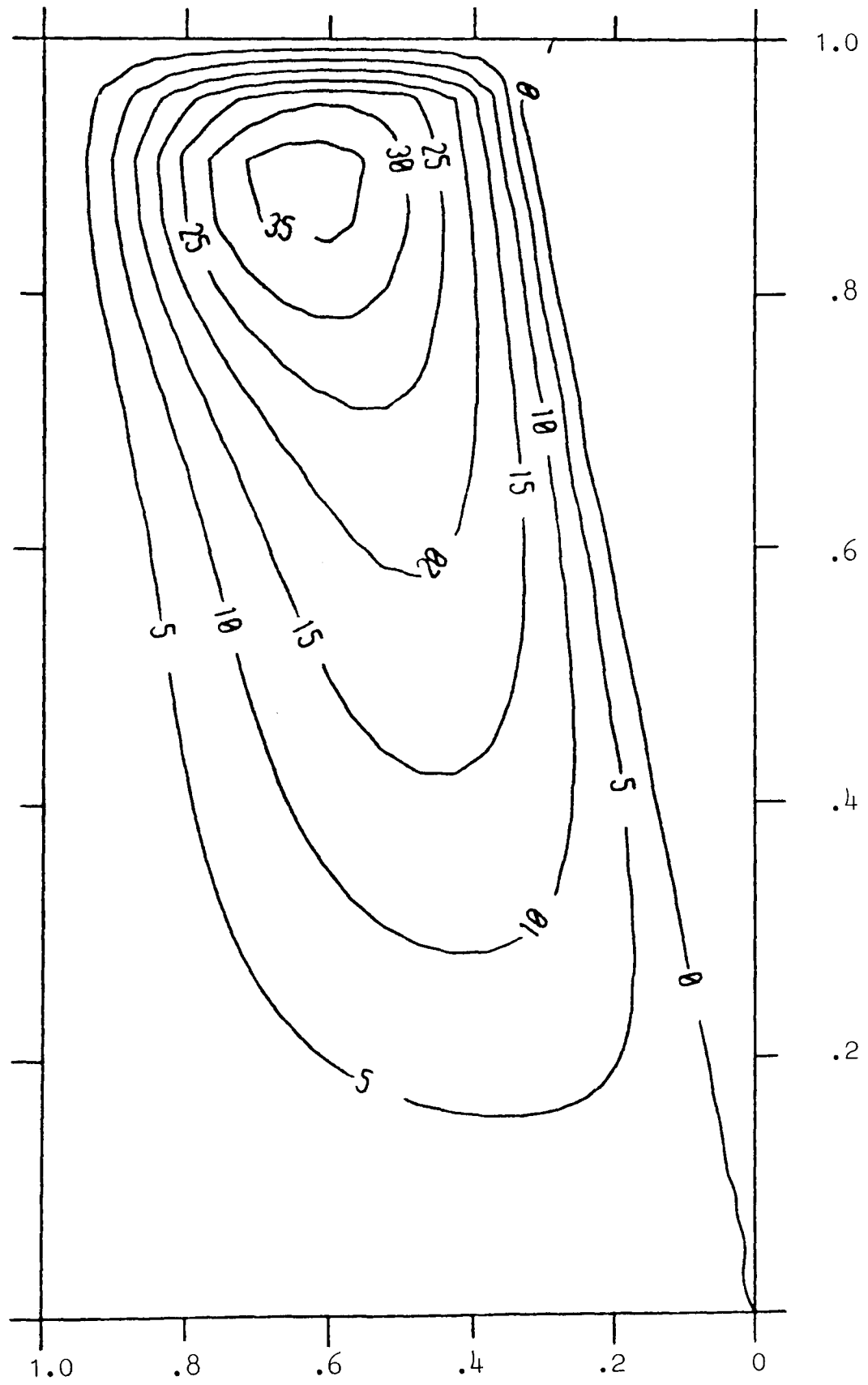


Figure 7.

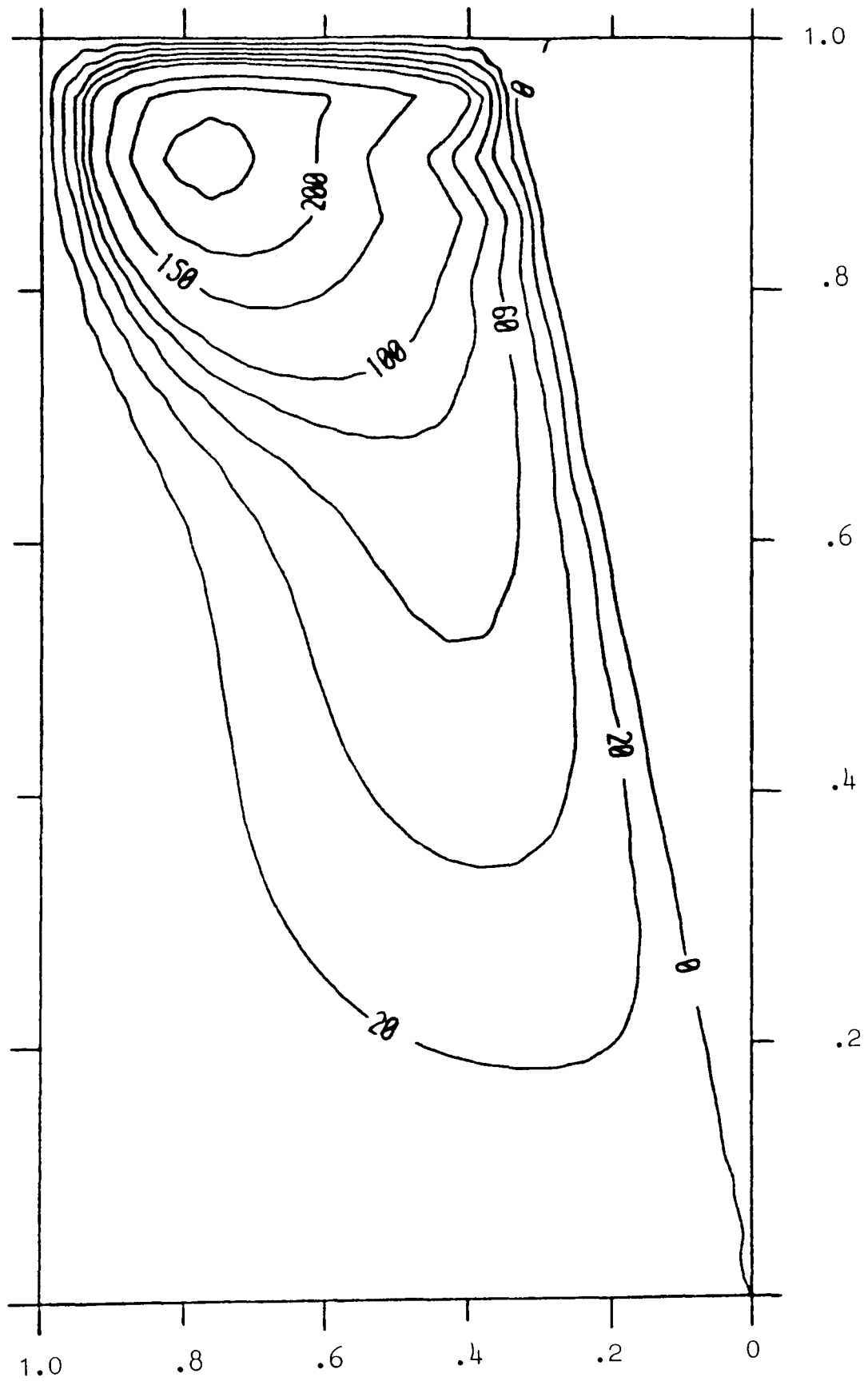


Figure 8.

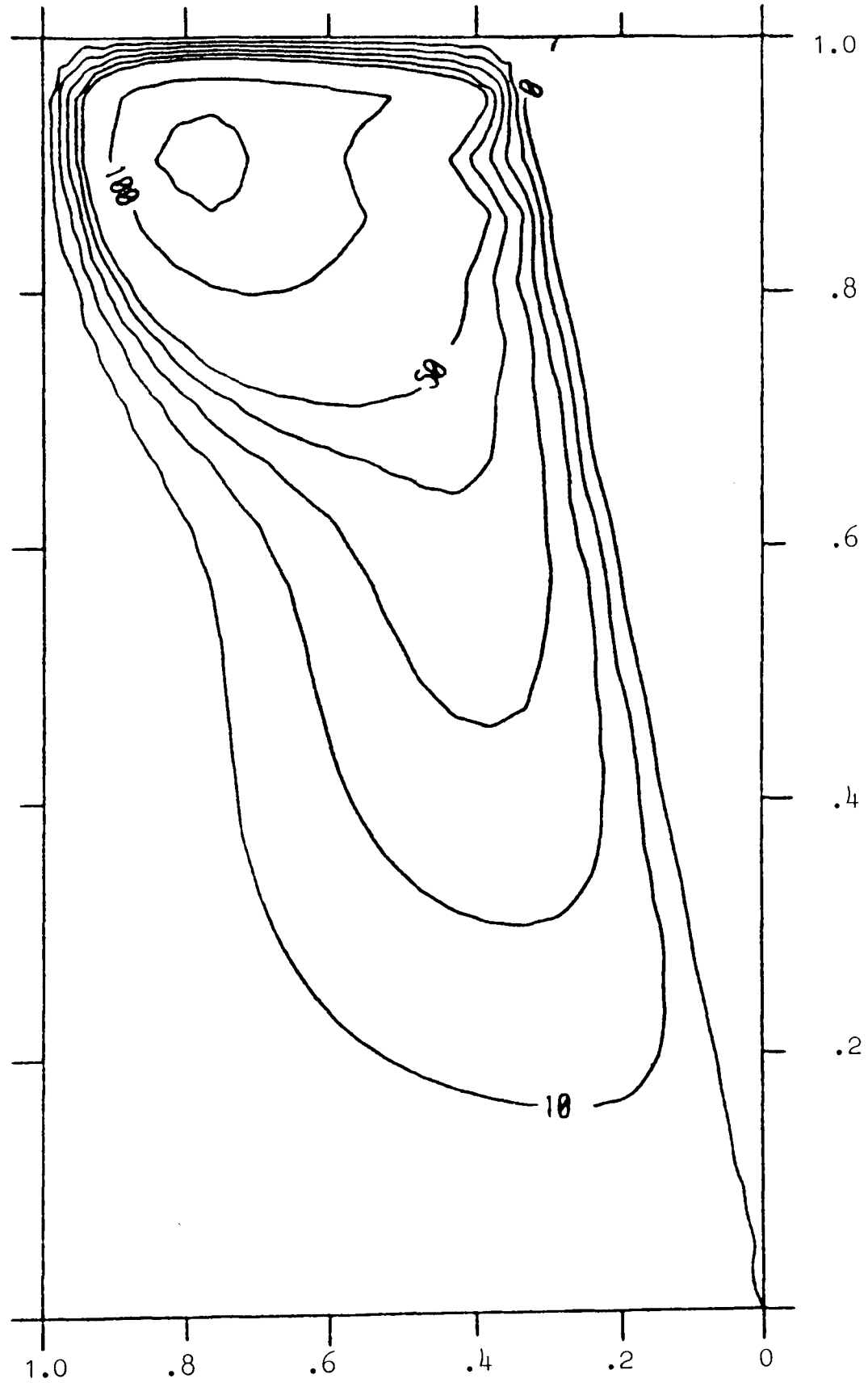


Figure 9.

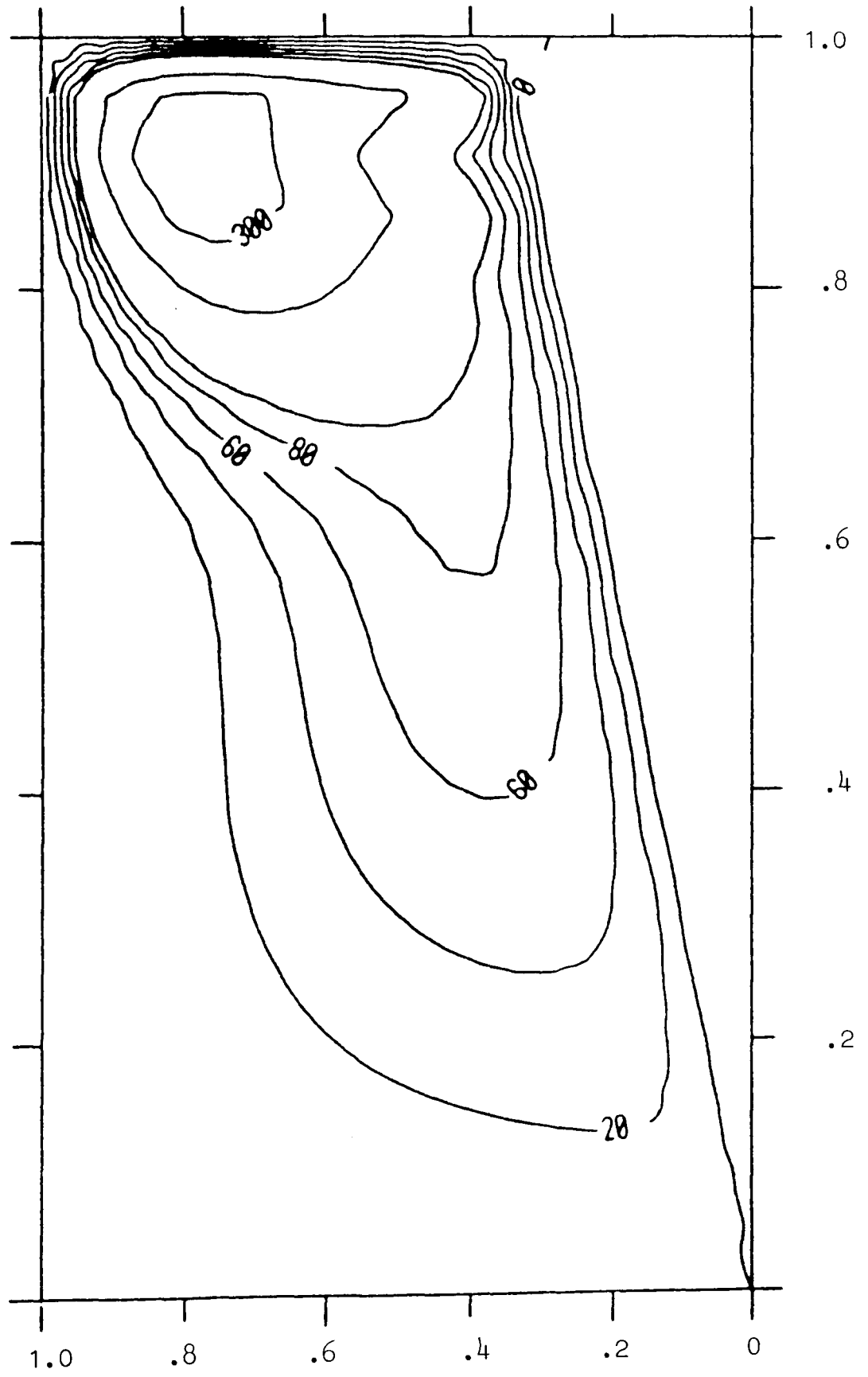


Figure 10(a).

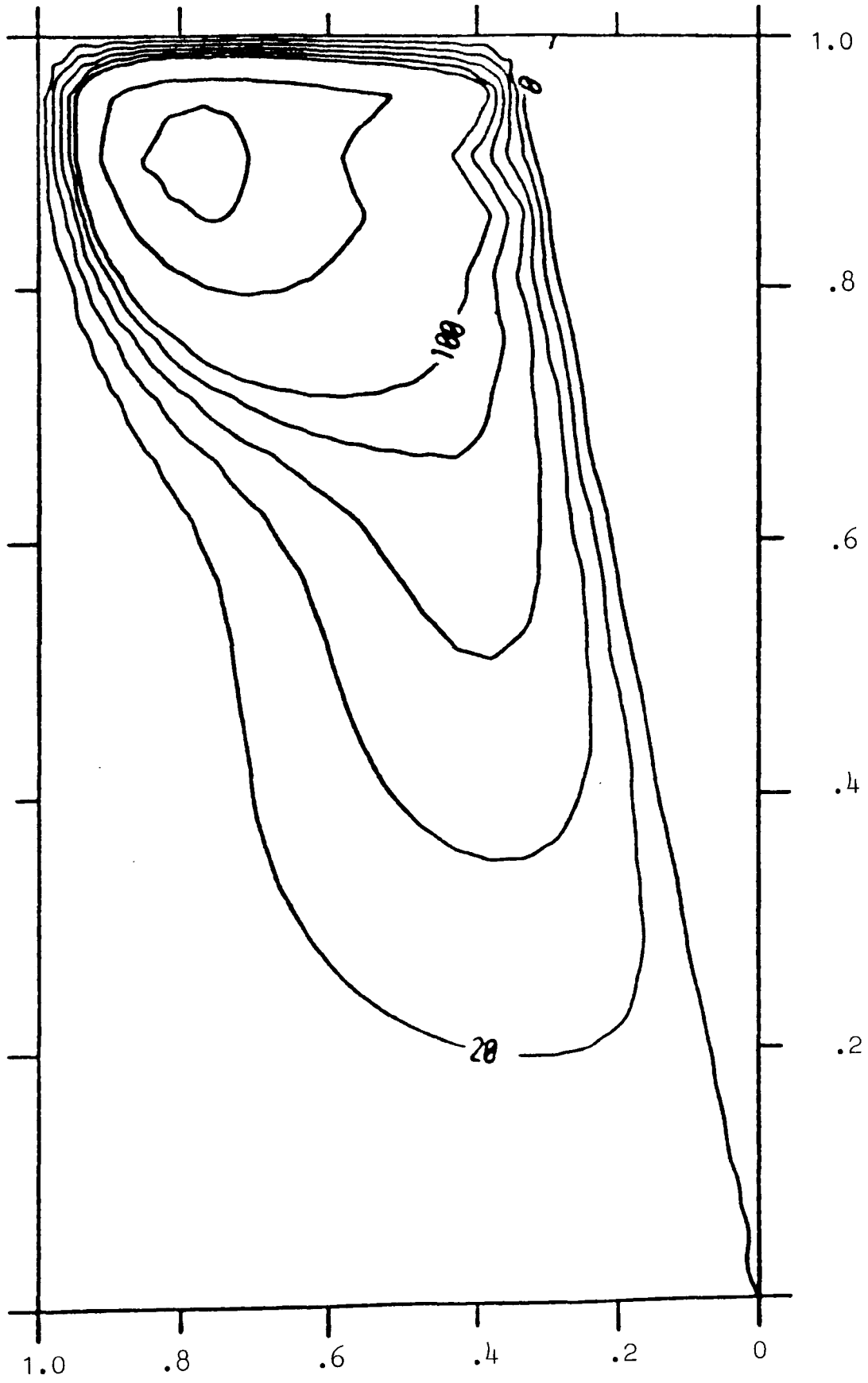


Figure 10(b)

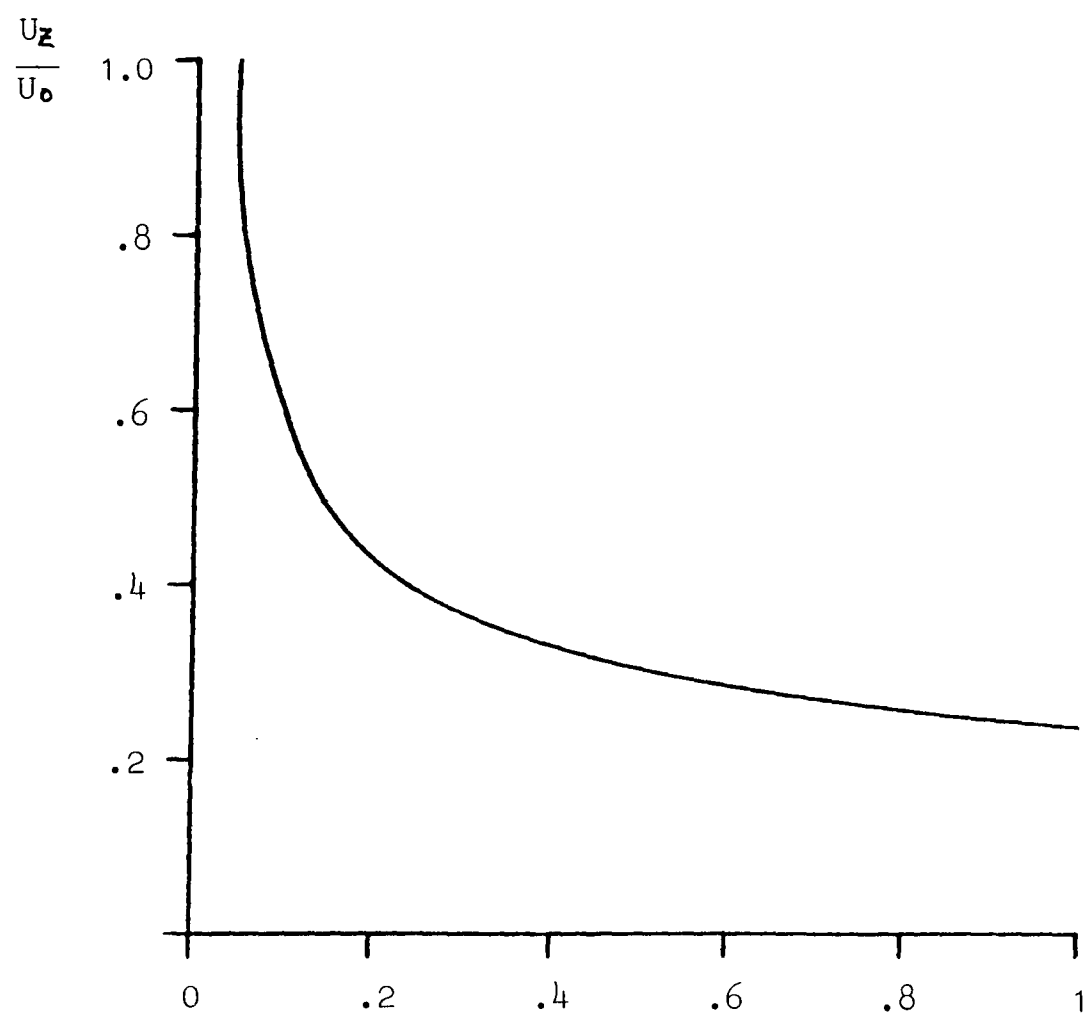


Figure 10(c)

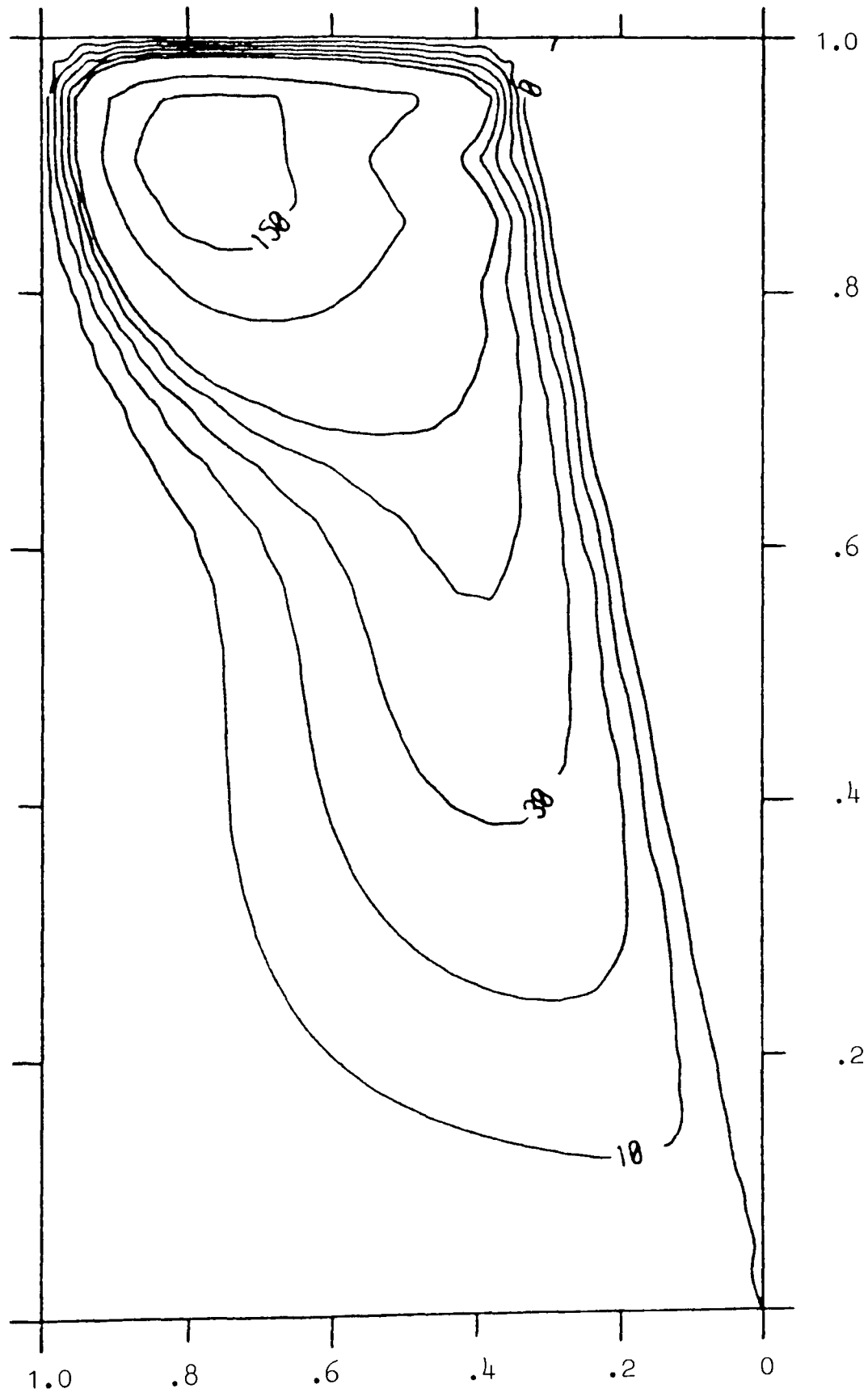


Figure 11(a)

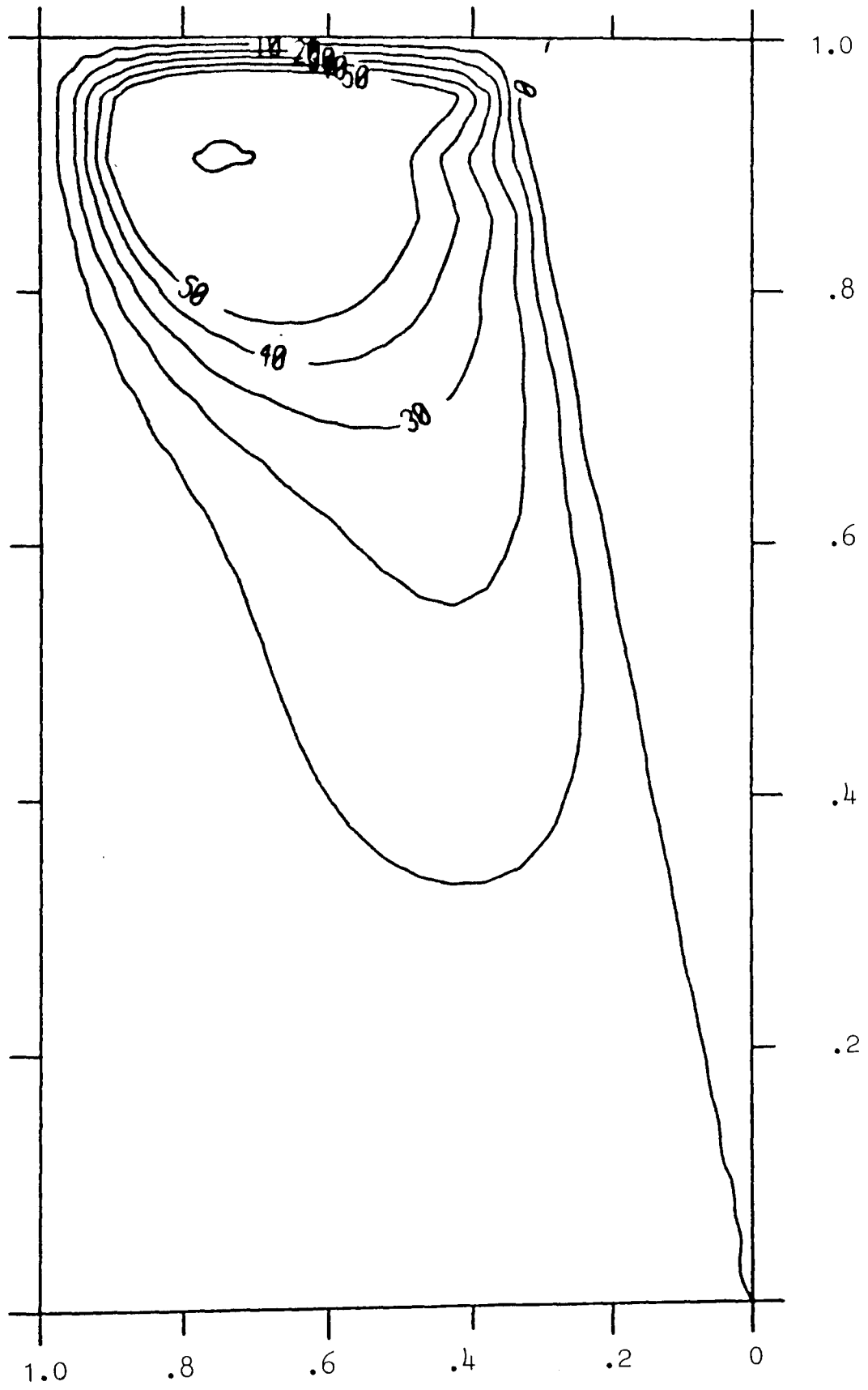


Figure 11(b)

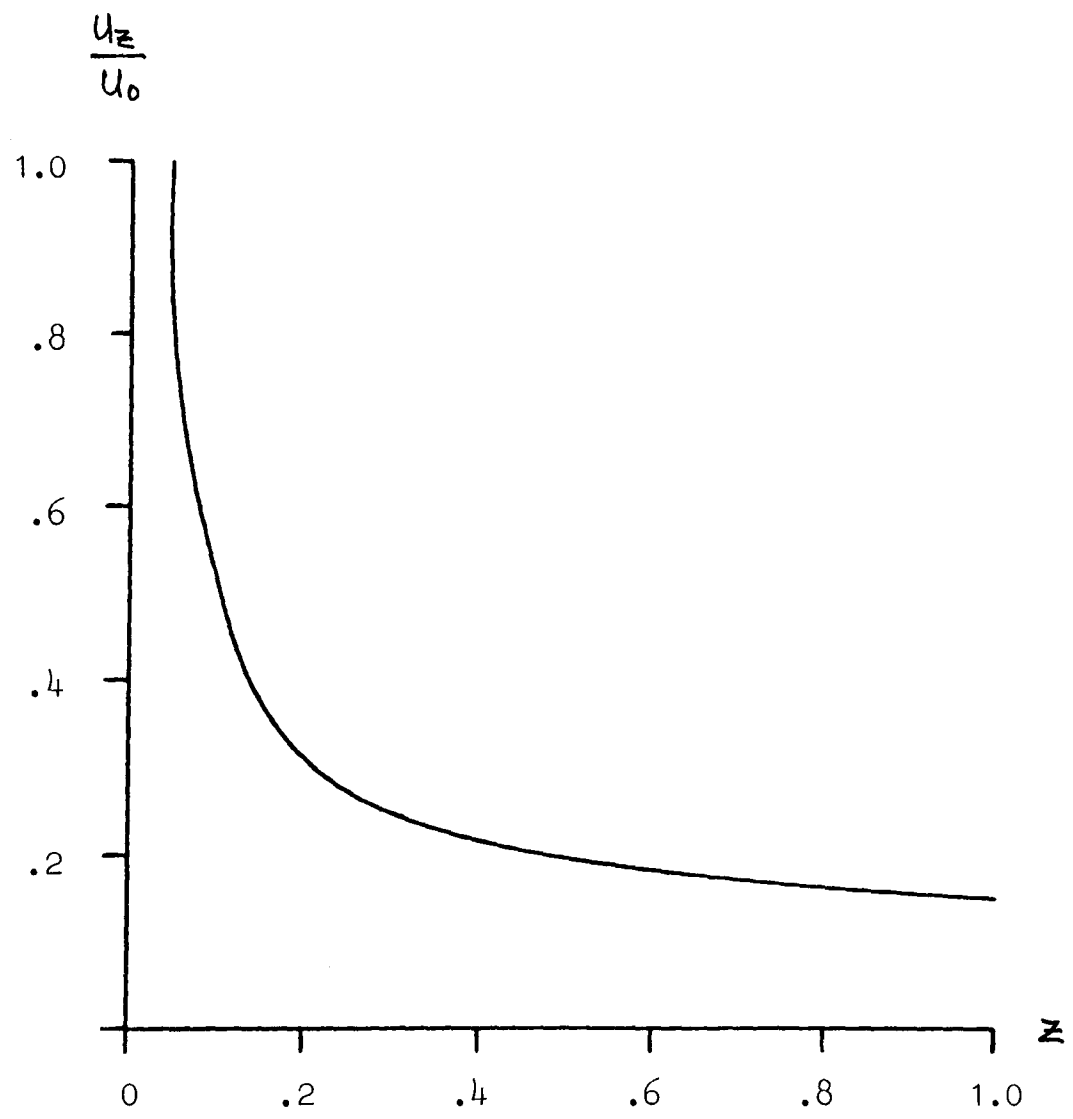


Figure 11(c)

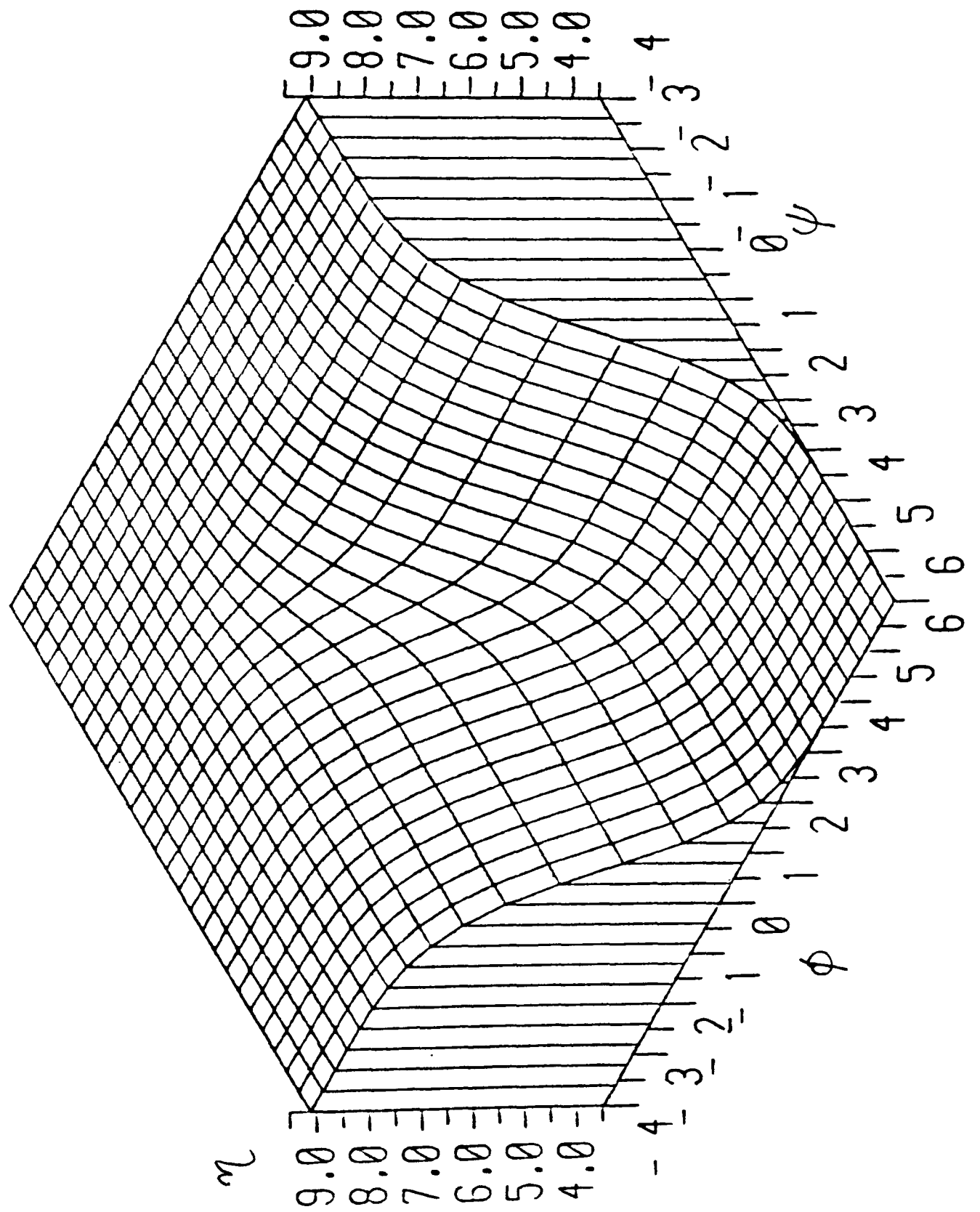


Figure 12.

Interface location for wall temperature given by
 2.2.84. $\beta = 0.3$, $\tau = 0.2$

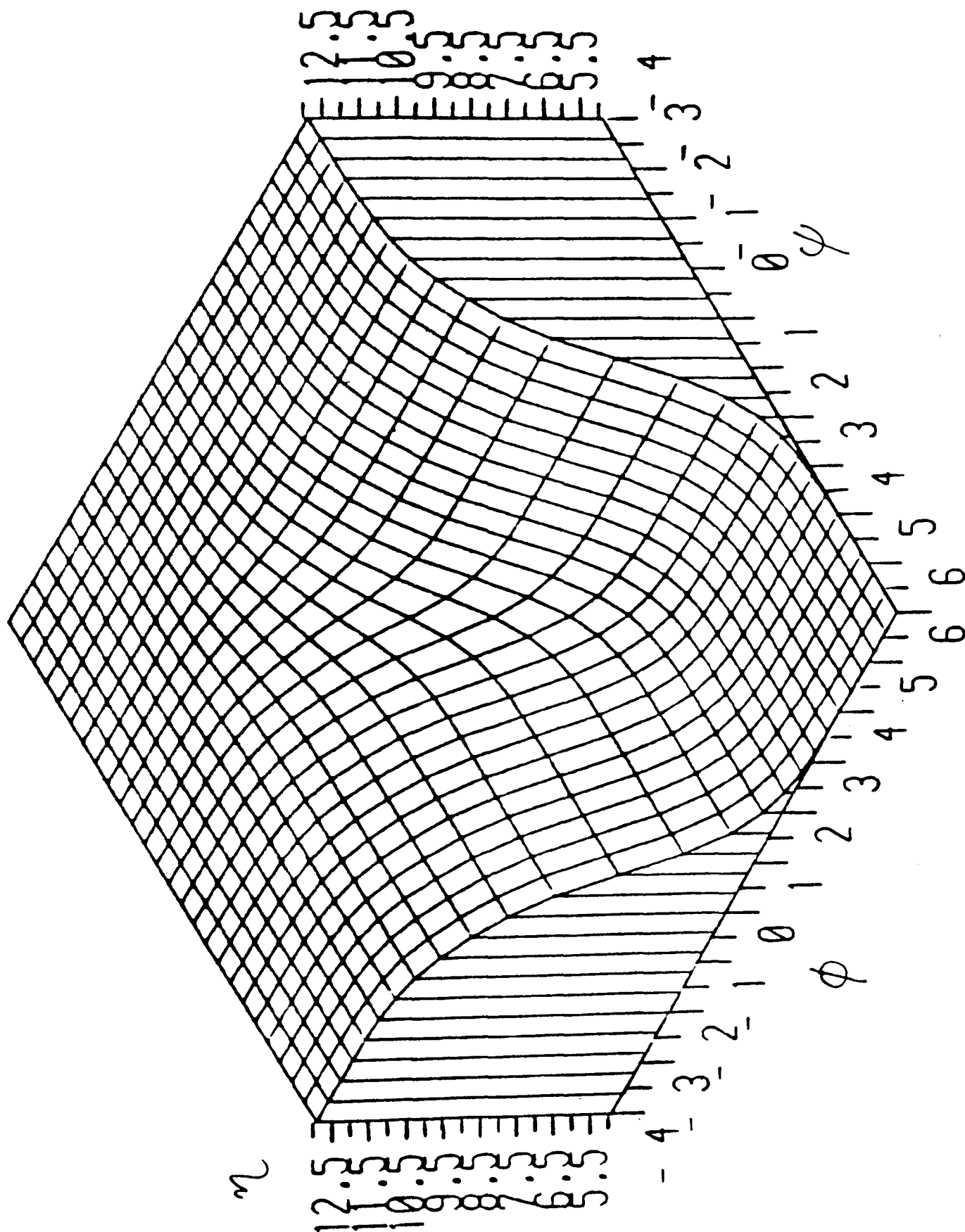


Figure 13.

Interface location for wall temperature given by
 (2.2.84) $\beta = 0.3$, $\tau = 0.4$

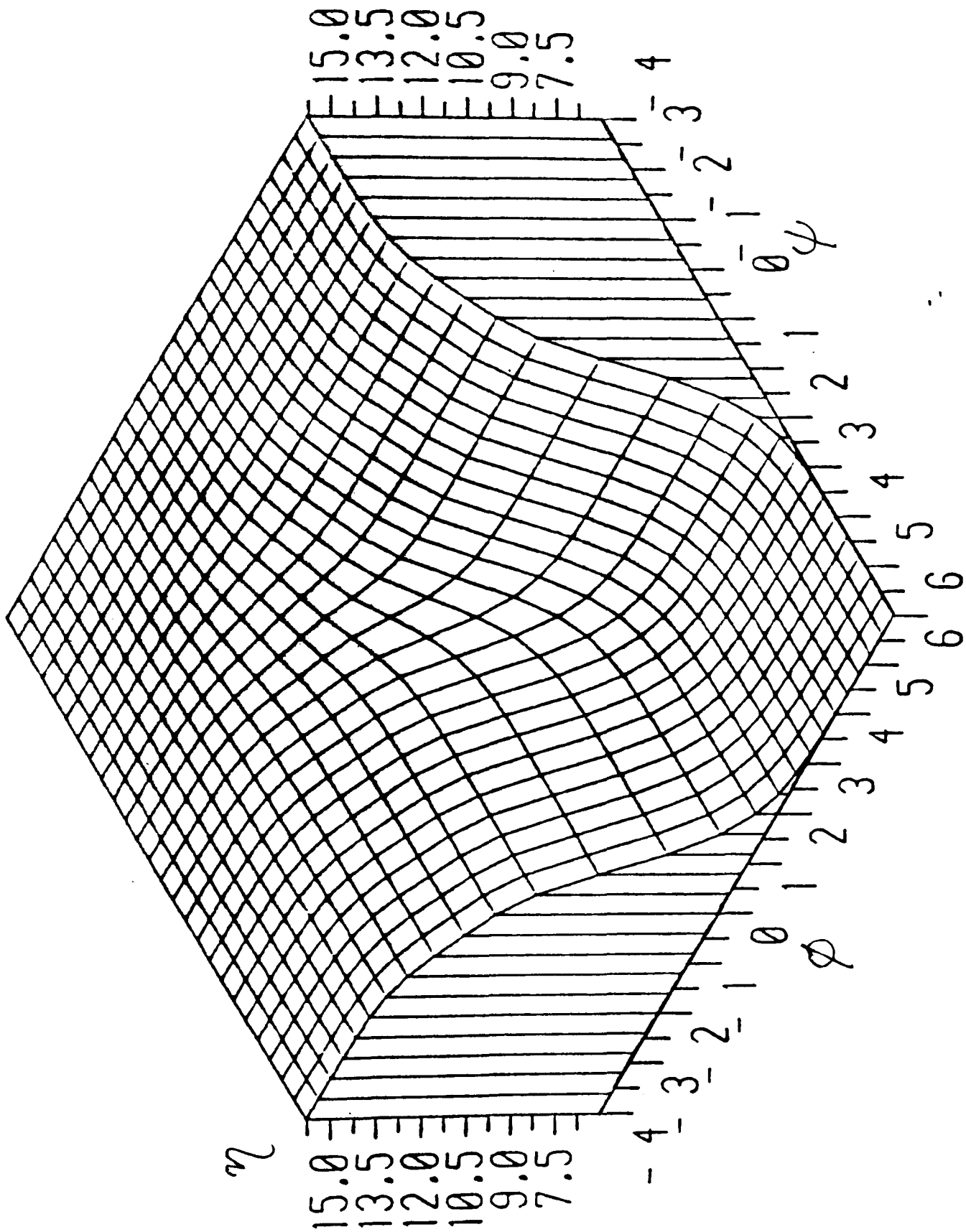


Figure 14.

Interface location for wall temperature given by
 (2.2.84) $\tau = 0.6$

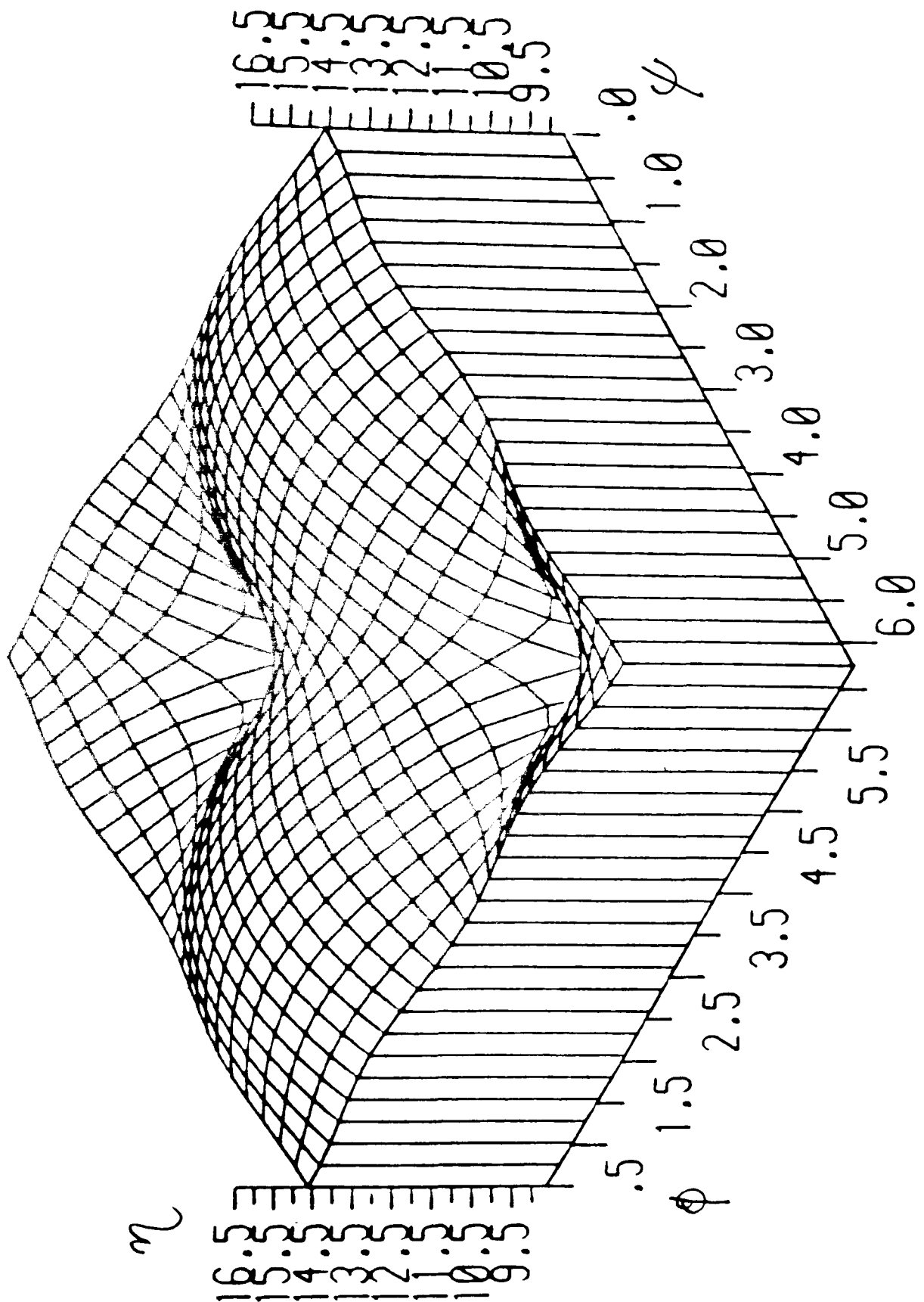


Figure 15.

Interface location for wall temperature given by
 (2.2.85) $\tau = 0.6$

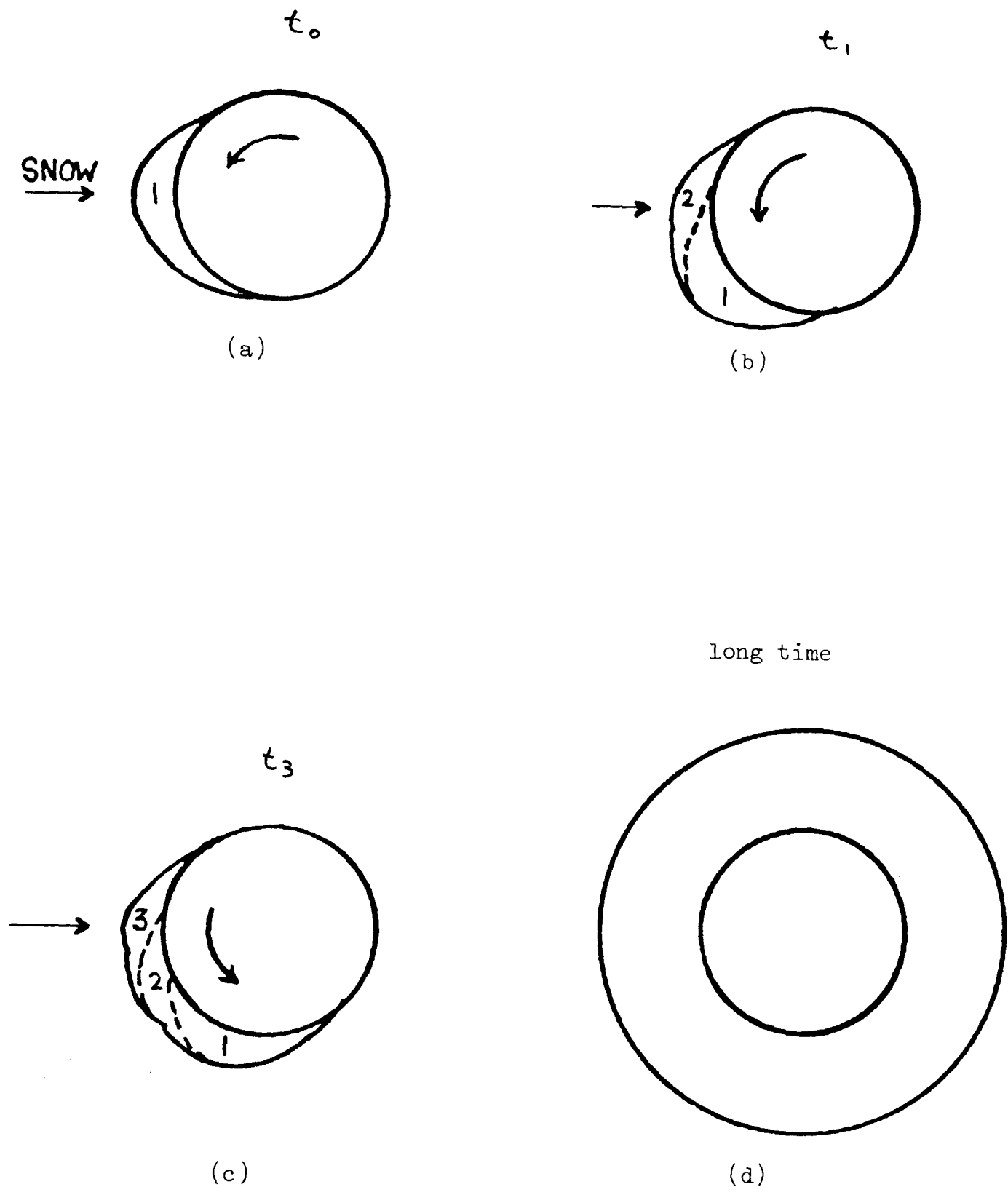


Figure 16.
Ice spike growth in an overnight snow environment.

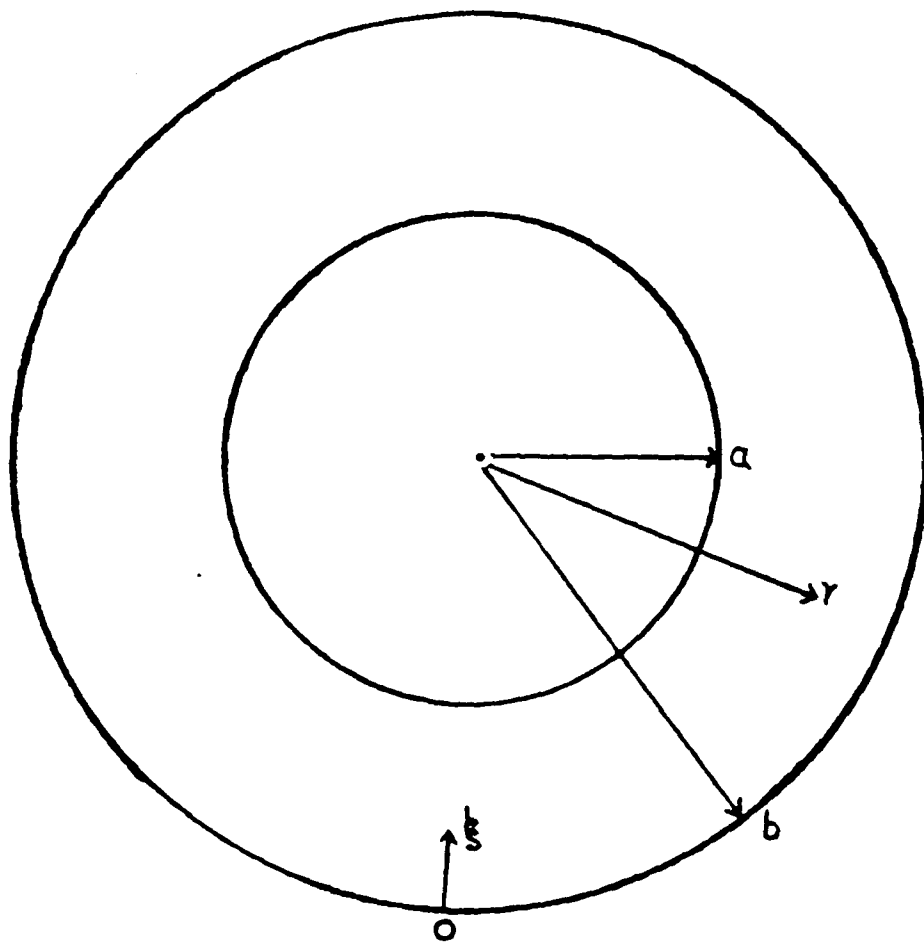


Figure 17.

Geometry of cylindrical system for warm-up problem.

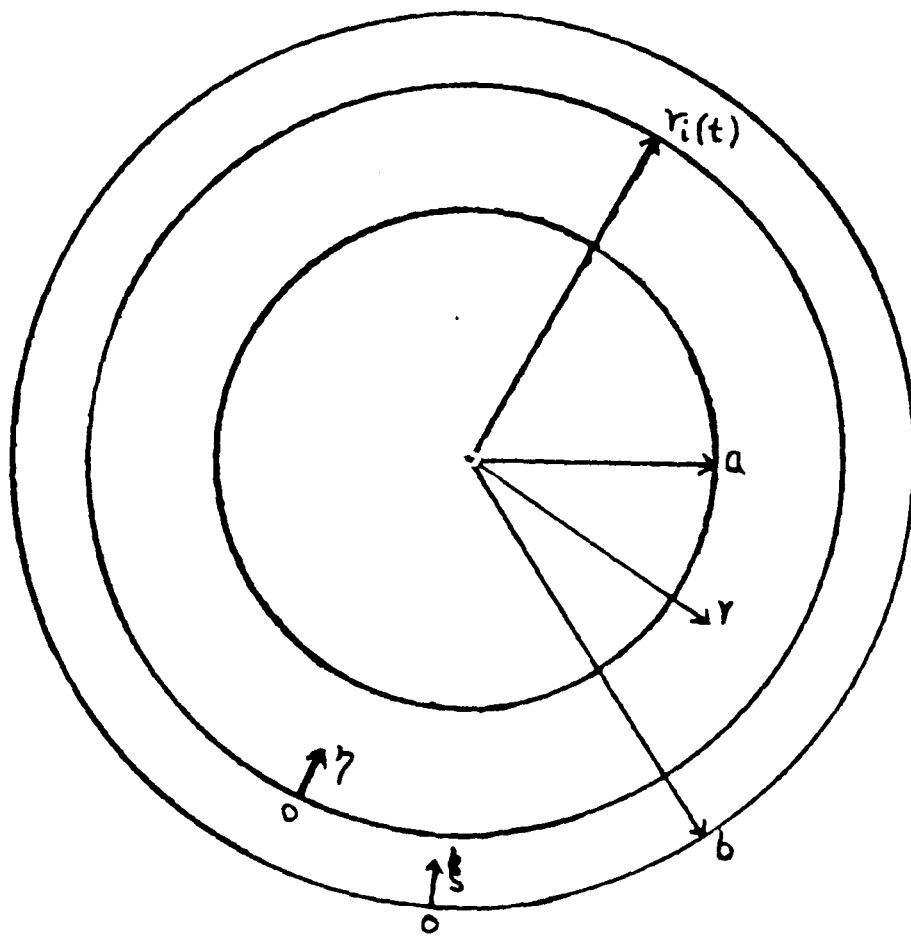


Figure 18.

Geometry of cylindrical system for the Stefan Problem.

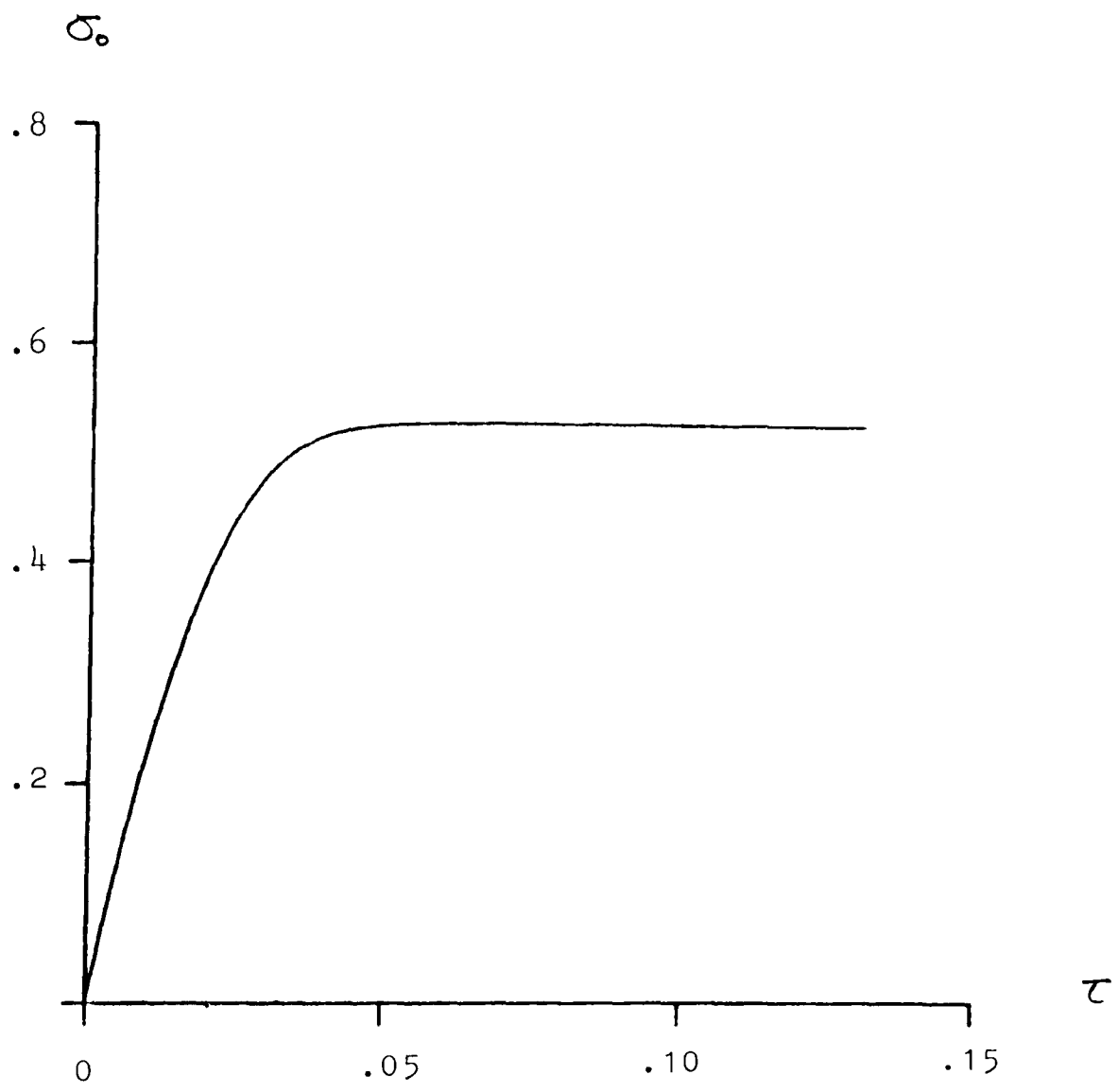


Figure 19.

Variation of σ_0 with τ

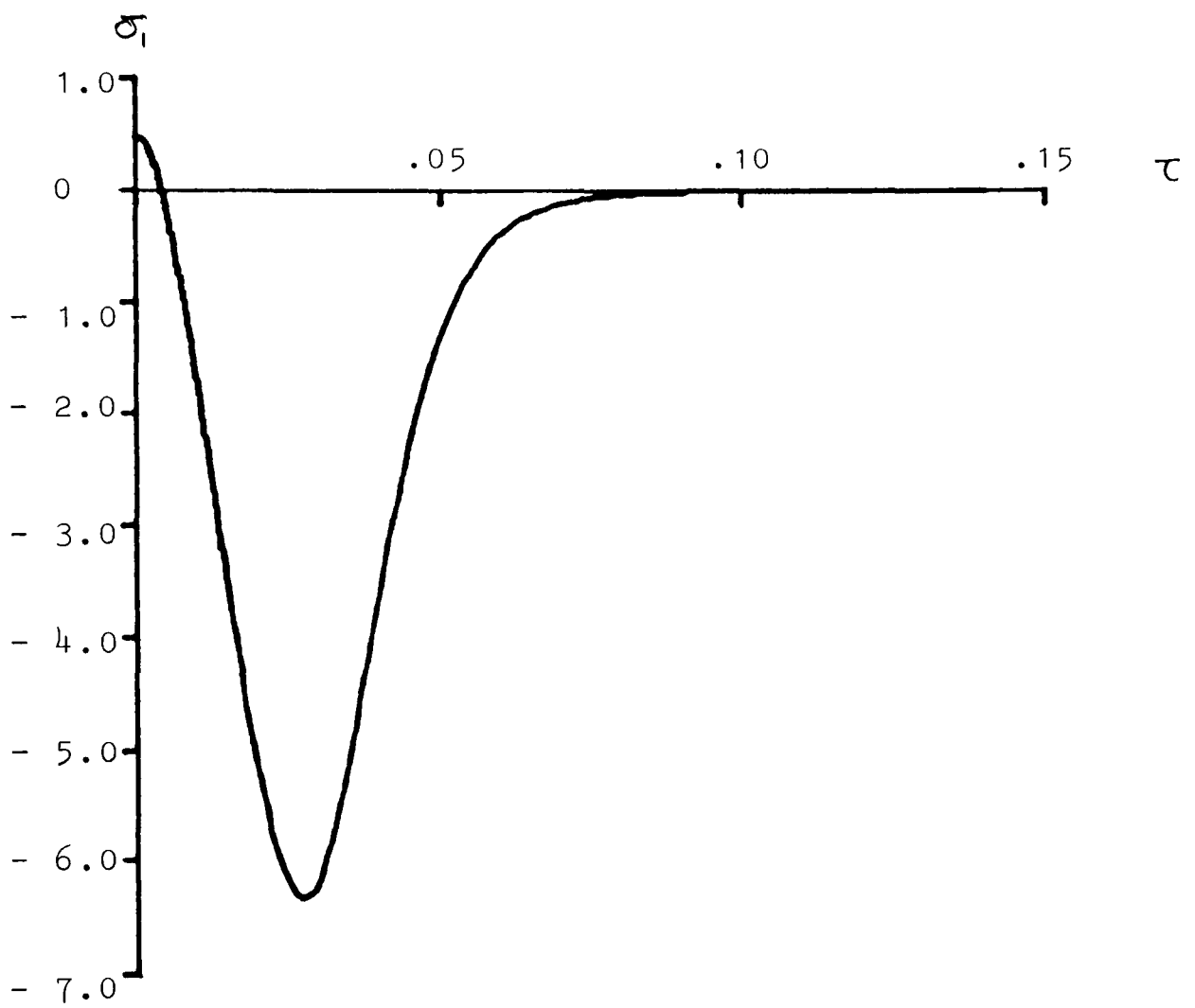


Figure 20.

Variation of σ_1 with τ

APPENDIX 1

The coefficients appearing in the differential operators defined by equations (1.3.36) - (1.3.38) are given here. For convenience introduce a new variable

$$s = \frac{1}{1 + \beta \eta} \quad . \quad (A1.1)$$

The required coefficients are as follows:

$$L_1 = 2\beta^2 \gamma^3 s - \frac{4\beta^2 \gamma^3 \xi s^3}{\xi - s} \quad ; \quad (A1.2)$$

$$L_2 = 4\beta^2 \gamma^3 \xi s^3 - \frac{\gamma(3 + 2\beta^2 \gamma^2 \xi^2) s^3}{\xi - s} \quad ; \quad (A1.3)$$

$$L_3 = \frac{4\beta \gamma^4 \xi s^2}{\xi - s} - 2\beta \gamma^3 s^2 \quad ; \quad (A1.4)$$

$$L_4 = -\frac{2\gamma^3 s}{\xi - s} \quad ; \quad (A1.5)$$

$$L_5 = \gamma(1 + \beta^2 \gamma^2 \xi^2) s^3 \quad ; \quad (A1.6)$$

$$L_6 = -2\beta \gamma^3 \xi s^2 \quad ; \quad (A1.7)$$

$$L_7 = \gamma^3 S \quad ; \quad (A1.8)$$

$$M_1 = -\frac{\beta \gamma S^3}{\xi - S} - \frac{3\beta \gamma \xi S^2}{\xi - S} + 6\beta^3 \gamma^3 \xi S^3 \quad ; \quad (A1.9)$$

$$M_2 = \frac{3\gamma S^2}{(\xi - S)^2} \quad ; \quad (A1.10)$$

$$M_3 = -\frac{\beta \gamma \xi S^3}{\xi - S} + 2\beta \gamma (1 + 3\beta^2 \gamma^2 \xi^2) S^3 \quad ; \quad (A1.11)$$

$$M_4 = \frac{\gamma S^2}{\xi - S} - 6\beta^2 \gamma^3 \xi S^2 \quad ; \quad (A1.12)$$

$$M_5 = \beta \gamma \xi (1 + \beta^2 \gamma^2 \xi^2) S^3 \quad ; \quad (A1.13)$$

$$M_6 = -\gamma (1 + 3\beta^2 \gamma^2 \xi^2) S^2 \quad ; \quad (A1.14)$$

$$M_7 = 3\beta \gamma^3 \xi S \quad ; \quad (A1.15)$$

$$M_8 = -\gamma^3 \quad ; \quad (A1.16)$$

$$N_1 = \frac{3s^4}{(\xi-s)^3} + \frac{4\beta^2\gamma^2s^4}{\xi-s} - 24\beta^4\gamma^4\xi s^4 ; \quad (\text{A1.17})$$

$$N_2 = \frac{-3s^4}{(\xi-s)^2} + \frac{8\beta^2\gamma^2\xi s^4}{\xi-s} - 12\beta^2\gamma^2s^4(1+3\beta^2\gamma^2\xi^2) ; \quad (\text{A1.18})$$

$$N_3 = -\frac{4\beta\gamma^2s^3}{\xi-s} + 24\beta^3\gamma^4\xi s^3 ; \quad (\text{A1.19})$$

$$N_4 = \frac{2(1+\beta^2\gamma^2\xi^2)s^4}{\xi-s} - 12\beta^2\gamma^2\xi(1+\beta^2\gamma^2\xi^2)s^4 ; \quad (\text{A1.20})$$

$$N_5 = -\frac{4\beta\gamma^2\xi s^3}{\xi-s} + 8\beta\gamma^2(1+3\beta^2\gamma^2\xi^2)s^3 ; \quad (\text{A1.21})$$

$$N_6 = \frac{2\gamma^2s^2}{\xi-s} - 12\beta^2\gamma^4\xi s^2 ; \quad (\text{A1.22})$$

$$N_7 = -s^4(1+\beta^2\gamma^2\xi^2(2+\beta^2\gamma^2\xi^2)) ; \quad (\text{A1.23})$$

$$N_8 = 4\beta\gamma^2\xi(1+\beta^2\gamma^2\xi^2)s^3 ; \quad (\text{A1.24})$$

$$N_9 = -2\gamma^2(1+3\beta^2\gamma^2\xi^2)s^2 ; \quad (\text{A1.25})$$

$$N_{10} = 4\beta\gamma^4 \xi S \quad ; \quad (\text{A1.26})$$

and finally

$$N_{11} = -\gamma^4 \quad (\text{A1.27})$$

APPENDIX 2

The coefficients appearing in the finite difference representations (1.4.14) - (1.4.16) and (1.4.19) are given here.

$$C_1 = \frac{N_{10}}{2hk^3} \quad ; \quad (A2.1)$$

$$C_2 = \frac{N_{11}}{k^4} \quad ; \quad (A2.2)$$

$$C_3 = -\frac{N_{10}}{2hk^3} \quad ; \quad (A2.3)$$

$$C_4 = \frac{N_8}{2h^3k} \quad (A2.4)$$

$$C_5 = \frac{N_3}{4hk} - \frac{N_5}{2h^2k} - \frac{N_6}{2hk^2} - \frac{N_7}{h^3k} + \frac{N_9}{h^2k^2} - \frac{N_{10}}{hk^3} \quad ; \quad (A2.5)$$

$$C_6 = \frac{N_5}{h^2k} - \frac{2N_6}{h^2k^2} - \frac{4N_{11}}{k^4} \quad ; \quad (A2.6)$$

$$C_7 = -\frac{N_3}{4hk} - \frac{N_5}{2h^2k} + \frac{N_6}{2hk^2} + \frac{N_8}{h^3k} + \frac{N_9}{h^2k^2} + \frac{N_{10}}{hk^3} ; \quad (\text{A2.7})$$

$$C_8 = -\frac{N_8}{2h^3k} ; \quad (\text{A2.8})$$

$$C_9 = \frac{N_2}{h^4} - \frac{N_4}{2h^3} ; \quad (\text{A2.9})$$

$$C_{10} = -\frac{N_1}{2h} + \frac{N_2}{h^2} + \frac{N_4}{h^3} + \frac{N_6}{hk^2} - \frac{4N_7}{h^4} - \frac{2N_9}{h^2k^2} ; \quad (\text{A2.10})$$

$$C_{11} = -\frac{2N_2}{h^2} + \frac{6N_7}{h^4} + \frac{4N_9}{h^2k^2} + \frac{6N_{11}}{k^4} ; \quad (\text{A2.11})$$

$$C_{12} = \frac{N_1}{2h} + \frac{N_2}{h^2} - \frac{N_4}{h^3} - \frac{N_6}{hk^2} - \frac{4N_7}{h^4} - \frac{2N_9}{h^2k^2} ; \quad (\text{A2.12})$$

$$C_{13} = \frac{N_4}{2h^3} + \frac{N_7}{h^4} ; \quad (\text{A2.13})$$

$$C_{14} = -\frac{N_8}{2h^3k} ; \quad (\text{A2.14})$$

$$C_{15} = -\frac{N_3}{4hk} + \frac{N_5}{2h^2k} - \frac{N_6}{2hk^2} + \frac{N_8}{h^3k} + \frac{N_9}{h^2k^2} + \frac{N_{10}}{hk^3} ; \quad (\text{A2.15})$$

$$C_{16} = -\frac{N_5}{h^2k} - \frac{2N_9}{h^2k^2} - \frac{4N_{11}}{R^4} ; \quad (\text{A2.16})$$

$$C_{17} = \frac{N_3}{4hk} + \frac{N_5}{2h^2k} + \frac{N_6}{2hk^2} - \frac{N_8}{h^3k} + \frac{N_9}{h^2k^2} - \frac{N_{10}}{hk^3} ; \quad (\text{A2.17})$$

$$C_{18} = \frac{N_8}{2h^3k} ; \quad (\text{A2.18})$$

$$C_{19} = -\frac{N_{10}}{2hk^3} ; \quad (\text{A2.19})$$

$$C_{20} = \frac{N_{11}}{R^4} ; \quad (\text{A2.20})$$

$$C_{21} = \frac{N_{10}}{2hk^3} ; \quad (\text{A2.21})$$

$$D_2 = -\frac{M_8}{2h^3} ; \quad (\text{A2.22})$$

$$D_5 = \frac{M_4}{2hk} - \frac{M_6}{2h^2k} - \frac{M_7}{2hk^2} ; \quad (\text{A2.23})$$

$$D_6 = \frac{M_6}{h^2k} + \frac{M_8}{k^3} - \frac{M_2}{2k} ; \quad (\text{A2.24})$$

$$D_7 = \frac{M_7}{2hk^2} - \frac{M_6}{2h^2k} - \frac{M_4}{4hk} ; \quad (\text{A2.25})$$

$$D_9 = -\frac{M_5}{2h^3} ; \quad (\text{A2.26})$$

$$D_{10} = \frac{M_7}{hk^2} + \frac{M_5}{h^3} + \frac{M_3}{h^2} - \frac{M_1}{2h} ; \quad (\text{A2.27})$$

$$D_{11} = -\frac{2M_3}{h^2} ; \quad (\text{A2.28})$$

$$D_{12} = \frac{M_1}{2h} + \frac{M_3}{h^2} - \frac{M_5}{h^3} - \frac{M_7}{hk^2} ; \quad (\text{A2.29})$$

$$D_{13} = \frac{M_5}{2h^3} ; \quad (\text{A2.30})$$

$$D_{15} = \frac{M_6}{2h^2k} - \frac{M_7}{2hk^2} - \frac{M_4}{4hk} ; \quad (\text{A2.31})$$

$$D_{16} = \frac{M_2}{2k} - \frac{M_6}{h^2k} - \frac{M_8}{k^3} ; \quad (\text{A2.32})$$

$$D_{17} = \frac{M_4}{4hk} + \frac{M_6}{2h^2k} + \frac{M_7}{2hk^2} ; \quad (\text{A2.33})$$

$$D_{20} = \frac{M_8}{2h^3} ; \quad (\text{A2.34})$$

$$E_5 = \frac{L_3}{4hk} - \frac{L_6}{2h^2k} - \frac{L_7}{2hk^2} ; \quad (\text{A2.35})$$

$$E_6 = \frac{L_4}{k^2} + \frac{L_6}{h^2k} ; \quad (\text{A2.36})$$

$$E_7 = \frac{L_7}{2hk^2} - \frac{L_3}{4hk} - \frac{L_6}{2h^2k} ; \quad (\text{A2.37})$$

$$E_9 = -\frac{L_5}{2h^3} ; \quad (\text{A2.38})$$

$$E_{10} = -\frac{L_1}{2h} + \frac{L_2}{h^2} + \frac{L_5}{h^3} + \frac{L_7}{hk^2} \quad ; \quad (\text{A2.39})$$

$$E_{11} = -\frac{2L_2}{h^2} - \frac{2L_4}{k^2} \quad ; \quad (\text{A2.40})$$

$$E_{12} = \frac{L_1}{2h} + \frac{L_2}{h^2} - \frac{L_3}{h^3} - \frac{L_7}{hk^2} \quad ; \quad (\text{A2.41})$$

$$E_{13} = \frac{L_5}{2h^3} \quad ; \quad (\text{A2.42})$$

$$E_{15} = \frac{L_6}{2h^2k} - \frac{L_3}{4hk} - \frac{L_7}{2hk^2} \quad ; \quad (\text{A2.43})$$

$$E_{16} = \frac{L_4}{k^2} - \frac{L_6}{h^2k} \quad ; \quad (\text{A2.44})$$

$$E_{17} = \frac{L_3}{4hk} + \frac{L_6}{2h^2k} + \frac{L_7}{2hk} \quad ; \quad (\text{A2.45})$$

$$S_1 = C_1 \quad ; \quad (\text{A2.46})$$

$$S_2 = C_2 - \text{Re } D_2 D_2 \bar{\Psi}_{i,j} \quad ; \quad (\text{A2.47})$$

$$S_3 = C_3 \quad ; \quad (\text{A2.48})$$

$$S_4 = C_4 \quad ; \quad (\text{A2.49})$$

$$S_5 = C_5 - \text{Re} (E_5 D_1 \bar{\Psi}_{i,j} + D_5 D_2 \bar{\Psi}_{i,j}) \quad ; \quad (\text{A2.50})$$

$$S_6 = C_6 - \text{Re} (E_6 D_1 \bar{\Psi}_{i,j} + D_6 D_2 \bar{\Psi}_{i,j} - L \bar{\Psi}_{i,j} / 2R) \quad ; \quad (\text{A2.51})$$

$$S_7 = C_7 - \text{Re} (E_7 D_1 \bar{\Psi}_{i,j} + D_7 D_2 \bar{\Psi}_{i,j}) \quad ; \quad (\text{A2.52})$$

$$S_8 = C_8 \quad ; \quad (\text{A2.53})$$

$$S_9 = C_9 - \text{Re} (E_9 D_1 \bar{\Psi}_{i,j} + D_9 D_2 \bar{\Psi}_{i,j}) \quad ; \quad (\text{A2.54})$$

$$S_{10} = C_{10} - \text{Re} (E_{10} D_1 \bar{\Psi}_{i,j} + D_{10} D_2 \bar{\Psi}_{i,j} - (\beta \xi_i L \bar{\Psi}_{i,j} + M \bar{\Psi}_{i,j}) / (2h(1 + \beta \eta_j))) \quad ; \quad (\text{A2.55})$$

$$S_{11} = C_{11} - \text{Re} (E_{11} D_1 \bar{\Psi}_{i,j} + D_{11} D_2 \bar{\Psi}_{i,j}) ; \quad (\text{A2.56})$$

$$S_{12} = C_{12} - \text{Re} (E_{12} D_1 \bar{\Psi}_{i,j} + D_{12} D_2 \bar{\Psi}_{i,j} - (\beta k_j L \bar{\Psi}_{i,j} + M \bar{\Psi}_{i,j}) / (2h(1 + \beta \eta_j))) ; \quad (\text{A2.57})$$

$$S_{13} = C_{13} - \text{Re} (E_{13} D_1 \bar{\Psi}_{i,j} + D_{13} D_2 \bar{\Psi}_{i,j}) ; \quad (\text{A2.58})$$

$$S_{14} = C_{14} ; \quad (\text{A2.59})$$

$$S_{15} = C_{15} - \text{Re} (E_{15} D_1 \bar{\Psi}_{i,j} + D_{15} D_2 \bar{\Psi}_{i,j}) ; \quad (\text{A2.60})$$

$$S_{16} = C_{16} - \text{Re} (E_{16} D_1 \bar{\Psi}_{i,j} + D_{16} D_2 \bar{\Psi}_{i,j} - L \bar{\Psi}_{i,j} / 2R) ; \quad (\text{A2.61})$$

$$S_{17} = C_{17} - \text{Re} (E_{17} D_1 \bar{\Psi}_{i,j} + D_{17} D_2 \bar{\Psi}_{i,j}) \quad (\text{A2.62})$$

$$S_{18} = C_{18} \quad (\text{A2.63})$$

$$S_{19} = C_{19} \quad (\text{A2.64})$$

$$S_{20} = C_{20} - \text{Re} D_{20} D_2 \bar{\Psi}_{i,j} \quad ; \quad (\text{A2.65})$$

$$S_{21} = C_{21} \quad ; \quad \text{and finally} \quad (\text{A2.66})$$

$$V_{i,j} = - \text{Re} (D_1 \Psi_{i,j} L \bar{\Psi}_{i,j} + D_2 \bar{\Psi}_{i,j} M \bar{\Psi}_{i,j}) . \quad (\text{A2.67})$$

Appendix 3

This appendix is the paper published in Mech. Res.
Com., 11, 1984.

ANALYTICAL SOLUTIONS TO A CLASS OF THREE DIMENSIONAL SOLIDIFICATION PROBLEMS

W. Kunda and G. Poots
Department of Applied Mathematics, University of Hull,
England.

(Received 9 March 1984; accepted for print 2 April 1984)

Introduction

It is the purpose of this paper to present analytical solutions to a certain class of three-dimensional solidification problems. The availability of such work is useful in producing reliable computer algorithms for the numerical solution of three dimensional moving interface problems. The analytical solutions presented are generalizations of the classical one-dimensional problem of Neumann (see Carslaw and Jaeger [1]) for the half space domain. They augment the small time two-dimensional solutions of Schulze [2] et al. and the earlier work of Boley and Yagoda [3]. In the latter three-dimensional solutions for small time have been obtained for the melting (or solidification) of a half space by a general surface heat input (or output); the imbedding technique used is fully described by Boley in Ockendon and Hodgkins [4].

The following three dimensional problems, see [2], are investigated:

1. At time $t = 0$, the half space $z > 0$ is filled with liquid at fusion temperature and for $t < 0$ the wall $z = 0$ is maintained at a lower temperature given by $T_0 - (T_F - T_0)g(\frac{x}{a}, \frac{y}{a})$, where x and y are measured along the wall and a is a representative length. Here $g(\frac{x}{a}, \frac{y}{a}) > -1$ for $|\underline{x}| < \infty$ and $T_0 < T_F$.
2. At time $t = 0$ the half space $z > 0$ is filled with liquid at fusion temperature T_F and for $t > 0$ there is Newton cooling at the wall $z = 0$ into the environment $z < 0$. The wall heat transfer coefficient is taken as varying with the co-ordinates x and y measured along the wall.

Following the method developed in [2] small time solutions are obtained. For specific examples results on the location of the solidification surface are presented graphically for various times.

Mathematical Formulation

Let the solid/liquid interface at time t be

$$C(\underline{x}, z, t) = z - \check{\chi}(\underline{x}, t) = 0. \quad (1)$$

Then we have for the solidified phase the governing equations

$$K\nabla^2 T = \rho c_p \partial T / \partial t, \quad (2)$$

$$T = T_F, \quad K\nabla T \cdot \nabla C = -\rho L \partial C / \partial t \text{ on } z = \tilde{\chi}(x, t), \quad (3)$$

either

$$T = T_0 + (T_F - T_0)g(\tilde{x}/a) \text{ or } K\partial T / \partial z = h(\tilde{x}/a)(T - T_0) \text{ on } z = 0, \quad (4a, b)$$

together with the initial conditions

$$T = T_F \text{ for } t = 0, \quad z > 0 \quad (5a)$$

$$\text{and } \tilde{\chi}(x, 0) = 0 \quad (5b)$$

In conditions (4) it is assumed that $g(\tilde{x}/a)$ is a bounded function and $g(\tilde{x}/a) > -1$ for $|\tilde{x}| < \infty$. Moreover the wall heat transfer coefficient must also be bounded with $h(\tilde{x}/a) > 0$ for $|\tilde{x}| < \infty$ and the temperature $T_0 (< T_F)$ is used to denote a reference condition of the environment. In the above L is the latent heat of fusion of the liquid, ρ the density, K the thermal conductivity, c_p the specific heat and T the temperature of the solid.

With use of the dimensionless variables

$$\tilde{x} = x/a, \quad Z = z/a, \quad \tau = kt/a^2, \quad \theta = (T - T_0)/(T_F - T_0), \quad \chi = \tilde{\chi}/a,$$

where k is the thermal diffusivity, the governing equations (1) - (5) transform to the following:

$$\partial^2 \theta / \partial X^2 + \partial^2 \theta / \partial Y^2 + \partial^2 \theta / \partial Z^2 = \partial \theta / \partial \tau \quad (6)$$

$$\theta(X, Z, \tau) = 1, \quad \nabla \theta \cdot \nabla C = -\beta \partial C / \partial \tau \text{ on } C = Z - \chi(X, \tau) = 0. \quad (7)$$

$$\text{Either } \theta = -g(X) \text{ or } \partial \theta / \partial Z = Bi(X)\theta \text{ on } Z = 0. \quad (8a, b)$$

together with the initial conditions

$$\theta(X, Z, \tau) = 1, \quad \chi(X, \tau) = 0 \text{ at } \tau = 0. \quad (9)$$

Here the Stefan number is defined as $\beta = L/c_p(T_F - T_0)$ and the wall Biot number $Bi(X) = ah(x/a)/K$.

Small Time Solutions

Consider the case with the wall temperature specified by (8a). On employing the interface immobilization technique, as discussed in [2], introduce the new variables

$$\tilde{x} = X, \quad \eta = Z/\chi(X, \tau), \quad (10)$$

In the solidified phase the dimensionless temperature satisfies

$$\begin{aligned} \nabla_1^2 \theta + \frac{1}{2} \partial^2 \theta / \partial \eta^2 + (2\eta/\chi^2)(\nabla_1 \chi)^2 \partial \theta / \partial \eta - \\ - (\eta/\chi) \nabla_1^2 \chi \partial \theta / \partial \eta - 2(\eta/\chi) \nabla_1 \chi \cdot \nabla_1 (\partial \theta / \partial \eta) + \\ + \eta^2 (\nabla_1 \chi)^2 \partial^2 \theta / \partial \eta^2 = -(\eta/\chi) \partial \chi / \partial \tau \partial \theta / \partial \eta + \partial \theta / \partial \tau, \end{aligned} \quad (11)$$

subject to the conditions

$$\theta = 1, (1 + (V_1 \chi)^2) \partial \theta / \partial \eta = \beta \chi \partial \chi / \partial \tau \text{ on } \eta = 1, \quad (12)$$

$$\theta = -g(\tilde{x}) \text{ on } \eta = 0, \quad (13)$$

$$\text{and } \theta = 1, \chi = 0 \text{ at } \tau = 0. \quad (14)$$

In the above $V_1^2 = \partial^2 / \partial X^2 + \partial^2 / \partial Y^2$ and $V_1 = \text{grad} = (\partial / \partial X, \partial / \partial Y)$.

For small time assume regular perturbation expansions:

$$\theta(\tilde{x}, \eta, \tau) = \theta_0(\tilde{x}, \eta) + \tau \theta_1(\tilde{x}, \eta) + O(\tau^2), \quad (15)$$

$$\text{and } \chi(\tilde{x}, \tau) = 2\tau^{1/2} \chi_0(\tilde{x}) + 2\tau^{3/2} \chi_1(\tilde{x}) + O(\tau^{5/2}). \quad (16)$$

The zero-order perturbation solutions are:

$$\theta_0(\tilde{x}, \eta) = [1 + g(\tilde{x})] \frac{\text{erf}[\chi_0(\tilde{x}) \eta]}{\text{erf}[\chi_0(\tilde{x})]} - g(\tilde{x}) \quad (17)$$

where $\chi_0(\tilde{x})$ satisfies the transcendental equation

$$\chi_0(\tilde{x}) \exp[\chi_0^2(\tilde{x})] \text{erf}[\chi_0(\tilde{x})] = [1 + g(\tilde{x})] / \beta \pi^{1/2}. \quad (18)$$

The first order function $\theta_1(\tilde{x}, \eta)$ will not be quoted here. The interface perturbation function $\chi_1(\tilde{x})$ is determined from

$$\begin{aligned} & (3 + 2\chi_0^2 + 10\phi\chi_0^2 + 4\phi\chi_0^4) \beta \chi_1 = \\ & (1 + 2\chi_0^2 - \phi - 4\phi\chi_0^4 + 2\phi^2\chi_0^2 + 4\phi^2\chi_0^4) \chi_0 \nabla^2 g / (1 + 2\phi\chi_0^2) + \\ & 4\chi_0^3 (\phi - 1) (2 + \phi + 6\phi\chi_0^2 - 2\phi^2\chi_0^2 + 4\phi^2\chi_0^4) |\nabla g|^2 / (1 + g) (1 + 2\phi\chi_0^2)^3, \end{aligned} \quad (19)$$

where $\phi(X) = 1 + \beta / (1 + g(X))$. The above results are the three dimensional generalization of the expansions already discussed in [2].

The case of variable Newton cooling, as specified by the wall condition (8b), is examined by the method of Megerlin [5]. Following [2] the temperature field is written as

$$\theta = 1 + \sum_{n=1}^{\infty} G_n(\tilde{x}, \tau) [Z - \chi(\tilde{x}, \tau)]^n, \quad (20)$$

and because this has polynomial form in Z the solution will be valid for large β only. On employing subsidiary expansions for $G_n(\tilde{x}, \tau)$ and $\chi(\tilde{x}, \tau)$ for small τ yields the following result:

$$\begin{aligned} \gamma(\underline{x}, \tau) = & B_i(\underline{x}) \frac{\tau}{\beta} - \left[\frac{B_i(\underline{x})^3}{2} \right] \left(1 + \frac{1}{\beta} \right) \left(\frac{\tau}{\beta} \right)^2 + \\ & + B_i(\underline{x}) \left| \frac{v_g(\underline{x})}{1} \right|^2 + \left[\frac{B_i(\underline{x})^2}{2} \right] v^2 B_i(\underline{x}) + \left[\frac{B_i(\underline{x})^5}{2} \right] \left(1 + \frac{8}{3\beta} + \frac{5}{3\beta^2} \right) \tau, \end{aligned} \quad (21)$$

valid for large β .

Numerical Solutions

Interface locations have been calculated, from the two-term expansion (16), when the wall temperature is given in the form

$$\theta_w(x, y) = \theta(x, y, 0) = 0.3[(1 + \tanh x)(1 + \tanh y) - 1], \quad (22)$$

for $\beta = 0.3$. These results are self explanatory and are displayed in Figures 1, 2 and 3 for the dimensionless times $\tau = 0.2, 0.4$ and 0.6 , respectively. Note that the two dimensional equivalent of (16) is shown in [2] to yield results in exact agreement with numerical finite difference solutions up to the dimensionless time $\tau = 0.5$. It follows that expansion (16) is also valid in this region of time. The above results may be used to simulate heat transfer and solidification rates at the edges of an insulating tile inserted in an ingot mould of the type commonly employed in a steel making plant.

In Figure 4 the interface location at $\tau = 0.6$ for $\beta = 0.3$ and the bounded wall temperature

$$\theta_w(x, y) = 0.9 \sin x \sin y, \quad |x| \leq 2\pi, \quad |y| \leq 2\pi \quad (23)$$

is displayed. Note that in Figures 1 - 4 the scale on the z-axis is multiplied by a factor of 10.

The above analytical and numerical results may prove useful in producing and checking computer algorithms that may be developed for the numerical solution of three-dimensional moving interface problems. Moreover the vector form of the analytical results can be utilised in other applications where the geometry is expressed in curvilinear co-ordinates.

References

1. Carslaw, H. S. and Jaeger, J. C. Conduction of Heat in Solids, Oxford 1959,
2. Schulze, H. J., Beckett, P. M., Howarth, J. A., and Poots G., Proc. R. Soc. Lond. A 385, 313-343, 1983.
3. Boley, B. A. and Yagoda H. P., *ibid*, A 323, 89-110, 1971.
4. Ockendon J. R. and Hodgkins, W. R. (ed.) Moving boundary problems in heat flow and diffusion, 150-173. Oxford: The Clarendon Press, 1975.
5. Megerlin, F., Forsch. Geb. Ing. Wes 34, 40-46, 1968.

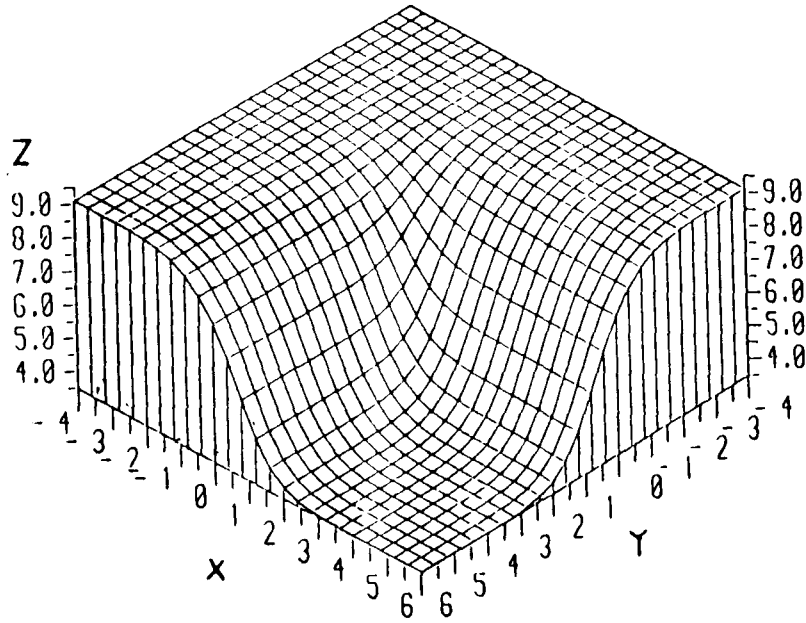


Figure 1 Interface location for wall temperature (22) for $\beta = 0.3$, $\tau = 0.2$

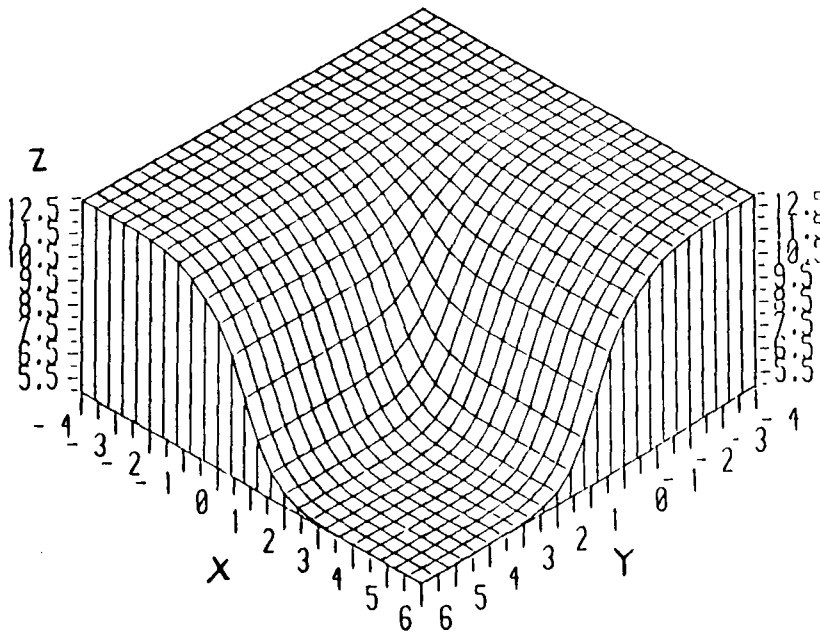


Figure 2 Interface location for wall temperature (22) for $\beta = 0.3$, $\tau = 0.4$

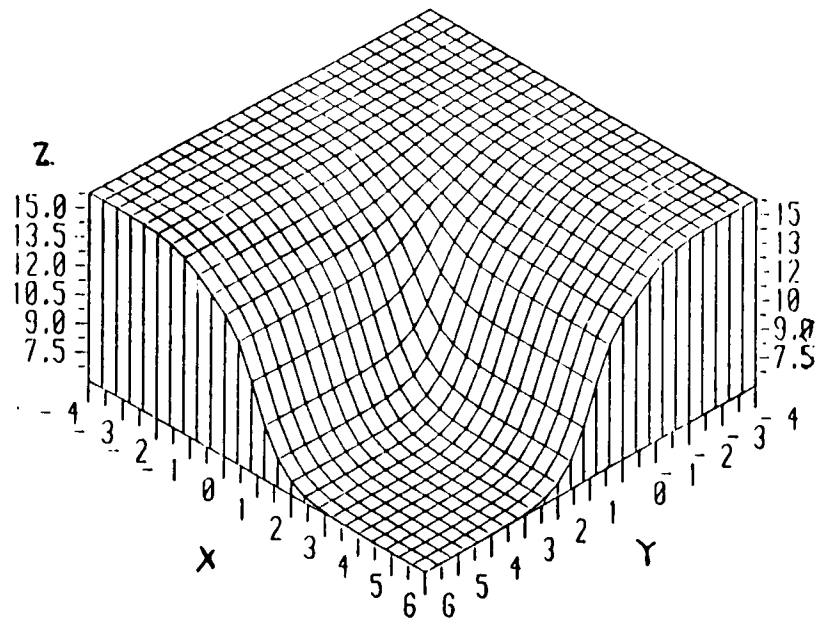


Figure 3 Interface location for wall temperature (22) for $\beta = 0.3$, $\tau = 0.6$

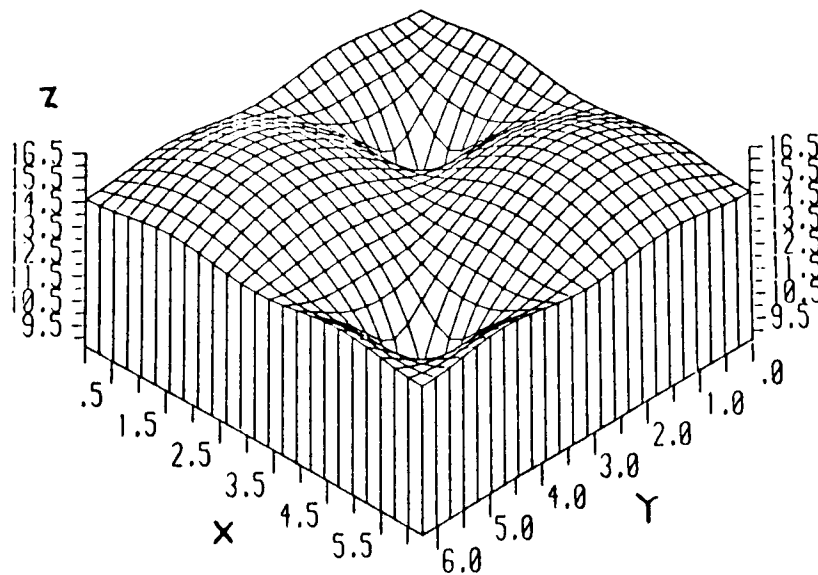


Figure 4 Interface location for wall temperature (23) for $\beta = 0.3$, $\tau = 0.6$.

REFERENCES

- DebRoy, T., Majumdar, A.K., and Spalding, D.B. "Numerical prediction of recirculation flows with free convection encountered in gas-agitated reactors." *Appl. Math. Modelling*, 2, 146-150, 1978.
- Durst, F., Taylor, A.M.K.P., and Whitelaw, J.H. "Experimental and Numerical investigation of bubble-driven laminar flow in an axisymmetric vessel." *Int. J. Multiphase flow* 10, 557-569, 1984.
- Grevet, J.H. "An experimental study of gas-agitated circulation systems of ladle metallurgy." MSc. Thesis, Massachusetts Institute of Technology. 1981.
- Grevet, J.H., Szekely, J., and El-Kaddah, N. "An experimental and theoretical study of gas bubble driven circulation systems." *Int. J. Heat and Mass Transfer*, 25, 487-497, 1982.
- Hudson, P.C., and O'Carroll, M.J., Eds. "Mathematical modelling of industrial processes." Emjoc Press, Northallerton, 1982.
- Olson, M.D. "Comparison problem No. 1, Recirculating flow in a square cavity." Structural research series, Report 22, University of British Columbia, Vancouver, 1979.

Pun, W.M. and Spalding, D.B. "A general computer program for two-dimensional elliptic flows." Rep. HTS/76/2, Heat transfer section, Imperial College, London, 1977.

Spalding D.B. "A novel finite difference formulation for differential expressions involving both first and second derivatives." Int. J. Numer. Meth. Engng, 4, 551-559, 1972.

Szekely, J., Dilawari, A.H., and Metz, R. "The mathematical and physical modelling of turbulent recirculating flows." Met. Trans. B, 10B, 33-41, 1979.

Szekely, J., El-Kaddah, N.H. and Grevet, J.H. "Flow phenomena in argon stirred ladles, room temperature measurements and analysis." Proc. Int. Conf. Injection metallurgy, Lulea, Sweden, 5:1 - 5: 32, 1980.

Szekely, J., Wang, H.J., and Kiser, K.M. "Flow pattern velocity and turbulence energy measurements and predictions in a water model of an argon-stirred ladle." Met. Trans. B, 7B, 287-295, 1976.

Tuann, S.-Y., and Olson, M.D. "Review of computing methods for recirculating flows." J. Computational Phys. 29, 1-19, 1978.

Baker, P.C., Poots, G, and Rodgers, G.G. "Ice accretion on cables of various cross-sections." I.M.A. Journ of Applied Mathematics, 1-18, 1986.

Boley, B.A., and Yogoda, H.P. "The three-dimensional starting solution for a melting slab." Proc. Roy. Soc. Lond. A.323, 89-110, 1971.

Carslaw, H.S., and Jaeger, J.C. "Conduction of heat in solids." 2nd ed. Clarendon Press, Oxford, 1959.

Crowley, A.B. "Numerical solution of Stefan problems." Int. J. Heat Mass Transfer, 21, 215-219, 1978.

Drew, T.B., Hoopes, J.W., and Vermuelen, T. Eds. "Advances in chemical engineering." Academic Press, New York, 1964.

Furzeland, R.M. "A comparative study of numerical methods for moving boundary problems." J. Inst. Math.Applics., 26. 411-429, 1980.

Goodman, T.R. "Applications of integral methods to transient non-linear heat transfer." Advances in heat transfer, 1, 52-120, 1964.

Jiji, L.M., and Weinbaum, S. "Perturbation solutions for melting or freezing in annular regions initially not at the fusion temperature." *Int.J.Heat and Mass Transfer*, 21, 581-592, 1978.

Landau, H.G. "Heat conduction in melting solid." *Quart. Applied Mathematics*, 8, 81-94, 1950.

Lazaradis, A. "A numerical solution of the multi-dimensional solidification and melting problems." *Int. J. Heat Mass Transfer*, 13, 1459-1477, 1970.

Mergerlin, F. "Geometrisch eindimensional Wärmeleitung beim schmelzen und erstarren." *Forsch. Ing. - Wes.*, 34, 40-46, 1968.

Muelbauer, J.C., and Sunderland, J.E. "Heat conduction with freezing and melting." *App. Mech. Rev.*, 18, 951-959, 1965.

Ockenden, J.R. and Hodgkins, W.R., Eds. "Moving boundary problems in heat flow and diffusion." Clarendon Press, Oxford, 1975.

Pedroso, R.I., and Domoto, G.A. "Inward spherical solidification by the method of strained coordinates." *Int. J. Heat Mass Transfer*, 16, 1037-1043, 1973.

Poots, G. "An approximate treatment of a heat conduction problem involving a two-dimensional solidification front." Int.J. Heat Mass Transfer, 5, 339-348, 1962.

Poots, G. "On the application of integral methods to the solution of problems involving the solidification of liquid initially at fusion temperature." Int. J. Heat Mass Transfer, 5, 525-531, 1962.

Poots, G., and Rodgers, G.G. "The Icing of a cable". J.I.M.A. 18, 203-217, 1976.

Poots, G. "Theoretical Solutions of ice accretion on cables". Proceedings of 2nd international workshop on ice accretion. Trondheim, Norway. 1984.

Rathjen, K.A., and Jiji, L.M. "Heat conduction with melting or freezing in a corner." Journ.Heat Transfer, 91, 101-109, 1971.

Riley, D.S., Smith, F.T., and Poots, G. "The inward solidification of spheres and circular cylinders." Int. J. Heat Mass Transfer, 17, 1507-1576, 1974.

Schulze, H.J., Beckett, P.M., and Howarth, J.A., and Poots, G. "Analytical and numerical solutions to two-dimensional moving interface problems with applications to the solidification of killed steel ingots." Proc. R.Soc. Lond. A.385, 313-343, 1983.

Sikarskie, D.L., and Boley, B.A. "The solution of a class of two-dimensional solidification problems." Int.Journ.Solids Struct. 1, 207-234, 1965.

Soward, A.M. "A unified approach to Stefan's problem for spheres and cylinders." Proc. R.Soc. Lond. A.373, 131-147, 1980.

Springer, G.S., and Olsen, D.R. "Method of solution of axi-symmetric solidification problems." ASME paper 62-WA-246, 1962.

Stewartson, K., and Waechter, R.T. "On Stefan's problem for spheres." Proc. R.Soc. Lond. A.348, 415-426, 1976.

Talwar, R., and Dilpare, A.L. "A two-dimensional numerical solution to freezing/melting in cylindrical coordinates." ASME paper 77-WA/HT-11, 1978.

Tien, L.C., and Wilkes, J.O. "Axi-symmetric normal freezing with convection above." 4th Int. Heat Transfer Conference, Versailles, 1970.

Wakaham. G, and Kuroiwa, D. "Snow accretion in electric wires and its prevention." Journ. of Glaciology, 19 (No. 81), 1977.